



High Energy Physics – Accelerating Science and Innovation

Particle Physics Landscape:

**History of Instrumentation /
Modern Tracking Detectors**

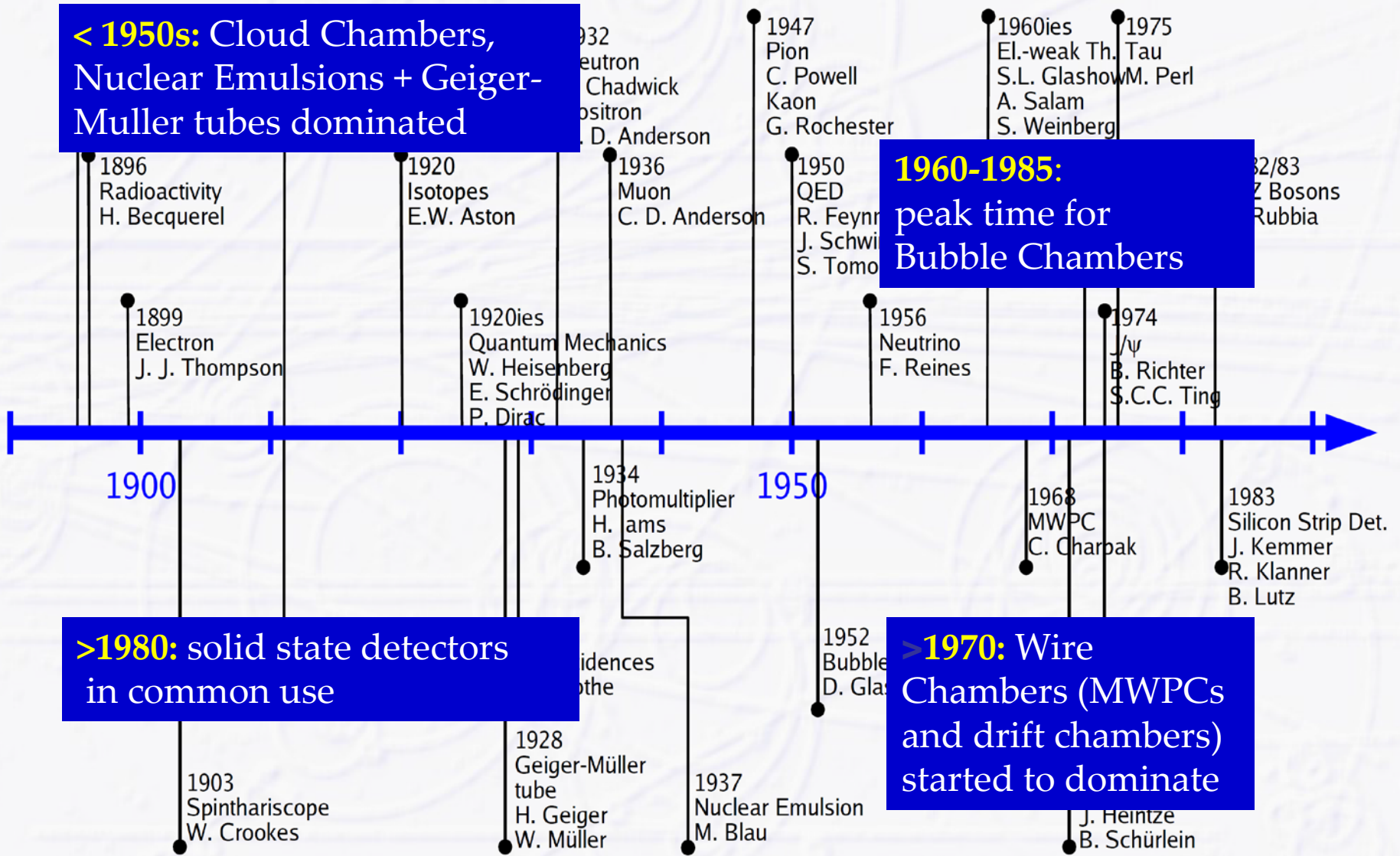
The History of Instrumentation is VERY Entertaining

- ❖ A look at the **history of instrumentation** in particle physics
 - **complementary view on the history of particle physics**, which is traditionally told from a theoretical point of view
- ❖ The importance and recognition of inventions in the field of instrumentation is proven by the fact that
 - several **Nobel Prizes in physics** were awarded mainly or exclusively for the **development of detection technologies**

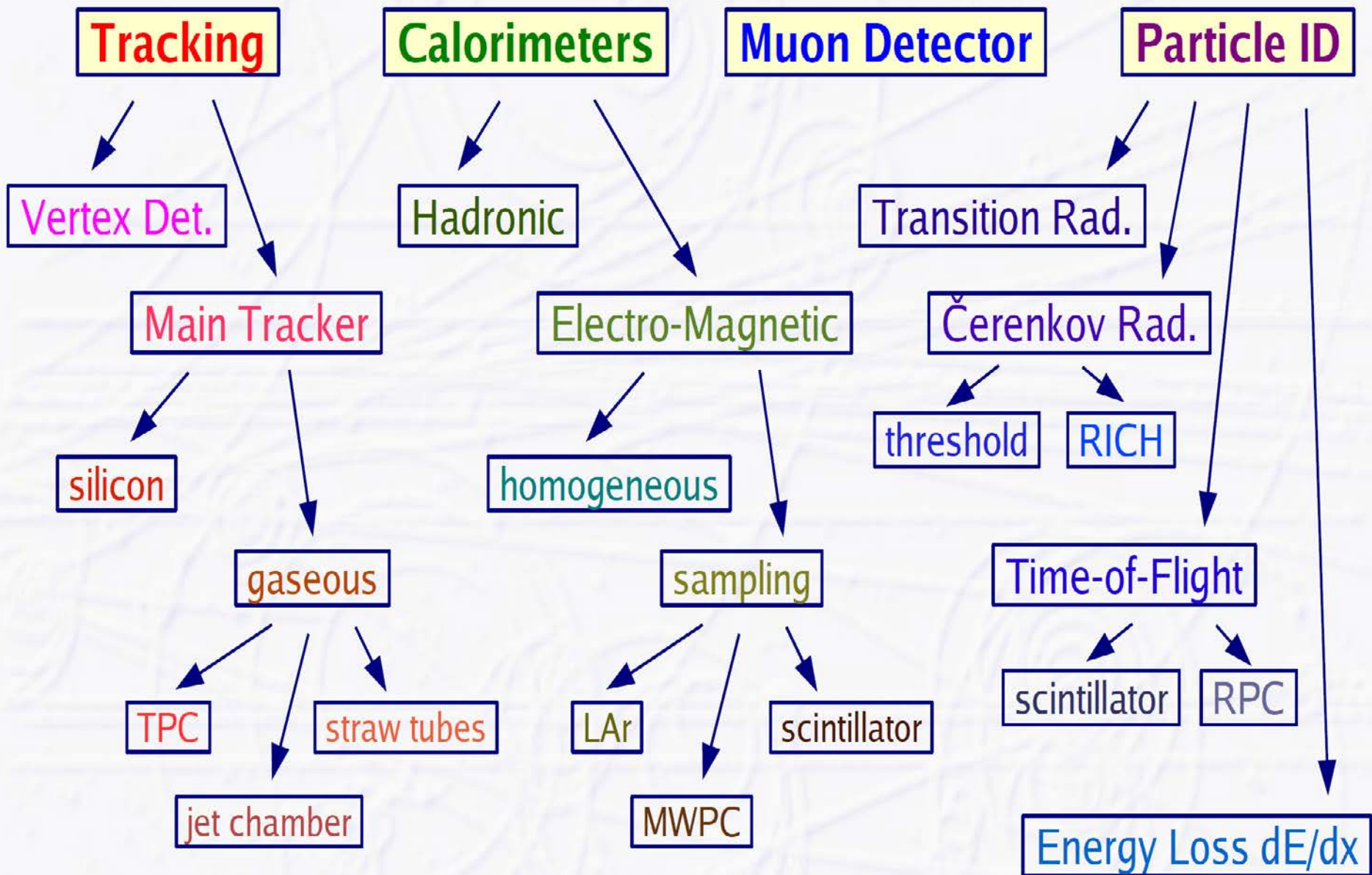
Nobel Prizes in instrumentation (“tracking concepts”):

- ❖ 1927: C.T.R. Wilson, Cloud Chamber
- ❖ 1960: Donald Glaser, Bubble Chamber
- ❖ 1992: Georges Charpak, Multi-Wire Proportional Chamber

Timeline of Particle Physics and Instrumentation



Modern Particle Physics Detectors Overview



Particle Physics Detectors: Major Components

Tracking Detector (or Tracker) = momentum measurement

- closest to interaction point: vertex detector (often silicon pixels)
 - measures **primary interaction vertex** and **secondary vertices** from decay particles
- main or central tracking detector
 - measures **momentum** by curvature in magnetic field
 - two technologies: solid state detectors, Si strips (CMS) or gaseous detectors (ALICE)

Calorimeters = energy measurement

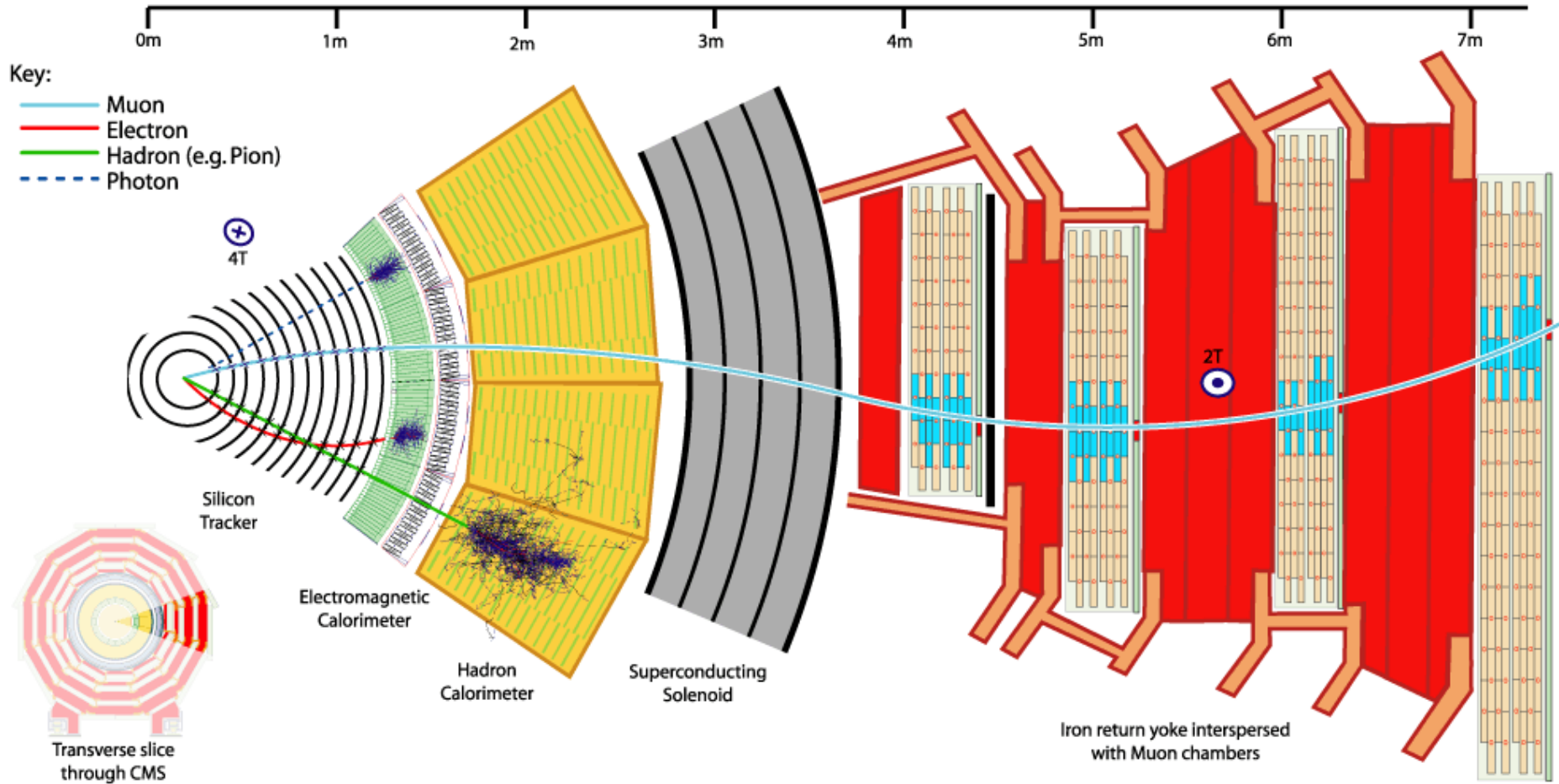
- electro-magnetic calorimeters
 - measures **energy of light EM particles** (electrons, positrons, photons) based on electro-magnetic showers by bremsstrahlung and pair production
 - two concepts: homogeneous (CMS) or sampling (ATLAS)
- hadron calorimeters
 - measures **energy of heavy (hadronic) particles** (pions, kaons, protons, neutrons) based on nuclear showers created by nuclear interactions

Muon Detectors = momentum measurement for muons (more precise)

- outermost detector layer, **basically a tracking detector**

A Typical Today's Particle Detector

● Cut-away view of CMS Experiment




















Tracker

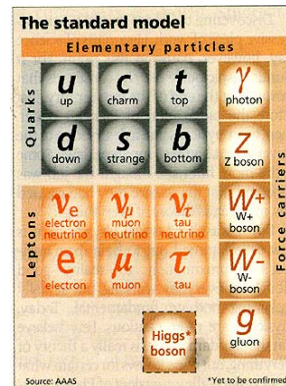
Calorimeter

Coil

Muon Detector and iron return yoke

The General Purpose Detector: Particle Identification Methods

Constituent	Vertex	Track	PID	Ecal	Hcal	Muon
electron	primary				—	—
Photon γ	primary	—	—		—	—
u, d, gluon	primary		—			—
Neutrino ν	—	—	—	—	—	—
s	primary					—
c, b, τ	secondary					—
μ	primary		—	MIP	MIP	



PID = Particle ID
(TOF, Cherenkov, dE/dx)

MIP = Minimum
Ionizing Particle

Tracking

Momentum measurement

Multiple scattering

Bethe-Bloch formula
/ Landau tails

Ionization of gases

Wire chambers

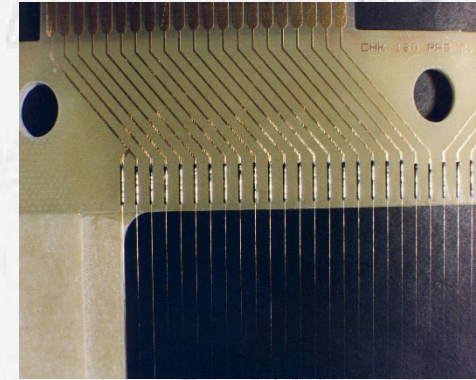
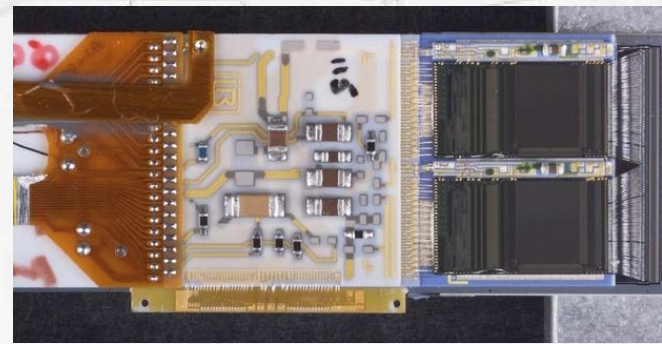
Drift and diffusion in gases

Drift chambers

Micro gas detectors

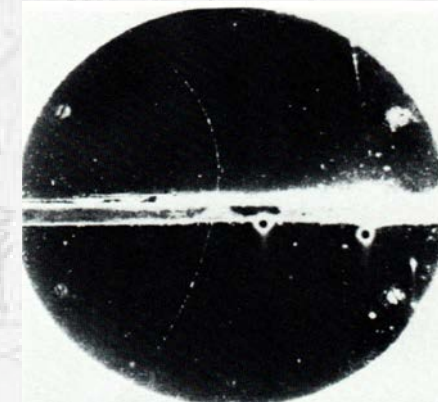
Silicon as a detection medium

Silicon detectors strips/pixels



Tracking Detectors

- **“Classic” Detectors (historical touch...)**
- **Momentum Measurement**
- **Wire Chambers, MPGDs**
- **Silicon Detectors**



Registration of Ionization: Tracking in Gas and Solid State Detectors

Charged particles leave a trail of ions (and excited atoms) along their path: Electron-Ion pairs in gases and liquids, electron hole pairs in solids.

The produced charges can be registered → Position measurement → Tracking Detectors.

- ❖ Cloud Chamber: Charges create drops → photography.
- ❖ Bubble Chamber: Charges create bubbles → photography.
- ❖ Emulsion: Charges 'blackened' the film.

Gas and Solid State Detectors: Moving Charges (electric fields) induce electronic signals on metallic electrodes that can be read by dedicated electronics.

→ In solid state detectors the charge created by the incoming particle is sufficient.

→ In gas detectors (e.g. wire chamber) the charges are internally multiplied in order to provide a measurable signal.

Geiger Counter



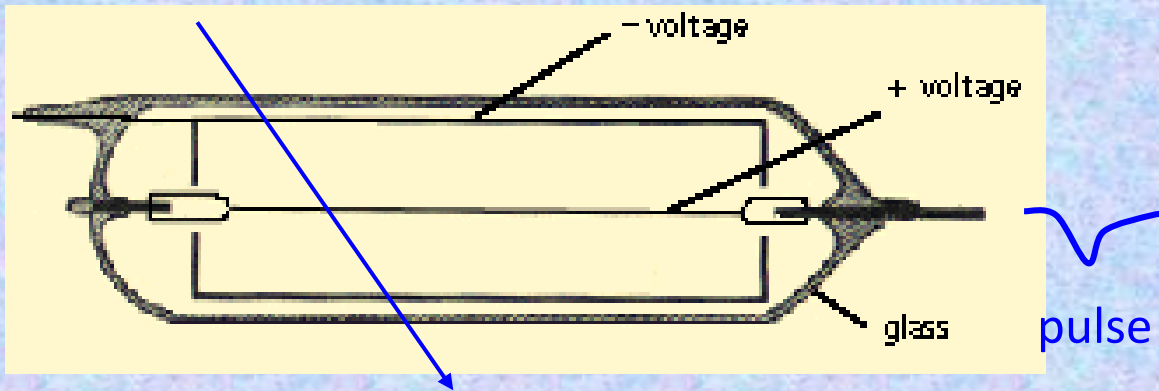
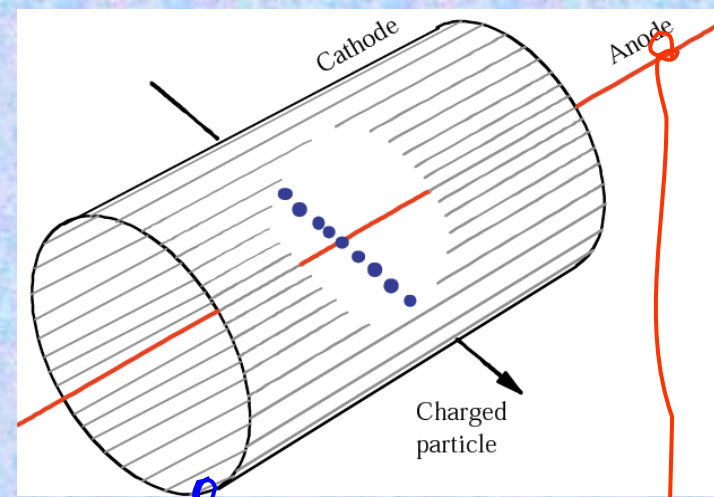
E. Rutherford

1909



H. Geiger

1927

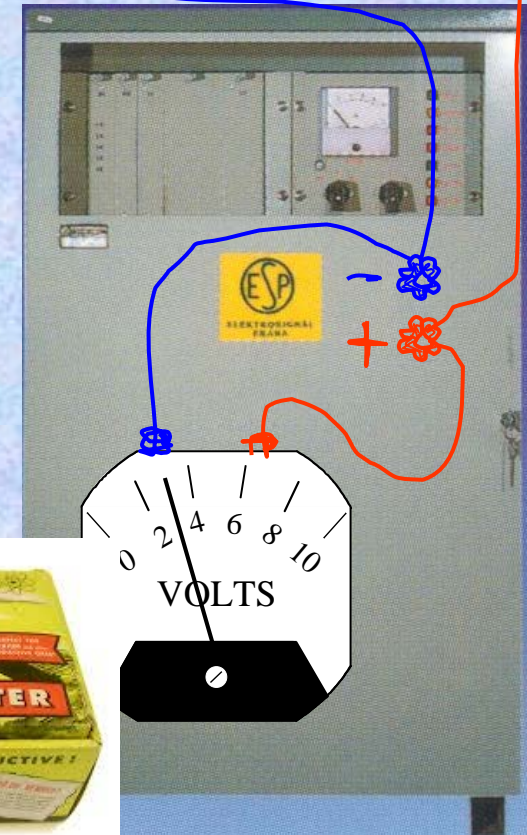


The Geiger counter, later further developed and then called Geiger-Müller counter

First electrical signal from a particle !!!

E. Rutherford and H. Geiger, Proc. Royall Soc. A81 (1908) 141

H. Geiger and W. Mülller, Phys. Zeits. 29 (1928) 839



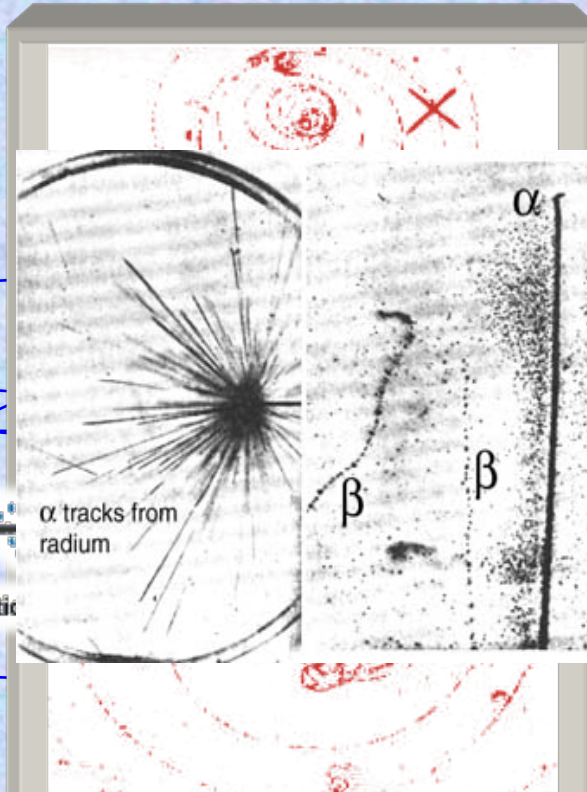
Classic Particle Tracking Detector: Cloud Chamber

Passage of charge particle would condense the vapor into tiny droplets, marking the particle's path → their number being proportional to dE/dx

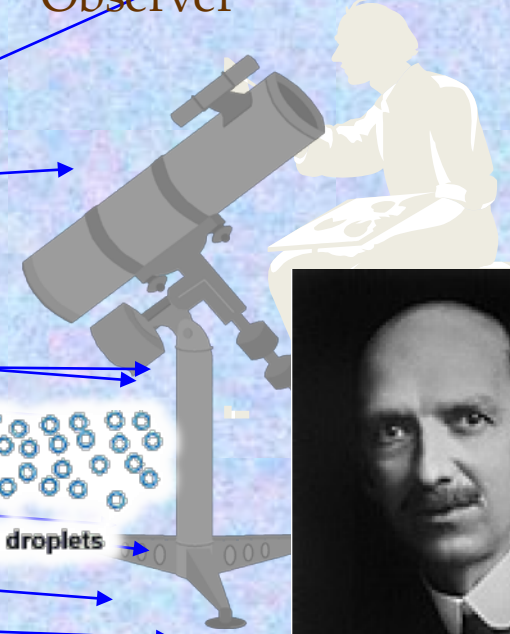
Flux of particles



Cloud Chamber
+ Magnet

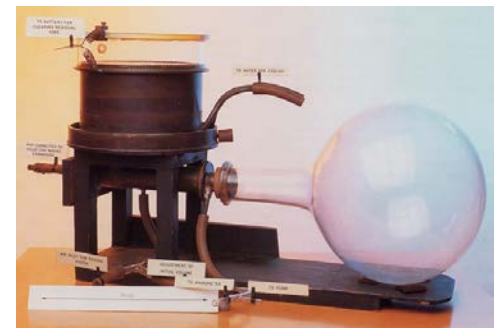


Observer



● Cloud chamber (1911 by Charles T. R. Wilson, Noble Prize 1927)

- chamber with over-saturated water vapour
 - originally developed to study formation of rain clouds
- charged particles leave trails of ions
 - water is condensing around ions
- visible track as line of small water droplets



Discovery of a Positron e^+ from Cosmic Rays

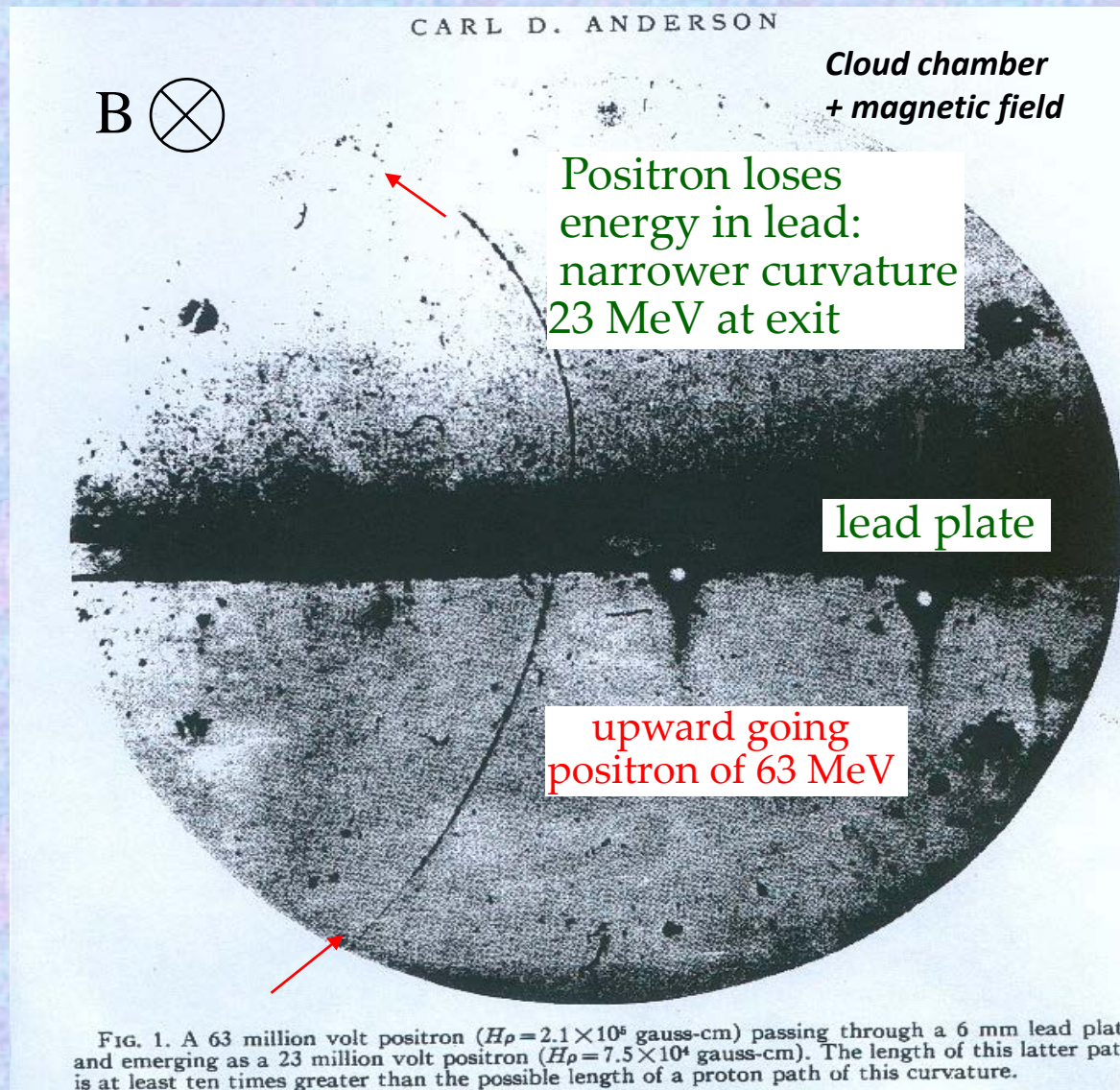
1932 C.D. Anderson :

- Particle with positive curvature and minimum ionisation (droplets size)
- Track length is at least 10 times greater than the possible length of a proton path of this curvature
- Energy loss in a 6 mm of Pb: compatible with that of electron

Hypothesis (discovery !) :

- particle with mass $\sim m_e$ and charge +1, the positron

❖ *First anti-particle*



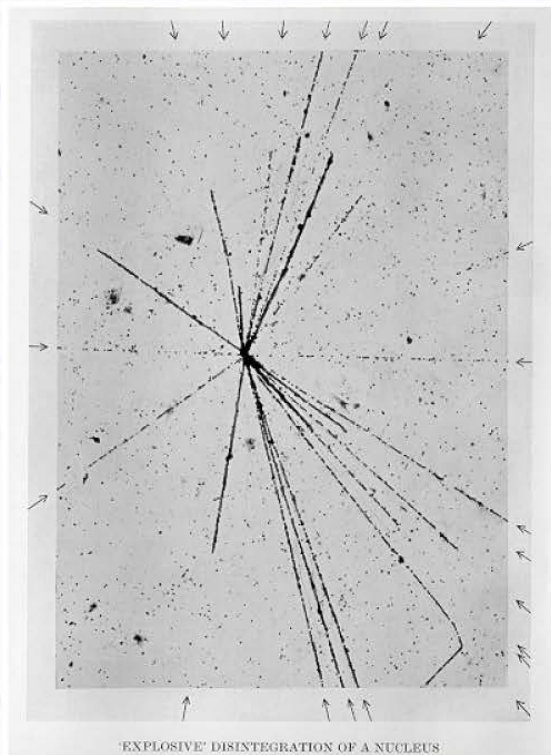
Discovery of the positron by Cloud Chamber
(1932 by Carl Anderson, Noble Prize 1936)

Nuclear Emulsion (I)

● Pioneered by Marietta Blau between 1923 – 1938 (no Nobel Prize)

- photographic emulsion layer, 10 – 200 μm thick, uniform grains of 0.1 – 0.3 μm size
- very high resolution for particle tracks
 - analysis of developed emulsion by microscope

Marietta Blau



nuclear disintegration from cosmic rays, observed 1937 for the first time

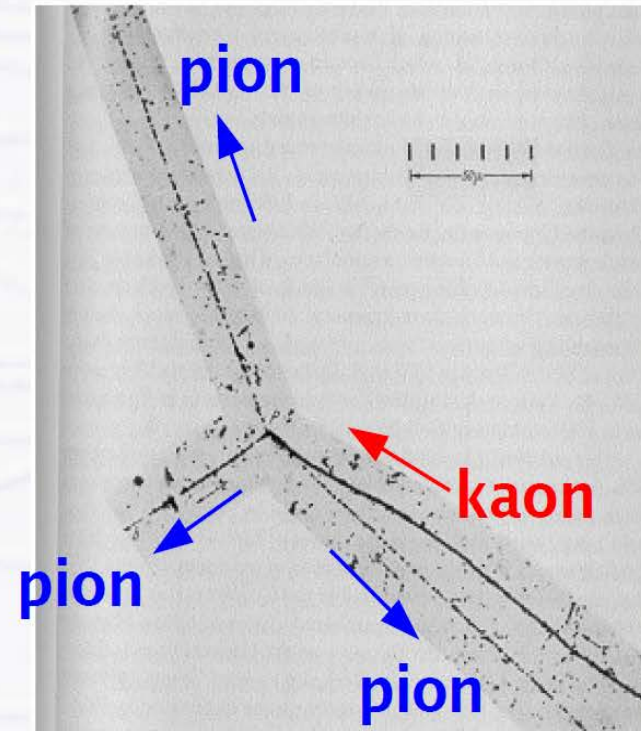
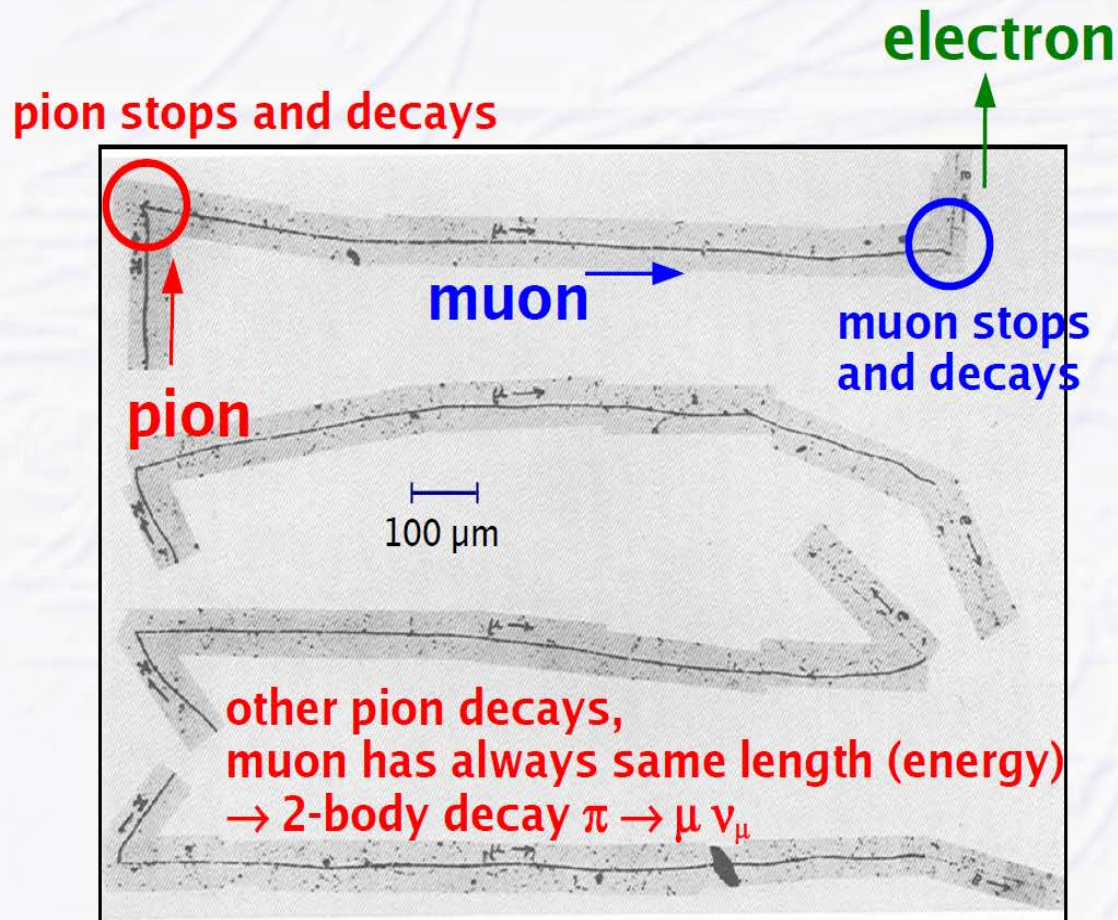
● Since early 20th century

- important role of photography to study radioactivity
- but capability to make individual tracks visible not seen until nuclear emulsion technique was developed

Nuclear Emulsion (II)

- Discovery of the **pion** in cosmic rays by Cecil Powell 1947 (Nobel Prize 1950)
- Discovery of the **kaon** 1949 (G. Rochester)

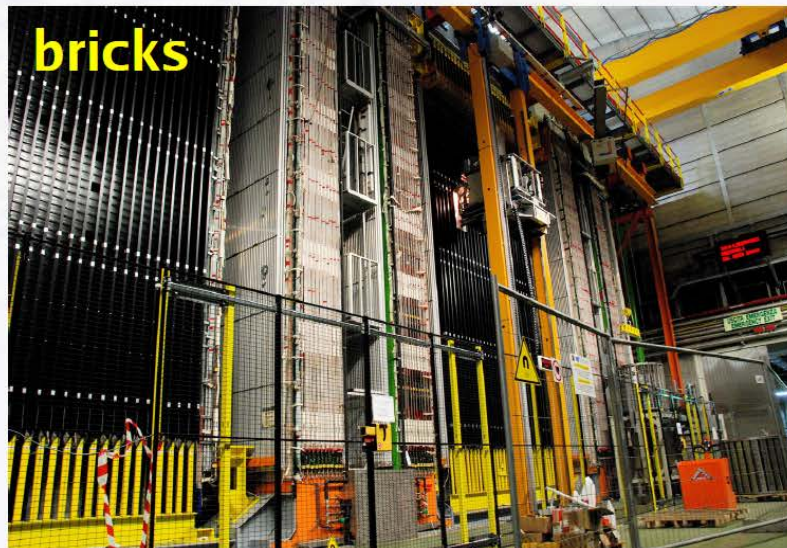
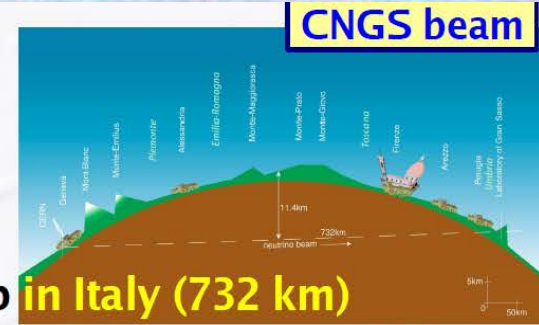
Cecil Powell



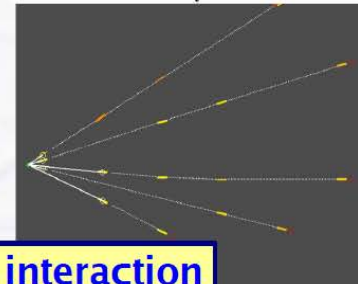
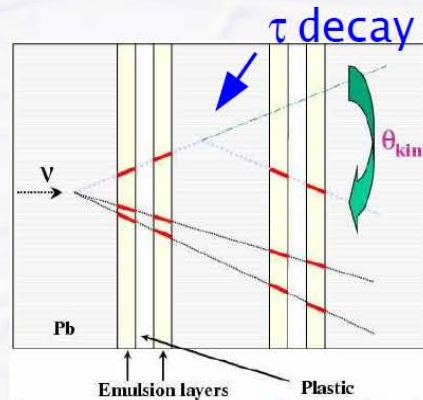
Nuclear Emulsion (III)

● Still used in actual experiments with highest precision requirements over a large volume

- ν_μ beam sent from CERN to Gran Sasso Underground lab in Italy (732 km)
- OPERA experiment is searching for ν_τ appearance after neutrino oscill. $\nu_\mu \rightarrow \nu_\tau$
 - need to reconstruct τ decays ($\nu_\tau + N \rightarrow \tau^- + X$) (few $\sim 100 \mu\text{m}$ track length)
 - 235'000 “bricks” (1.7 ktons) of lead + emulsion sheets



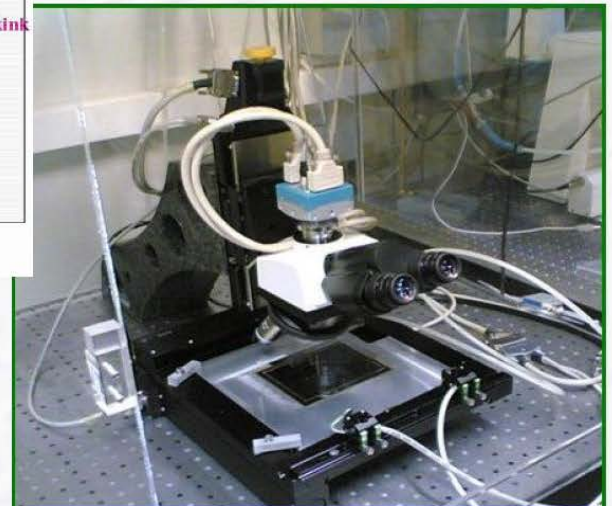
OPERA at Gran Sasso



ν_μ interaction



single brick



automatic emulsion scanning

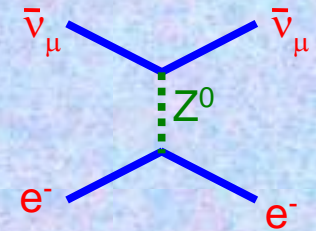
Bubble Chamber (I)

1952 by Donald Glaser, Noble Prize 1960

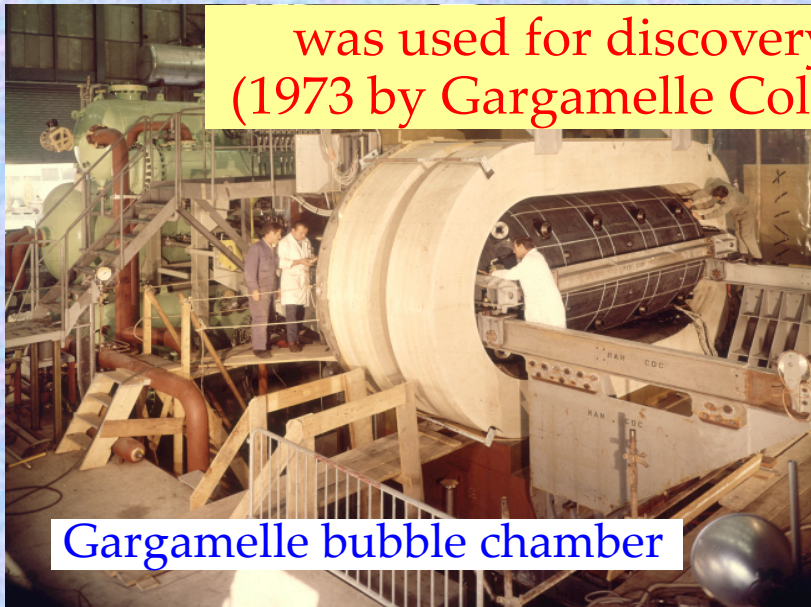
(4.8 x 1.85 m²) chamber with liquid (H₂) at boiling point (“superheated”)

Similar principle as cloud chamber:

- Instead of supersaturating a gas with a vapor one would superheat the liquid.
- A particle leave a trail of ions along its path → make a liquid boil, and form gas bubbles around ions

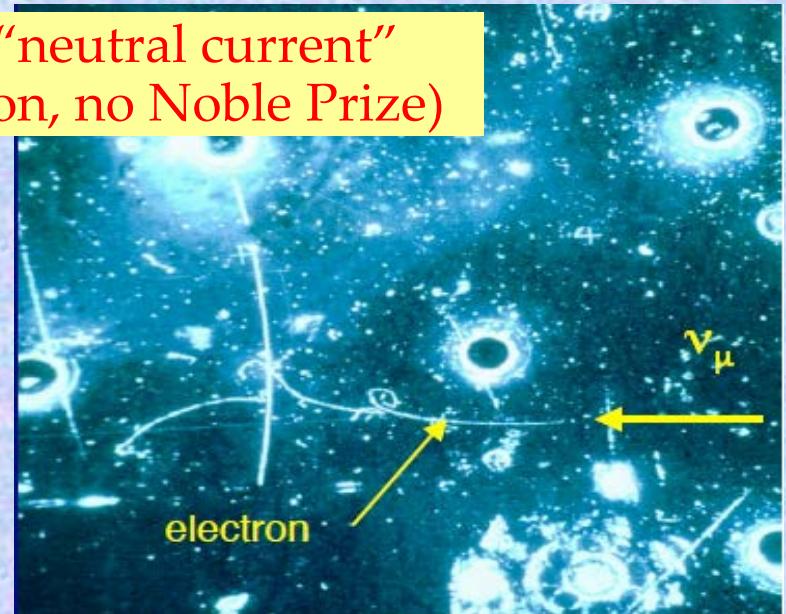


was used for discovery of the “neutral current”
(1973 by Gargamelle Collaboration, no Noble Prize)



Gargamelle bubble chamber

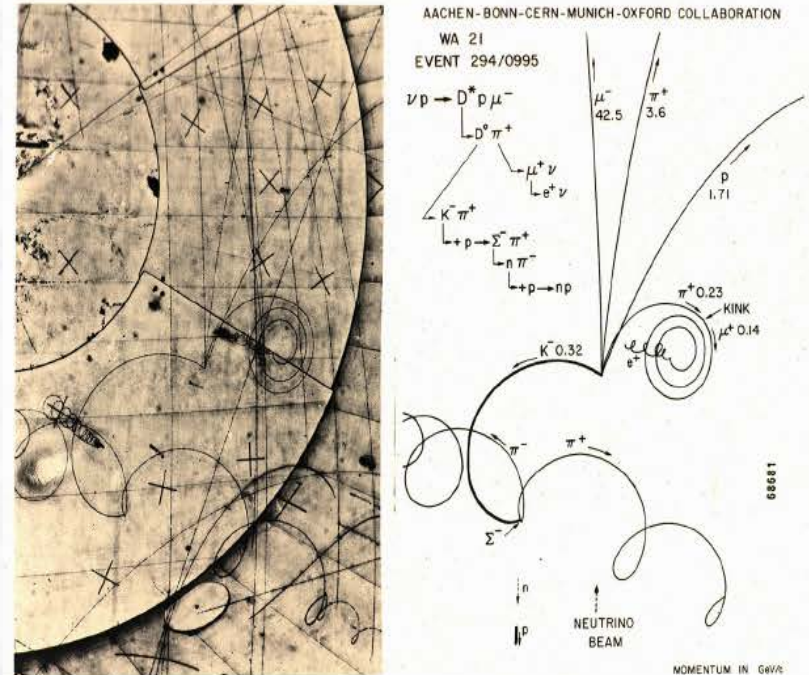
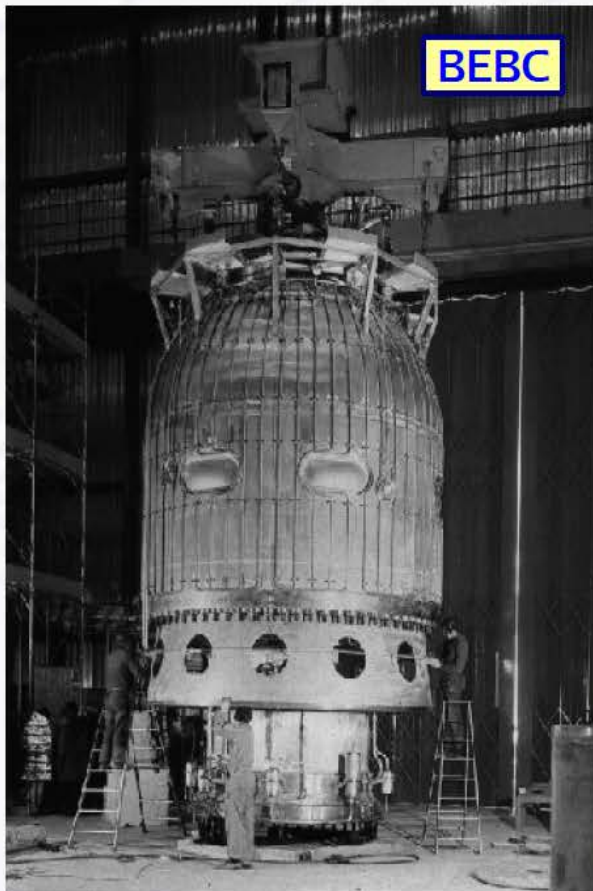
CERN



Bubble Chamber (II)

● BEBC (Big European Bubble Chamber) at CERN, 1973 – 1984

- largest bubble chamber ever built (and the last big one...), \varnothing 3.7 m
- 6.3 million photographs taken, 3000 km of developed film
- now displayed in permanent exhibition at CERN



production of D^* meson
with long decay chain

Bubble Chamber

- Advantages:

liquid (hydrogen) is
BOTH detector medium
AND target

high precision
($\sim 5 \mu\text{m}$)

- Disadvantages:

- NO TRIGGER ->
has to be in superheated
state when particle is
entering

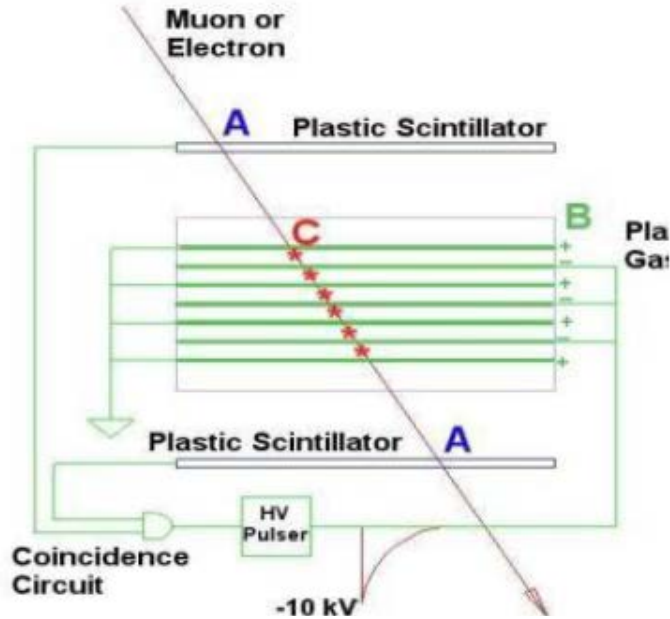
LOW RATE CAPABILITY
Need FASTER
detector (electronics !)

Liquid hydrogen “bubble chamber”



The hydrogen acts as a target (for
incoming particles) and a
detection medium

Spark Chamber



The Spark Chamber was developed in the early 60ies.

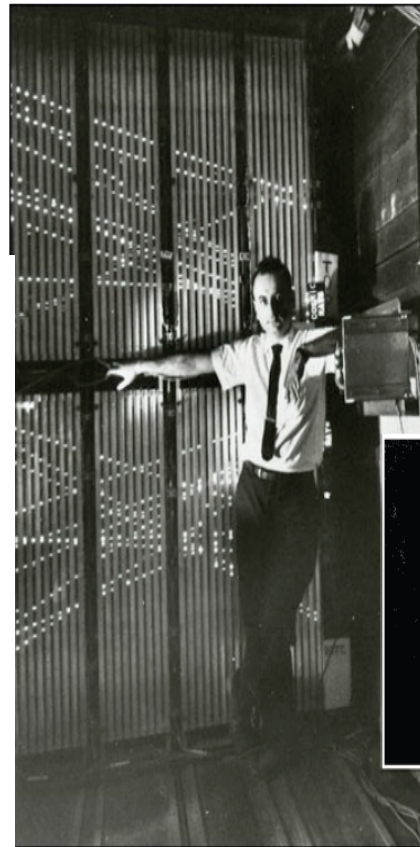
Schwartz, Steinberger and Lederman used it in discovery of the muon neutrino

Discovery of Muon Neutrino by Spark Chamber (1962 by Lederman, Schwartz, Stainberger; Noble Prize 1988)

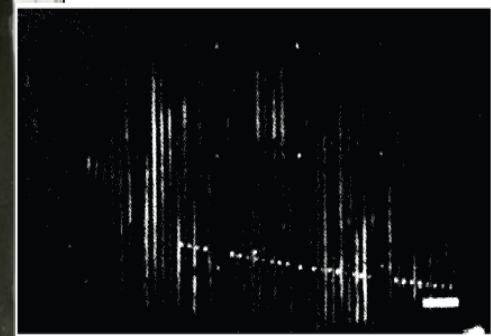
Beam of the energetic protons to produce π -mesons showers
→ Decaying into muons and neutrinos

Only neutrino could pass through a 5,000-ton 13-m thick steel wall into gas detector ("Spark Counter")

A tiny fraction of neutrinos react in the detector (90 layers of aluminum plates, 10 tons) giving rise to muon spark trails → existence of muon-neutrinos.

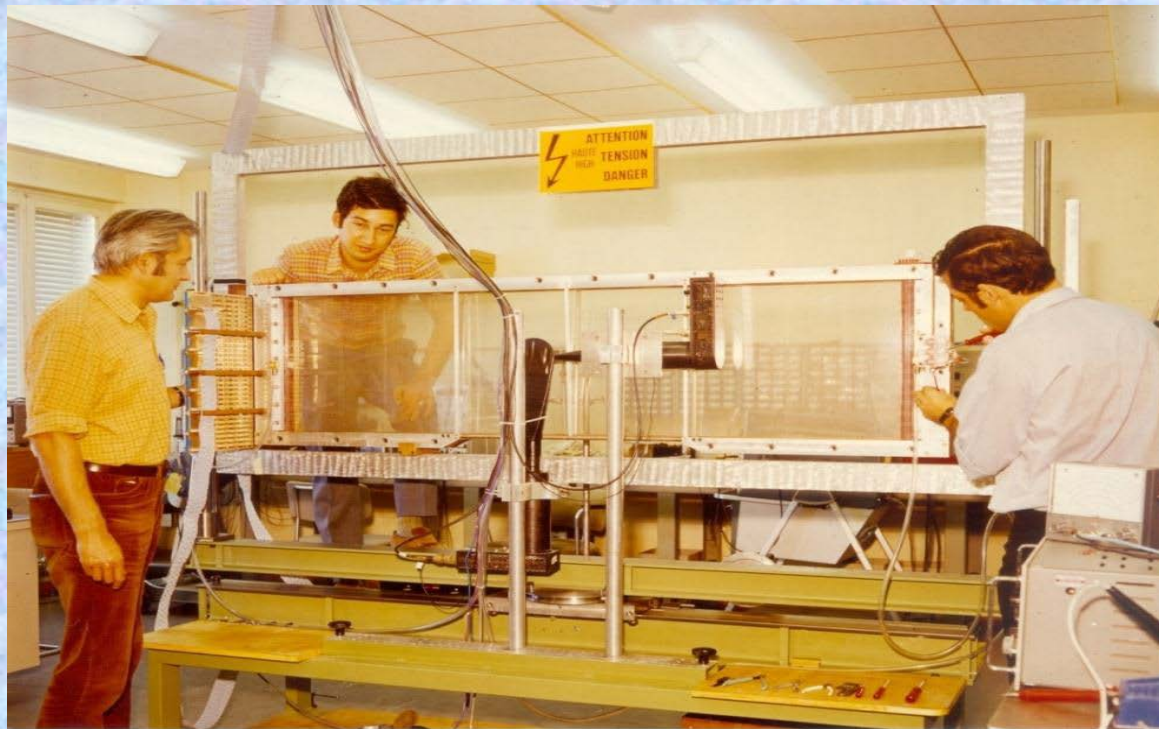


Melvin Schwartz in front of the spark chamber used to discover the muon neutrino



Single muon event from original publication

Multi-Wire Proportional Chamber (MWPC): Electronics Imaging Device



The 1st "Large Wire Chamber":

Georges Charpak with Fabio Sauli, Jean Claude Santiard

The invention revolutionized particle detection and High Energy Physics, which passed from the manual to the electronic era.



MWPC:

1968 by Georges Charpak;
Noble Prize 1992

Tracking Detectors: History and Trends

● Cloud Chambers, Nuclear Emulsions + Geiger-Müller tubes

→ dominated until the early 1950s: Cloud Chambers now very popular in public exhibitions related to particle physics

● Bubble Chambers had their peak time between 1960 and 1985

→ last big bubble chamber was BEBC at CERN

● Since 1970s: Wire Chambers (MWPCs and drift chambers) started to dominate

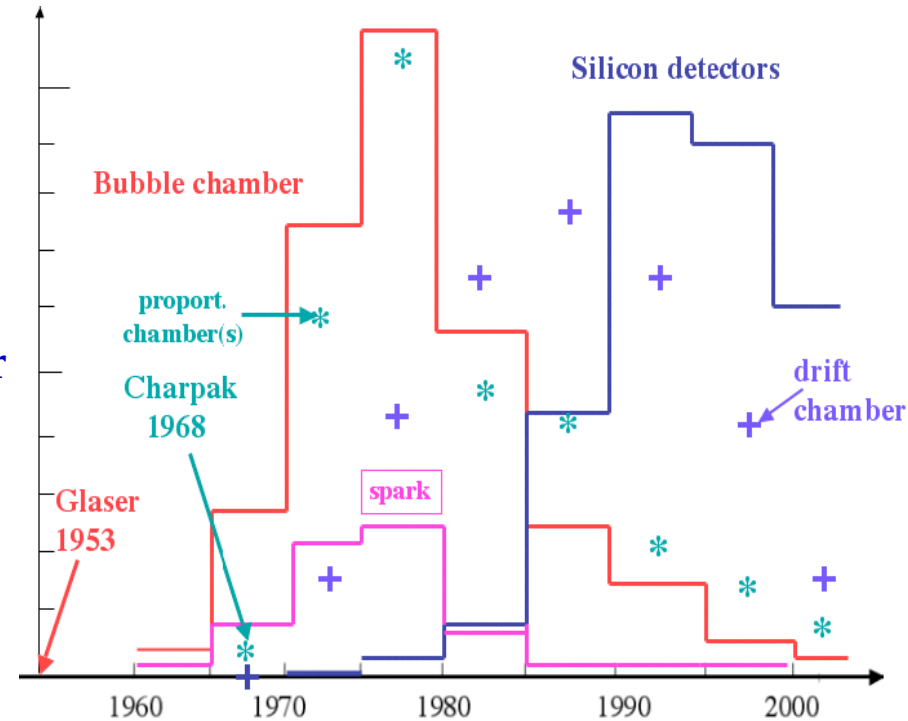
● Since late 1980s: Solid state detectors are in common use

→ started as small sized vertex detectors (at LEP and SLC)

→ now ~200 m² Si-surface in CMS tracker

● Most recent trend: hybrid detectors

→ combining both gaseous and solid state technologies



Tracking

Momentum measurement

Multiple scattering

Bethe-Bloch formula
/ Landau tails

Ionization of gases

Wire chambers

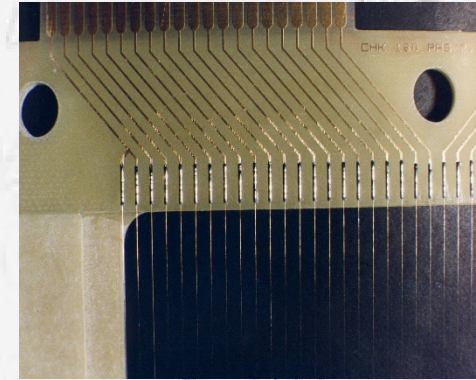
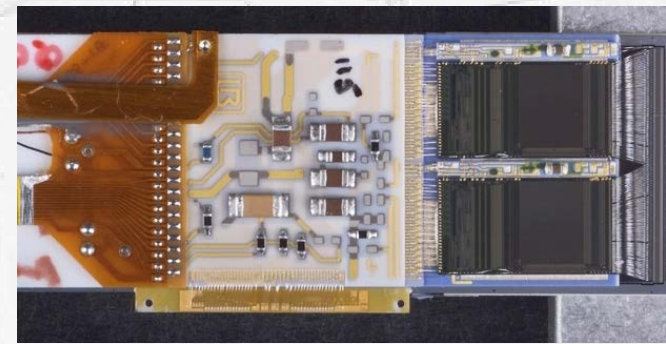
Drift and diffusion in gases

Drift chambers

Micro gas detectors

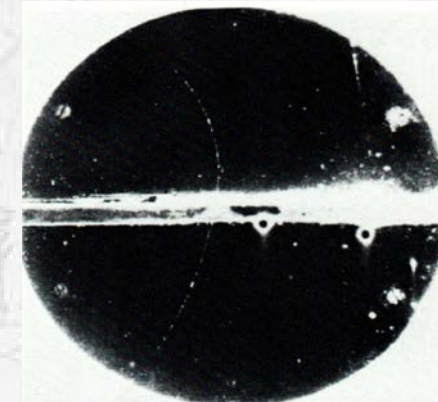
Silicon as a detection medium

Silicon detectors strips/pixels



Tracking Detectors

- “Classic” Detectors (historical touch...)
- Momentum Measurements
- Gaseous Chambers
- Silicon Detectors



Detector Systems: Perfect Detector

...should reconstruct any interaction of any type with 100% efficiency and unlimited resolution (get “4-momenta” of basic physics interaction)

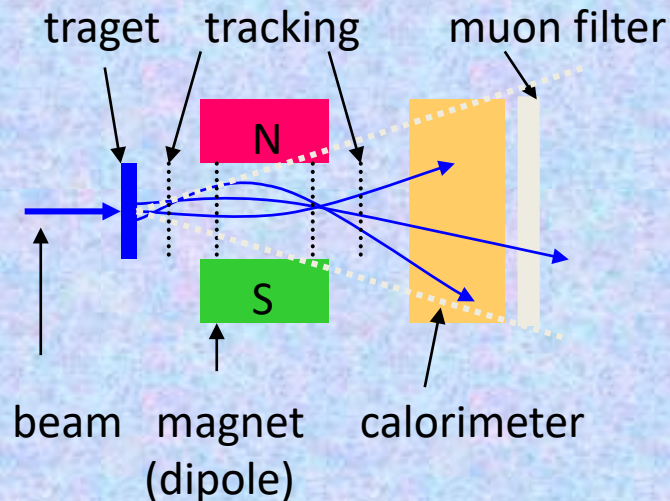
efficiency:

not all particles are detected, some leave the detector without any trace (neutrinos), some escape through not sensitive detector areas (holes, cracks for e.g. water cooling and gas pipes, cables, electronics, mechanics)

Geometrical concepts

Fixed target geometry

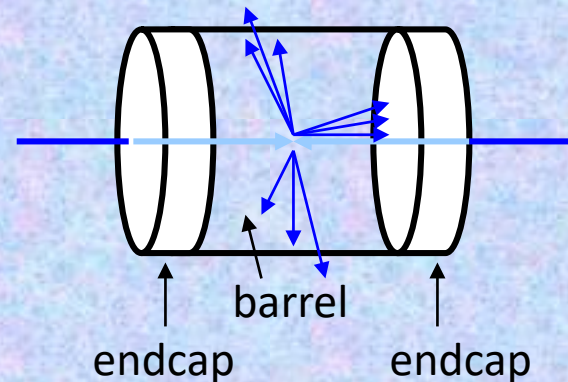
“Magnet spectrometer”



Limited solid angle $d\Omega$ coverage
rel. easy access (cables, maintenance)

Collider Geometry

“ 4π multi purpose detector”



“full” $d\Omega$ coverage
very restricted access

Momentum Measurement in a Magnetic Field

● Charged particles are deflected by magnetic fields

→ homogeneous B-field → particle follows a circle with radius r

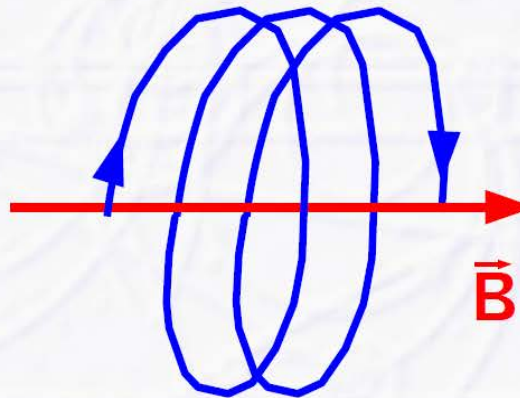
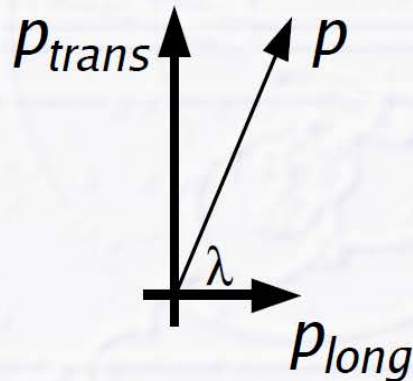
$$p_t [GeV/c] = 0.3 \cdot B [T] \cdot r [m]$$

measurement of p_t via measuring the radius

→ this is just the momentum component \perp to the B-field
transverse momentum p_t

→ no particle deflection parallel to magnetic field

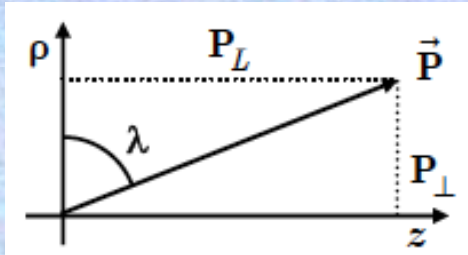
→ if particle has **longitudinal momentum** component
→ particle follows a **helix**



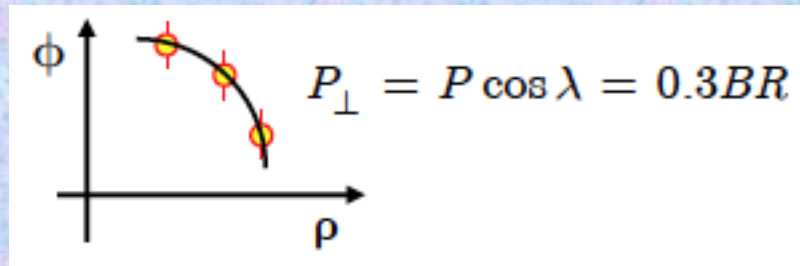
total momentum p to be measured via dip angle λ

$$p = \frac{p_t}{\sin \lambda}$$

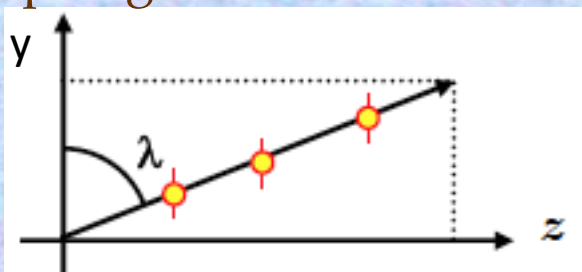
Momentum of particle is decomposed in transverse and longitudinal components



(ρ, ϕ) plane is used to determine the transverse momentum p_t



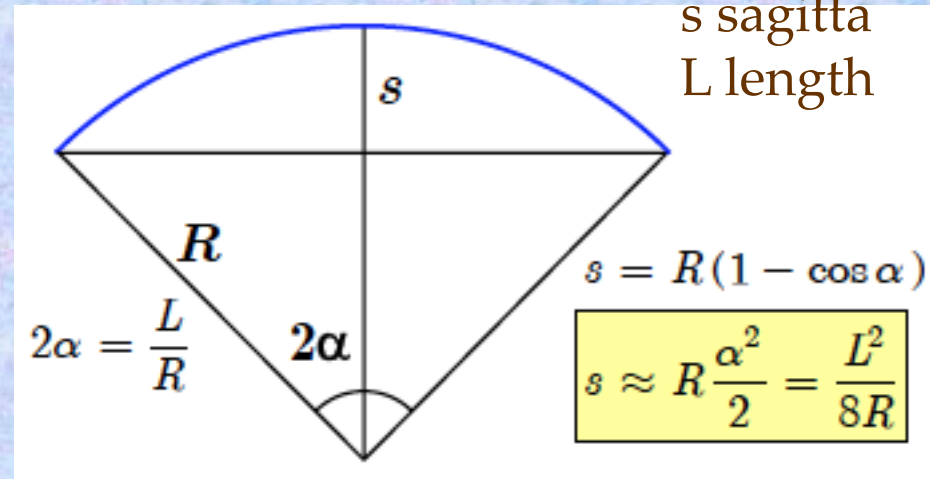
(ρ, z) plane is used to extract dip angle



Let's give some order of magnitude

$$P_{\perp} = 1 \text{ GeV} \quad B = 2 \text{ T} \quad R = 1.67 \text{ m}$$

$$P_{\perp} = 10 \text{ GeV} \quad B = 2 \text{ T} \quad R = 16.7 \text{ m}$$



For a track length of 1m :

$$P_{\perp} = 1 \text{ GeV} \quad s = 7.4 \text{ cm}$$

$$P_{\perp} = 10 \text{ GeV} \quad s = 0.74 \text{ cm}$$

Intermezzo: an interesting formula of classical electrodynamics

From G. Calderini

$$X = 0.5 E(\text{MJ})^{0.66}$$

E is the stored energy : $E = B^2V/2\mu_0$

where V is the volume : $V \sim \pi R^2d$

So what is X ?????? In which units ??????

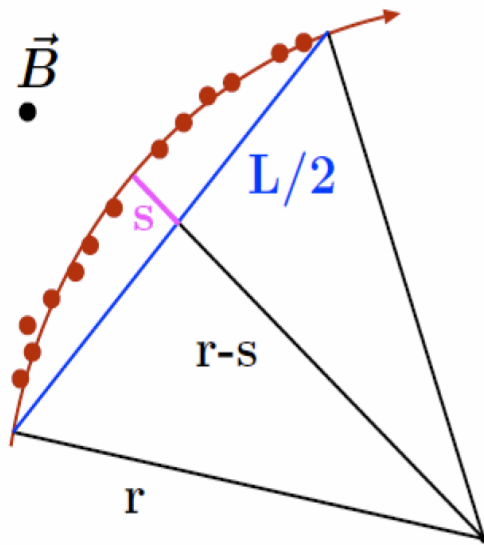
Answer: (believe it or not !)

X is the cost of the solenoid in M\$

Unfortunately solenoids with large B and large L are very expensive
The cost depends on the stored energy

As a cross-check, the CMS solenoid stores 2.6×10^9 J and costed about 100M\$ (source: G. Tonelli)

Momentum Measurement in a Magnetic Field



- In real applications usually only slightly bent track segments are measured
- Figure of merit: Sagitta

Segment of a circle: $s = r - \sqrt{r^2 - \frac{L^2}{4}}$

$$\Rightarrow r = \frac{s}{2} + \frac{L^2}{8s} \approx \frac{L^2}{8s} \quad (s \ll L)$$

With the radius-momentum-B-field relation: $r = \frac{p_T}{0.3 B} \Rightarrow s = \frac{0.3 B L^2}{8 p_T}$

In general, for many measurement points:

$$\frac{\sigma(p_T)}{p_T} = \frac{\sigma(x)}{0.3 B L^2} \sqrt{720/(N+4)} p_T$$

► Je larger the magnetic field B, the length L and the number of measurement points, and the better the spacial resolution, the better is the momentum resolution

ex.: $N = 7$, $L = 0.5$, $B = 2\text{T}$, $\sigma(x) = 20 \mu\text{m}$, $p_t = 5 \text{ GeV}/c$

$\Delta p_t / p_t = 0.5 \%$, $r = 8.3 \text{ m}$, $s = 3.75 \text{ mm}$

Today's Tracking Detectors and Technologies

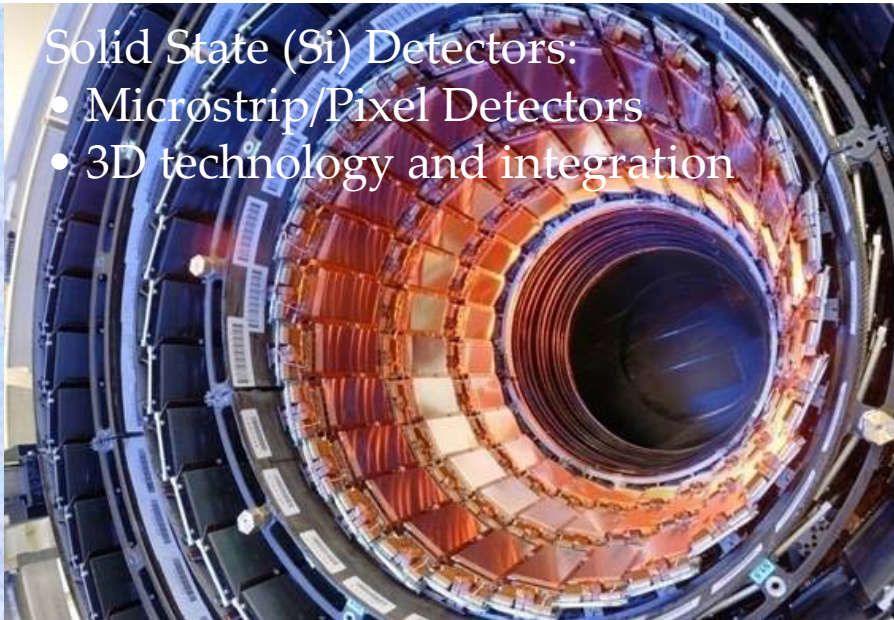
Gaseous Detectors:

- Wire Chambers, RPC, TPC
- Micro-Pattern Gas Detectors



Solid State (Si) Detectors:

- Microstrip/Pixel Detectors
- 3D technology and integration



3 major technologies of tracking detectors

❖ Gaseous detectors

→ ionization in gas

typically ~ 100 e-/cm, not sufficient to create significant signal height above noise for standard amplifiers

→ requires gas amplification $\sim 10^4$ to get enough signal over noise

❖ Silicon detectors

→ electron – hole pairs in solid state material

typically ~ 100 e- - hole pairs/ μm

300 μm thick detector creates high enough signal w/o gas amplification

❖ Fiber trackers

→ scintillating fibers

scintillation light detected with photon detectors (sensitive to single electrons)

Tracking

Momentum measurement

Multiple scattering

Bethe-Bloch formula
/ Landau tails

Ionization of gases

Wire chambers

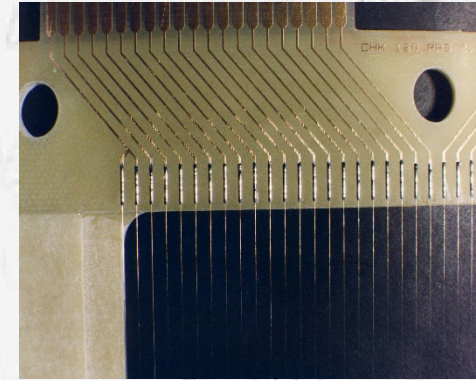
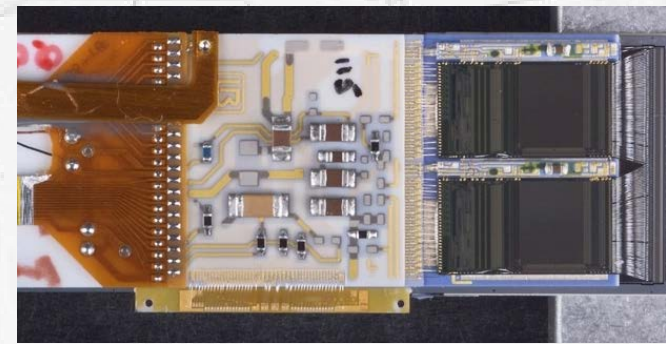
Drift and diffusion in gases

Drift chambers

Micro gas detectors

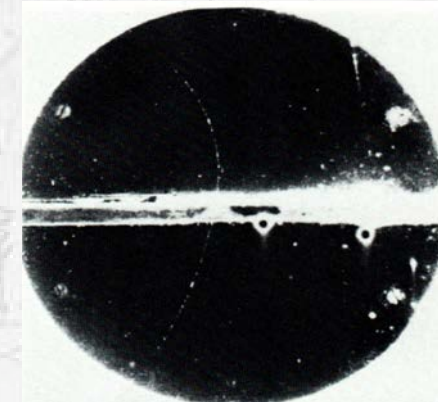
Silicon as a detection medium

Silicon detectors strips/pixels



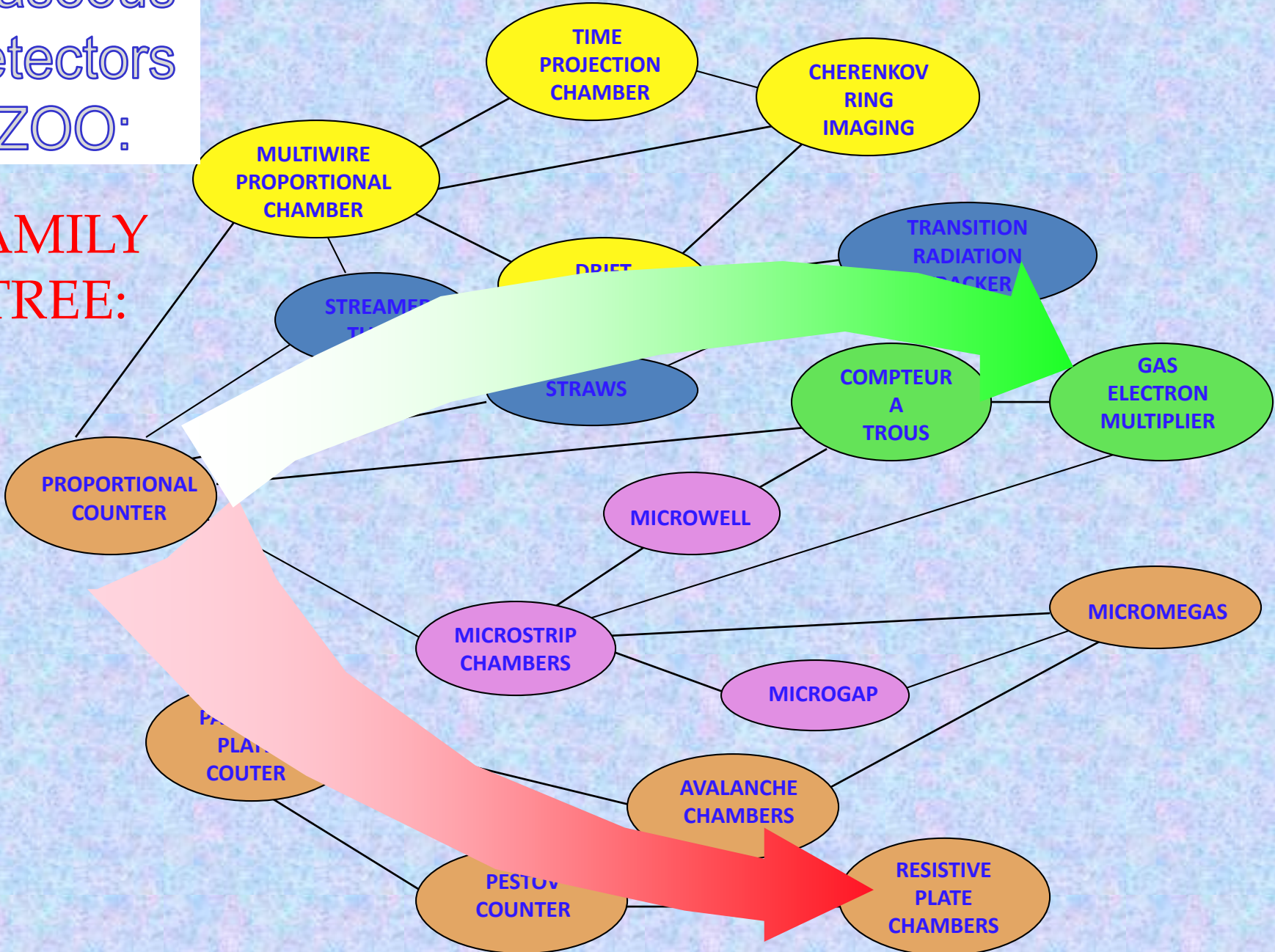
Tracking Detectors

- “Classic” Detectors (historical touch...)
- Momentum Measurements
- Gaseous Chambers
- Silicon Detectors



Gaseous Detectors ZOO:

FAMILY TREE:



Gas Detector History



Geiger Counter
H.Geiger/W.Mueller 1928

PPC
Parallel Plate Counter

PC
Proportional Counter

Pestov Counter
V.Pestov 1982

RPC
Resistive Plate Chambers
R.Santonico R.Cardarelli 1981



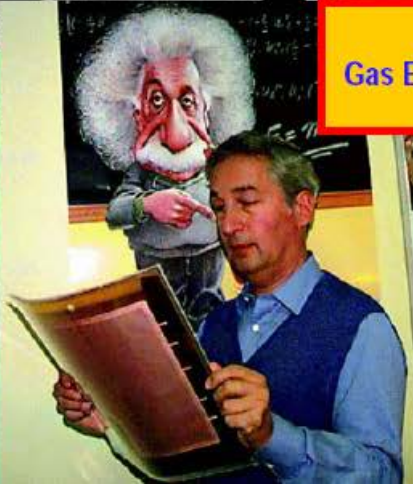
MWPC
Multiwire Proportional Chamber
G.Charpak et al 1968

TPC
Time Projection Chamber
D.R.Nygren et al 1974



MSGC
Microstrip Gas Chambers
A.Oed 1988

GEM
Gas Electron Multiplier
F.Sauli 1997



μ M
Micromegas
I.Giomataris et al 1996

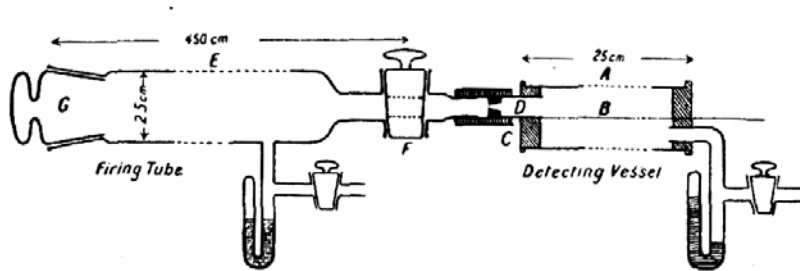


M. Hoch, 2004 Wire Chamber Conference

In the Family of Gaseous Detectors with a glorious tradition

1st Revolution: The invention of the MWPC revolutionized particle detection and HEP, which passed from the manual (optical) to the electronic era.

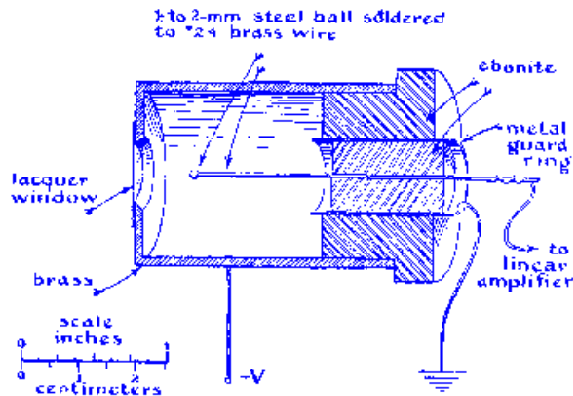
1908: FIRST WIRE COUNTER USED BY RUTHERFORD IN THE STUDY OF NATURAL RADIOACTIVITY



E. Rutherford and H. Geiger,
Proc. Royal Soc. A81 (1908) 141

Nobel Prize in Chemistry in 1908

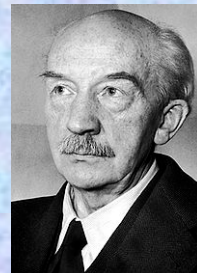
1928: GEIGER COUNTER SINGLE ELECTRON SENSITIVITY



H. Geiger and W. Müller,
Phys. Zeits. 29 (1928) 839

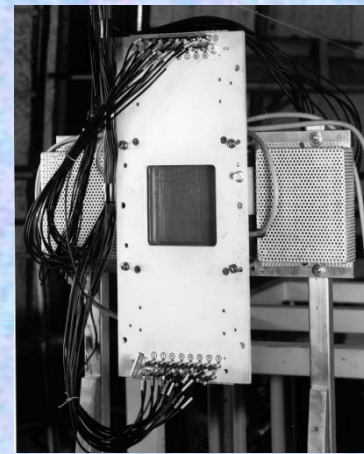


Hans Geiger



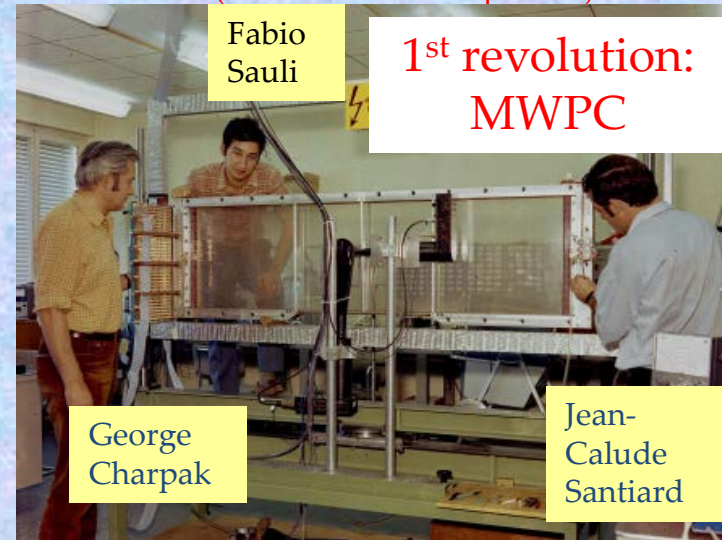
Walther Bothe
Nobel Prize in
1954 for the
"coincidence
method"

1968: MULTIWIRE PROPORTIONAL CHAMBER



Nobel Prize in 1992

G. Charpak, Proc. Int. Symp. Nuclear Electronics (Versailles 10-13 Sept 1968)



Fabio Sauli

**1st revolution:
MWPC**

George Charpak

Jean-Claude Santiard

Gaseous Detectors: Why do we use gas medium ?

Three states of matter:

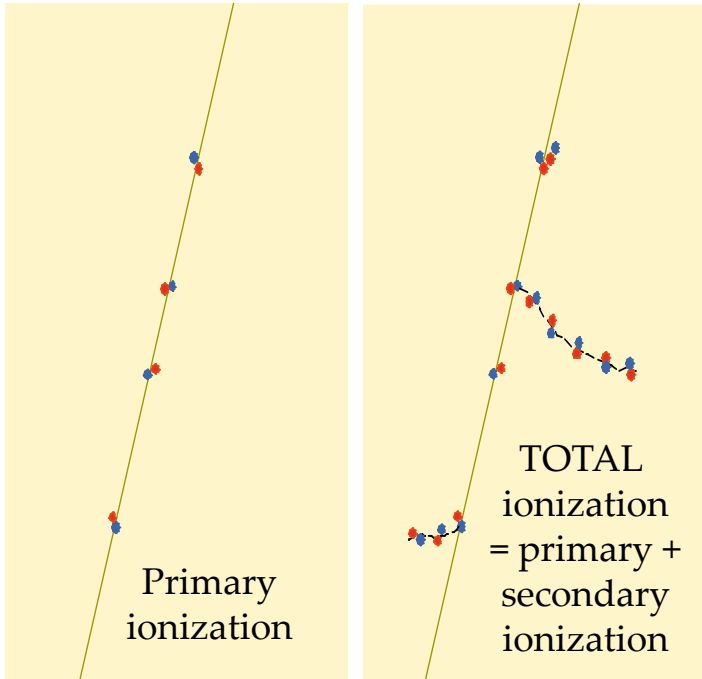
Solid, Liquid, Gas – why use Gas as a medium for ionization ?

- ⊙ Effectively quite light in terms of gm/cm^2 , requirement for reducing multiple scattering in particle physics
- ⊙ Few other technologies can easily realize detectors with as large a sensitive area as gas-filled devices
- ⊙ Gas-filled detectors are relatively cheap in terms of \$ per unit area/volume
- ⊙ There are optimized gas mixtures for **charged particles detection** (high energy and nuclear physics), **X-rays** (synchrotron physics, astronomy) **and neutrons** (neutron scattering, national security)
- ⊙ **Electron transport characteristics** are favorable and well characterized
- ⊙ **Gas gain, M** (electron multiplication factor), can be achieved, over many orders of magnitude (**large dynamic range**)
- ⊙ **Ionization collection or fluorescence** emission can form the signal

Gaseous Detectors: Ionization Statistics

TOTAL IONIZATION:

- **Primary electron-ion pairs**
 - Coulomb interactions of charged particles with molecules
 - typically ~ 30 primary ionization clusters /cm in gas at 1 bar
- **Secondary ionization: clusters and delta-electrons** → on average 90 electrons/cm in gas at 1 bar



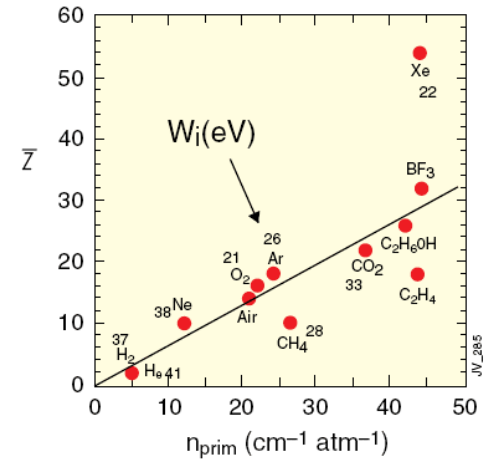
The actual number of **primary electron/ion pairs** (n_p) is **Poisson** distributed:

$$P(n_p, \langle n_p \rangle) = \frac{\langle n_p \rangle^{n_p} e^{-\langle n_p \rangle}}{n_p!}$$

σ_I : Ionization x-Section
 n_e : Electron density
 L : Thickness

$$\langle n_p \rangle = L/\lambda \quad \lambda = 1/(n_e \sigma_I)$$

Number of primary electron/ion pairs in frequently used gases:



Detection efficiency of a perfect detector is limited to:

→ for thin (L) layers ϵ can be significantly lower than 1

$$\epsilon = 1 - e^{-n_p}$$

$$\langle n_p \rangle = L/\lambda$$

GAS (STP)	thickness	ϵ (%)
Helium	1 mm	45
	2 mm	70
Argon	1 mm	91.8
	2 mm	99.3

Ionization Statistics: Table for most common gases

Properties of noble and molecular gases at normal temperature and pressure (NTP: 20° C, one atm). E_x , E_I : first excitation, ionization energy; W_I : average energy per ion pair; $dE/dx|_{\min}$, N_P , N_T : differential energy loss, primary and total number of electron-ion pairs per cm, for unit-charge minimum-ionizing particles. Values often differ, depending on the source, and those in the table should be taken only as approximate (Sauli and Titov 2010)

Gas	Density (mg cm ⁻³)	E_x (eV)	E_I (eV)	W_I (eV)	$dE/dx _{\min}$ (keV cm ⁻¹)	N_P (cm ⁻¹)	N_T (cm ⁻¹)
He	0.179	19.8	24.6	41.3	0.32	3.5	8
Ne	0.839	16.7	21.6	37	1.45	13	40
Ar	1.66	11.6	15.7	26	2.53	25	97
Xe	5.495	8.4	12.1	22	6.87	41	312
CH ₄	0.667	8.8	12.6	30	1.61	28	54
C ₂ H ₆	1.26	8.2	11.5	26	2.91	48	112
iC ₄ H ₁₀	2.49	6.5	10.6	26	5.67	90	220
CO ₂	1.84	7.0	13.8	34	3.35	35	100
CF ₄	3.78	10.0	16.0	54	6.38	63	120

Total ionization (N_T) ~ 3 times primary ionization (N_P)

$N_T \sim 100$ e-ion pairs during ionization process (typical number for 1 cm of gas) is not easy to detect \rightarrow typical noise of modern pixel ASICs is $\sim 100e^-$ (ENC)

Need to increase number of e-ion pairs \rightarrow ... ☹ ... how ??? – GAS AMPLIFICATION

Ionization Loss Distribution (brief reminder)

- **Number of interactions (ionizations) per unit length is Poisson-distributed** (typically 20-30 interactions/cm at 1 bar)
- **Number of created electrons per unit length is NOT**
 - most of the time: one single electron per interaction is created, this is the ideal case!
 - less often but more severe: more than one electron is created, can be a few, 10s, 100s, 1000s...
 - **LARGE** fluctuations in number of created electrons!
- **Usually, all detectors measure CHARGE deposited by a track (charge ~ number of electrons)**
 - sensitive to **LARGE** fluctuations -> makes dE/dx resolution bad
- **This is the fundamental, central problem of all dE/dx measurements**

Ionization Loss Distribution (brief reminder)

Cluster size fluctuations cause large variations of energy loss from track to track

→ Typical detector measures energy loss many times along track (samples)

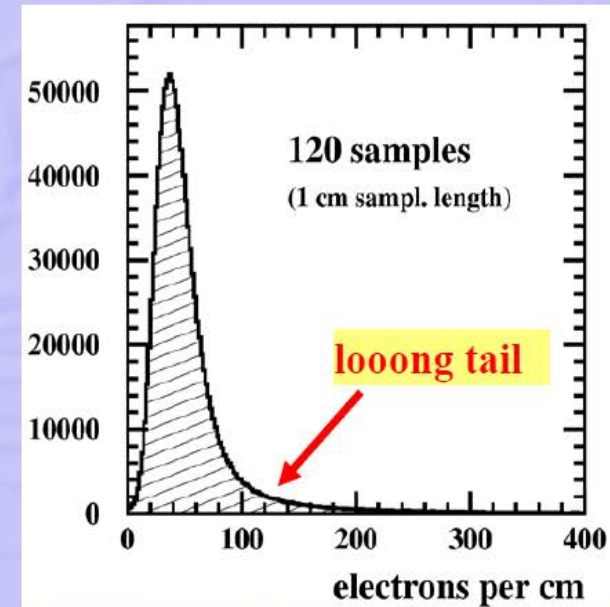
→ Landau distribution

- large broad peak (single or few el. clusters)

- soft collisions, interaction with whole gas molecule
- small energy transfer

- loong tail (multi el. clusters, δ -electrons)

- hard collisions, semi-free shell electrons, large energy transfer



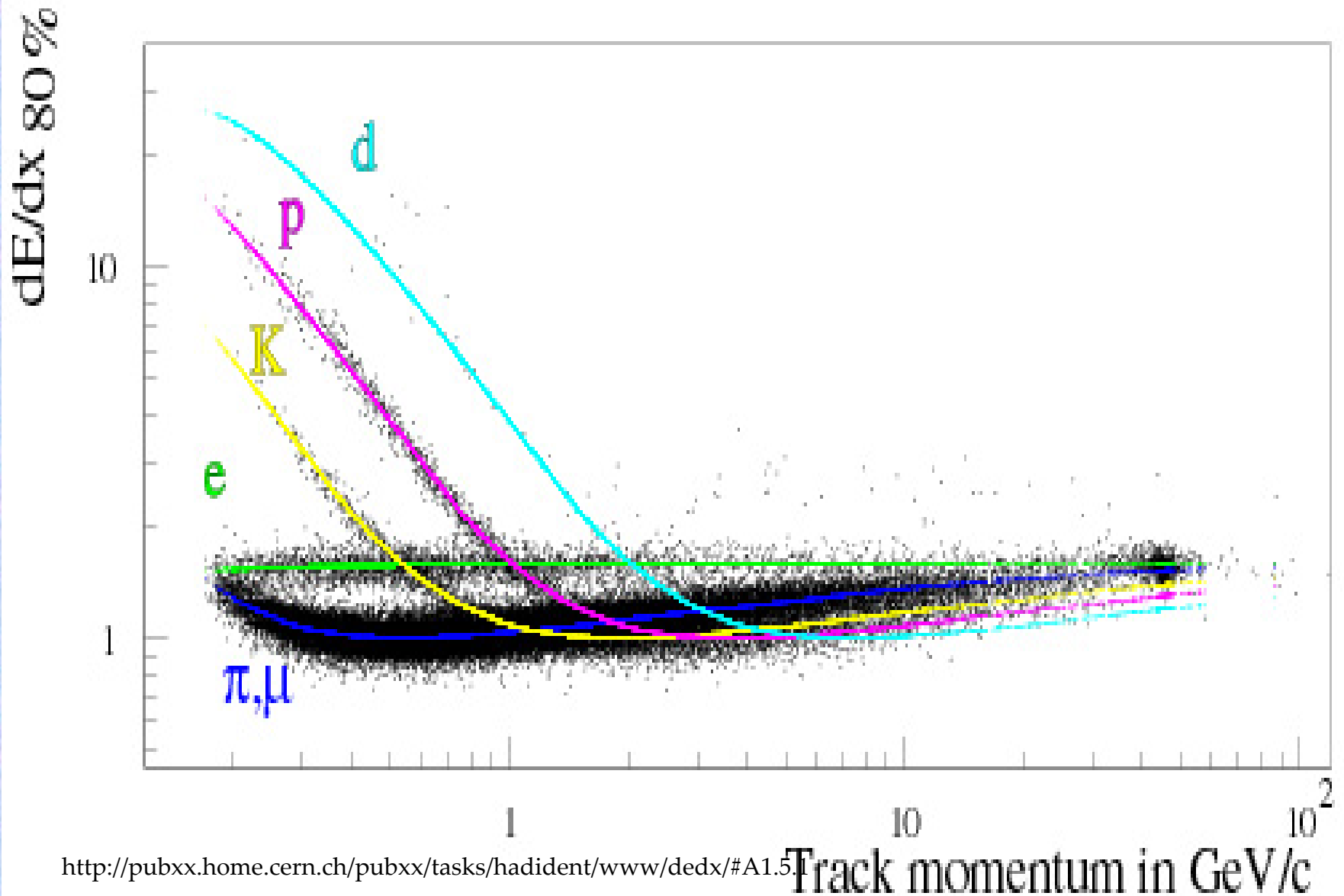
How to get best estimate of “mean” energy loss?

→ Most commonly used: “Truncated Mean” (robust)

→ Other methods:

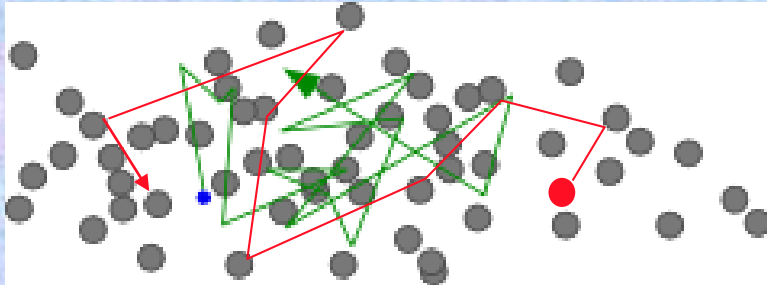
- Max.-Likelihood fit (but more sensitive to changes of Landau shape)
- Inverse transformation: mean of $(1/\sqrt{(dE/dx)_i})^{-1}$

dE/dx Measurement from DELPHI TPC



Transport of Electrons and Ions in Gases

ELECTRIC FIELD $E = 0$: THERMAL DIFFUSION



Maxwell energy distribution:

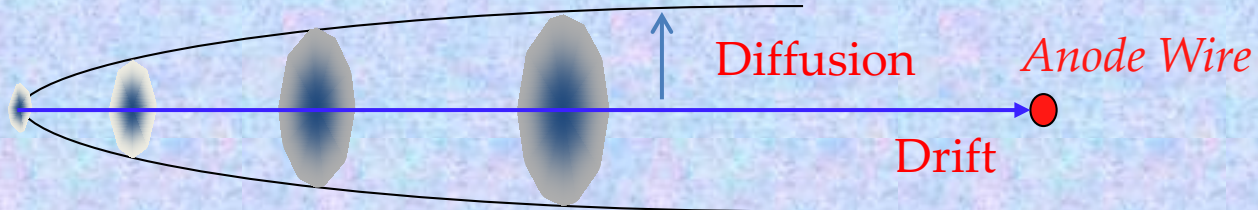
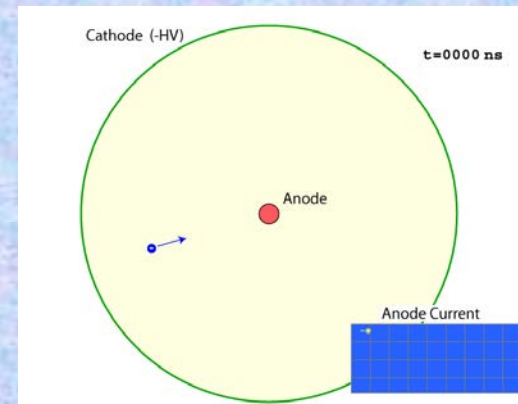
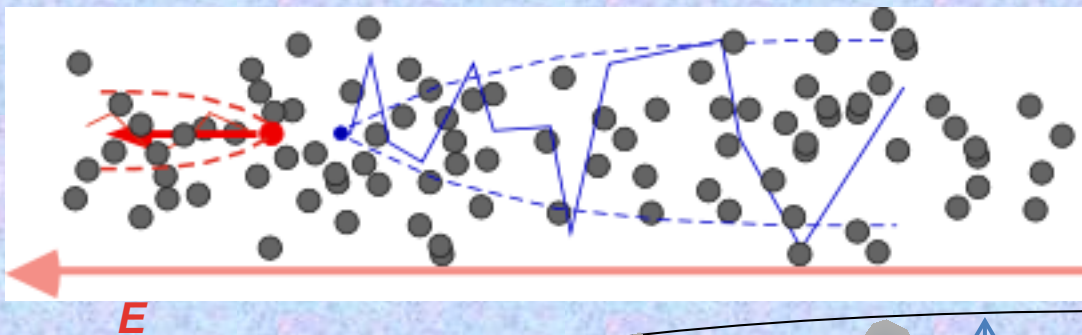
$$F(\varepsilon) = C\sqrt{\varepsilon} e^{-\frac{\varepsilon}{KT}}; \quad \langle \varepsilon \rangle \sim kT \sim 0.025 \text{ eV}$$

RMS of charge diffusion: $\sigma_x = \sqrt{2Dt}$

ELECTRIC FIELD $E > 0$: CHARGE TRANSPORT AND DIFFUSION

IONS

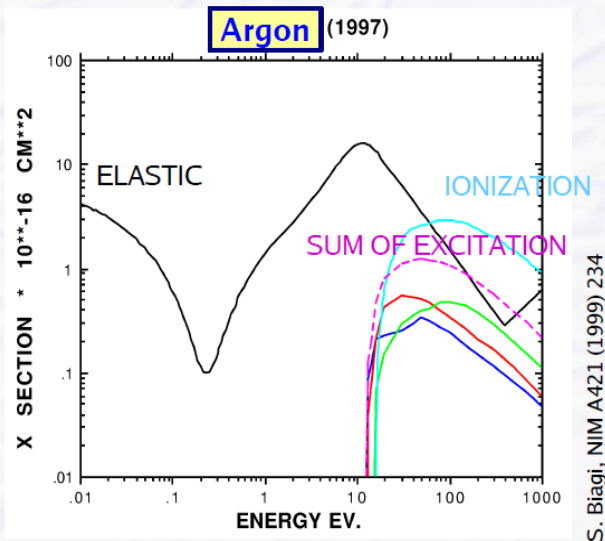
ELECTRONS



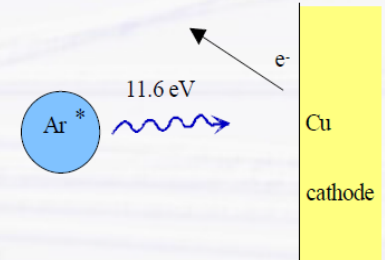
Selection of Gas Mixture: Quenching

Slight problem in gas avalanche

- Argon atoms can be ionized but also can be brought into excited states
- Excited Argon atoms can only de-excite by emission of high-UV photons



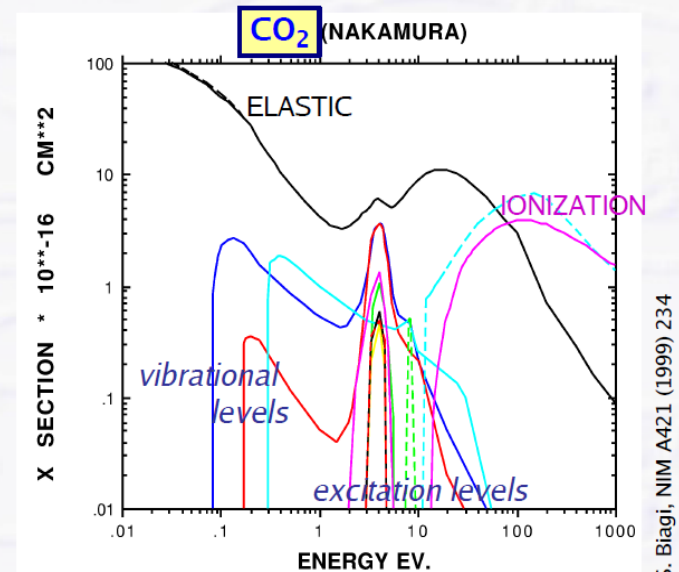
consequence: UV photons (>11.6 eV) hit surface of metals (cathode) and free new electrons, ionization energy of Cu = 7.7 eV



VERY unstable operation

Solution

- Add gases with many vibrational and rotational energy levels: CO₂, CH₄
- Absorption of UV photons over a wide energy range; dissipation by collisions



Selection of Gas Mixture: Drift Velocity

Large range of drift velocities in gases: 1 ... 10 cm/ μ s

Large drift velocities are obtained by adding polyatomic gas (CH_4 , CO_2 , CF_4) to Ar \rightarrow electrons cool due to energy transfer to rotational/ vibrational modes of the polyatomic gas

Typical categories

\rightarrow “slow” gases, e.g. CO_2 mixtures

- 1-2 cm/ μ s, almost linear dependence on E-field

\rightarrow “fast” gases, e.g. CF_4 mixtures

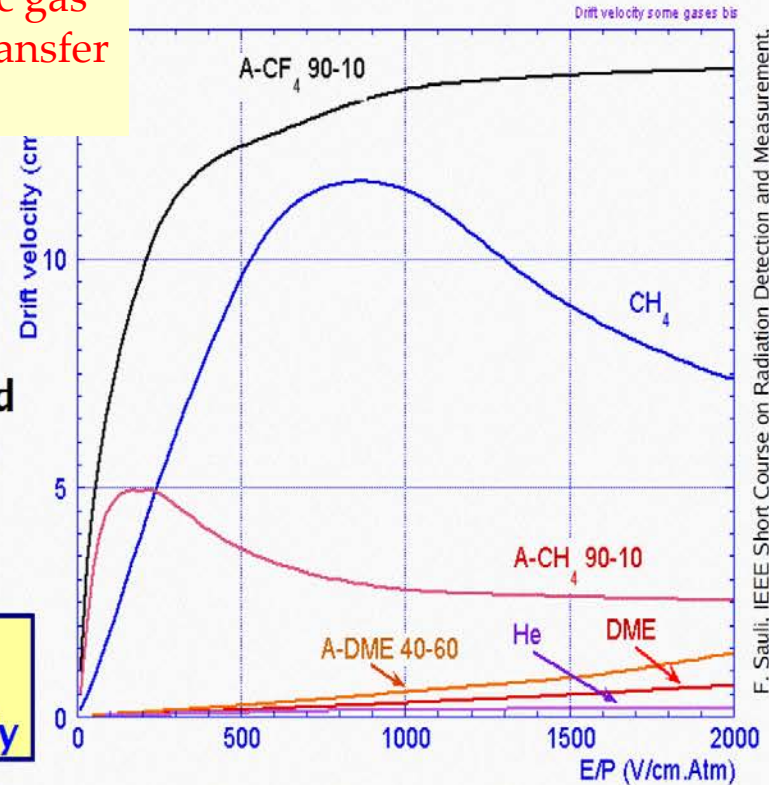
- ~ 10 cm/ μ s or more

LHC detectors need fast gases = short drift time to collect all electrons until next bunch crossing (25 ns) or at least within a few bunch crossings only

\rightarrow “saturated” gases, e.g. CH_4 mixtures

- have maximum of drift velocity at certain E-field
- widely used: Ar/ CH_4 (90/10)

gases with drift velocity maximum are rather convenient: drift velocity less sensitive to E-field variations and almost constant

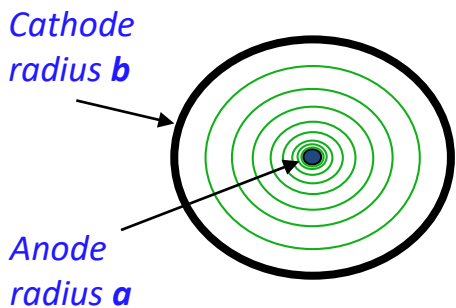


variety of gases allows multiple combinations: lots of *black magic!*

Single (Multi) Wire Proportional Counter

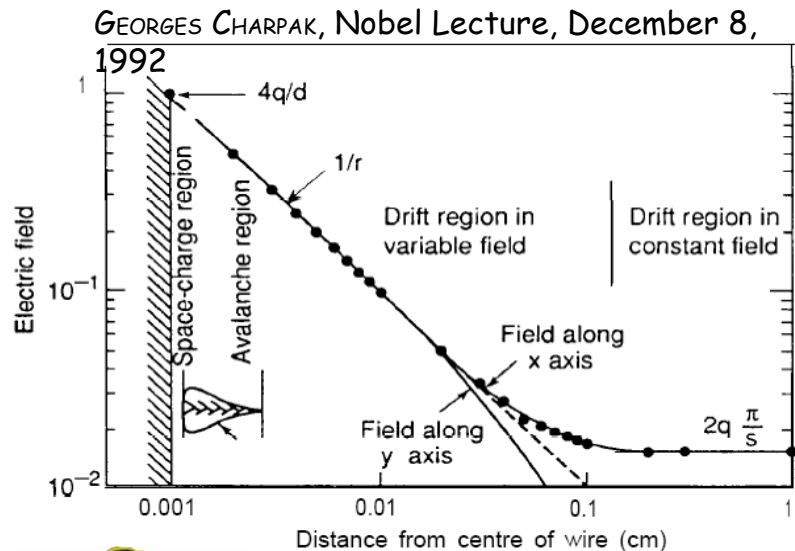
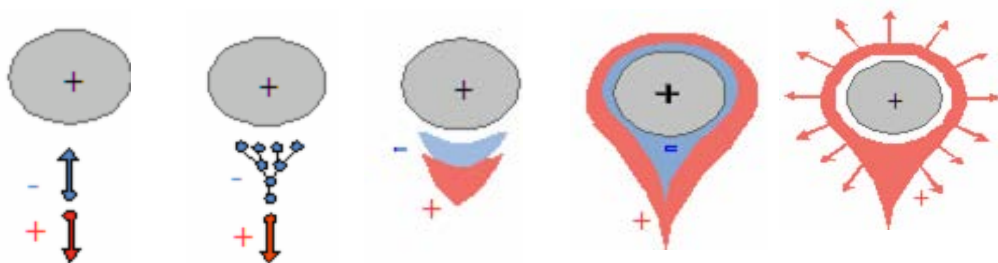
Thin anode wire (~20–50μm) coaxial with cathode:

Avalanche development in the high electric field (~ 250 kV/cm) around a thin wire (multiplication region ~ 100 μm):

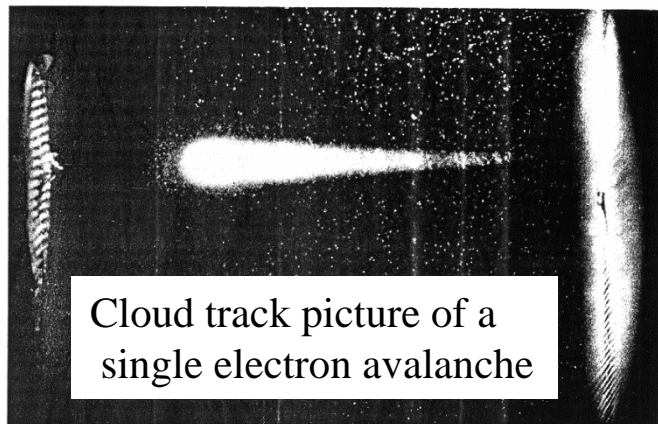
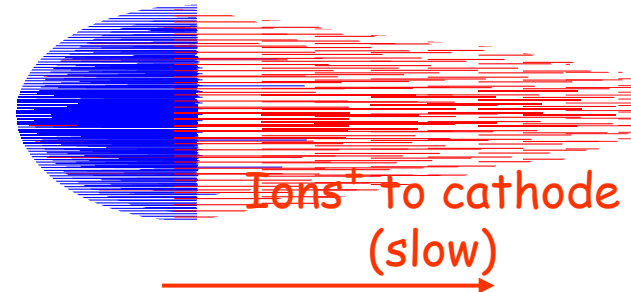


$$E(r) = \frac{CV_0}{2\pi\epsilon_0} \frac{1}{r}$$

Different stages in the gas amplification process next to the anode wire.



Electrons to anode
(fast)



Cloud track picture of a single electron avalanche

CLOUD TRACK PICTURE OF A SINGLE ELECTRON AVALANCHE (photograph H. Raether)

Operation Modes of Gaseous Detectors

- **Recombination before collection (I)**

- - ions recombine before collected

- **Ionization Mode (II)**

- - full charge ionization charge;
- - no charge multiplication yet; gain ~ 1

- **Proportional Mode (IIIa)**

- - multiplication of ionization
- - signal proportional to ionization
- - measurement of dE/dx
- - secondary avalanches need quenching;
- - gain $\approx 10^4 - 10^5$

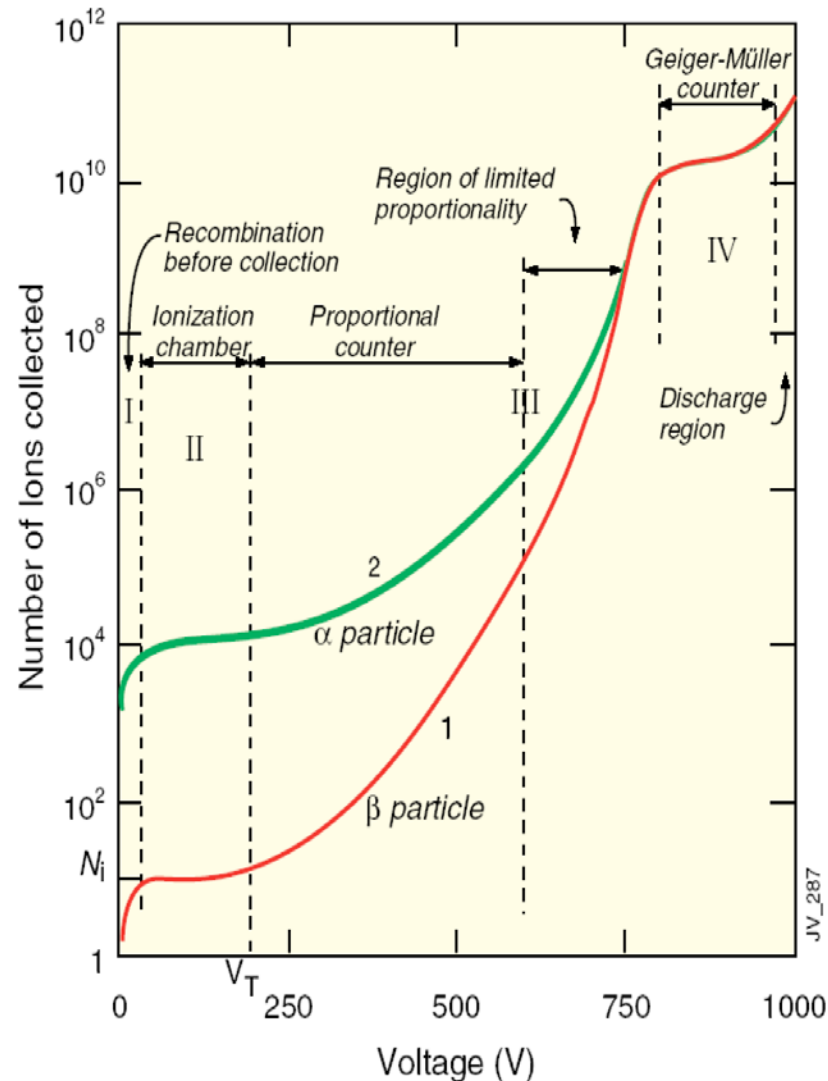
- **Limited Proportional Mode (IIIb) (saturated, streamer)**

- - secondary avalanches created by photoemission from primary ones;
- - signal no longer proportional to ionization \rightarrow requires strong quenchers or pulsed HV; gain $\sim 10^{10}$

- **Geiger Mode (IV)**

- - massive photoemission; full length of the anode wire affected;
- - discharge stopped by HV cut

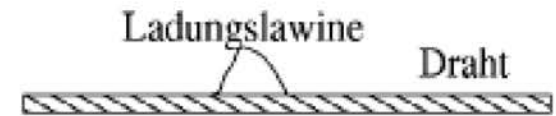
High Voltage



Wire Chamber: Electron Avalanches on the Wire

Proportional region: $A \approx 10^3 - 10^4$

LHC



Semi proportional region: $A \approx 10^4 - 10^5$
(space charge effect)

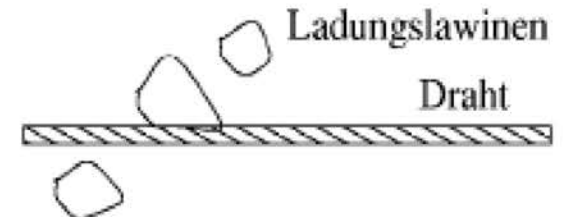


Saturation region: $A > 10^6$
Independent the number of primary electrons.

1970ies



Streamer region: $A > 10^7$
Avalanche along the particle track.

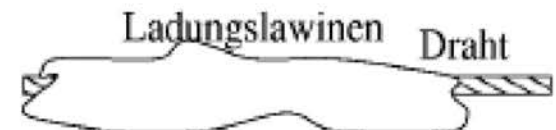


Limited Geiger region:
Avalanche propagated by UV photons.

1950ies

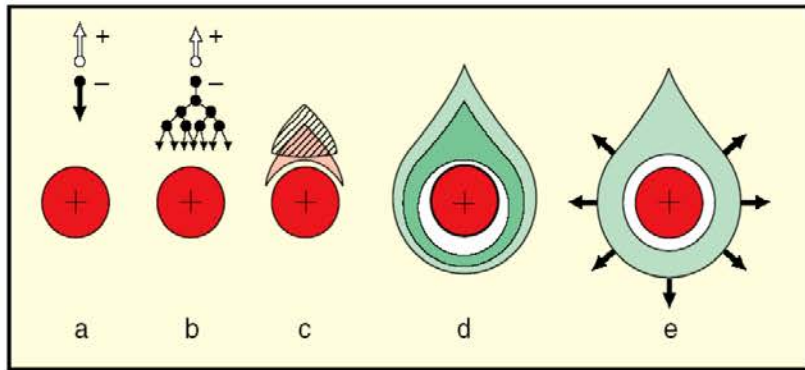


Geiger region: $A \approx 10^9$
Avalanche along the entire wire.



Wire Chamber – Signal Formation

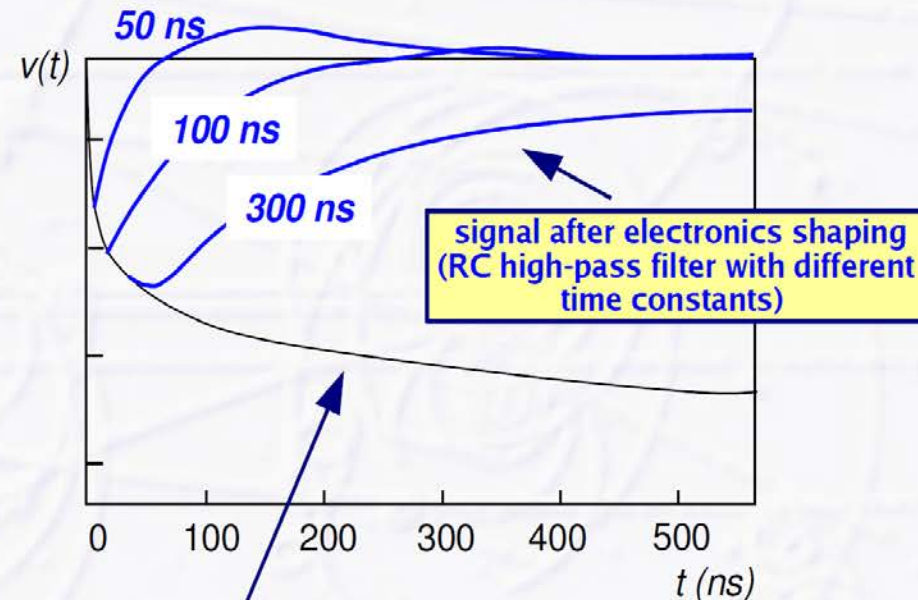
Signal formation is **DIFFERENT** to what you may think of



- Electrons from avalanche are collected within a very short time (few ns)
- Contribution of electrons to wire signal is rather small (few % only)

Main part of the signal comes from the **IONS**

- Ions drift back to cathode over long distance (several mm or cm) and time (many μs or even ms)
- Moving ion charge creates signal via influence (mirror charge in conductor)

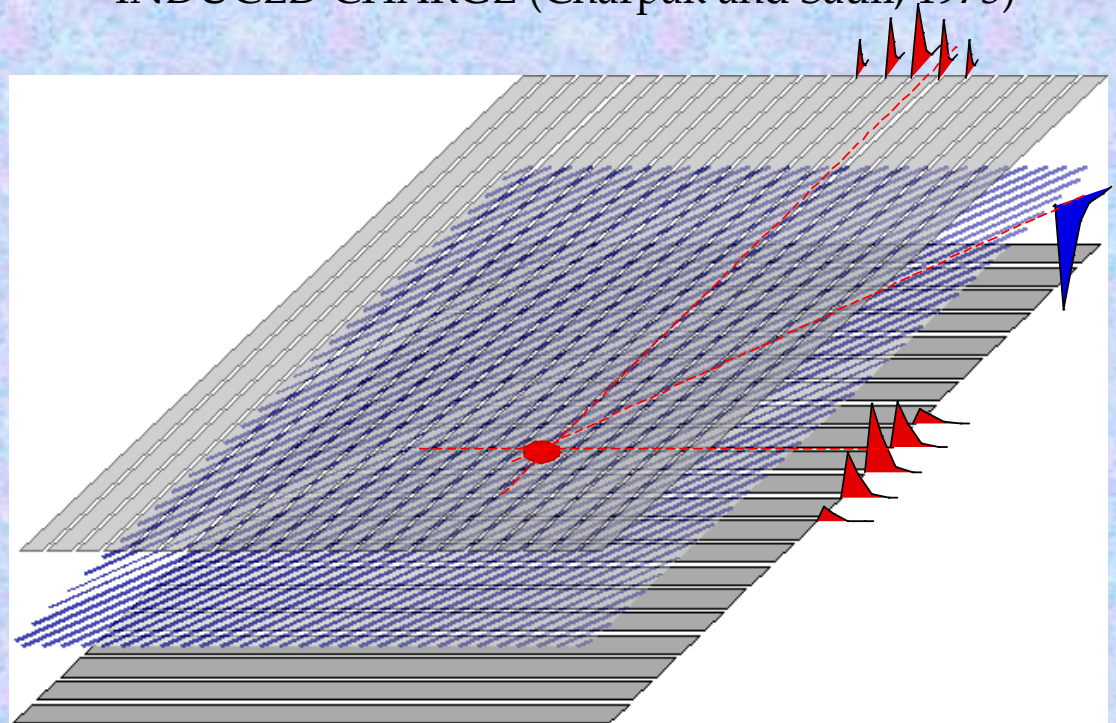
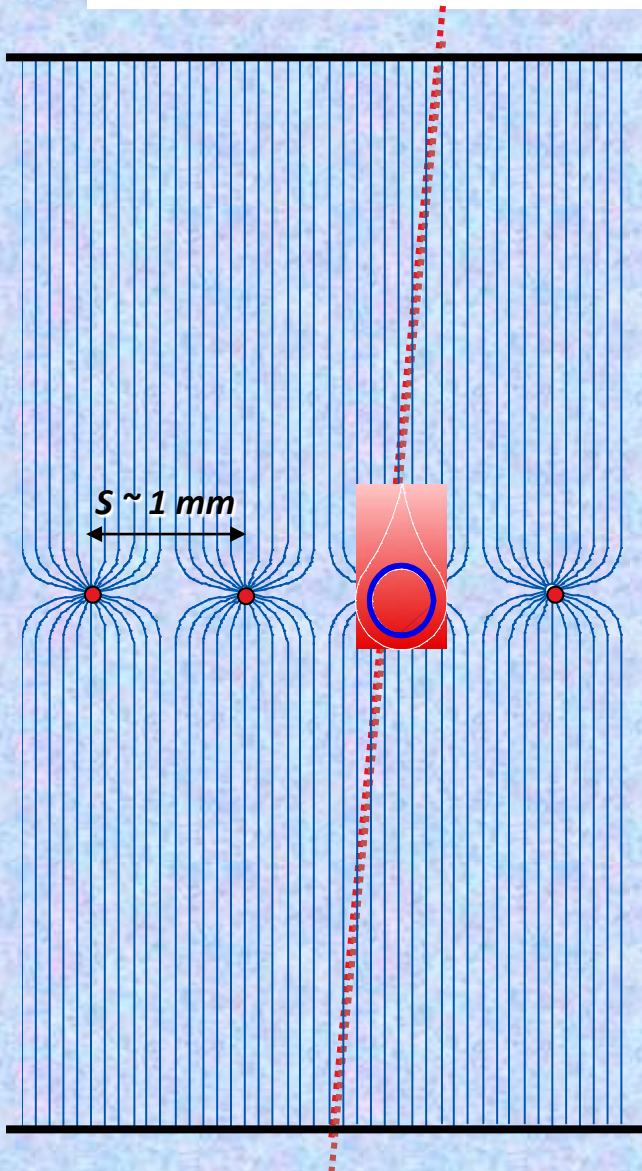


pure signal (no electronics shaping)
from ions drifting away from anode wire

Multi-Wire Proportional Chamber (MWPC)

High-rate MWPC with digital readout:
Spatial resolution is limited to $\sigma_x \sim s/\sqrt{12} \sim 300 \mu\text{m}$

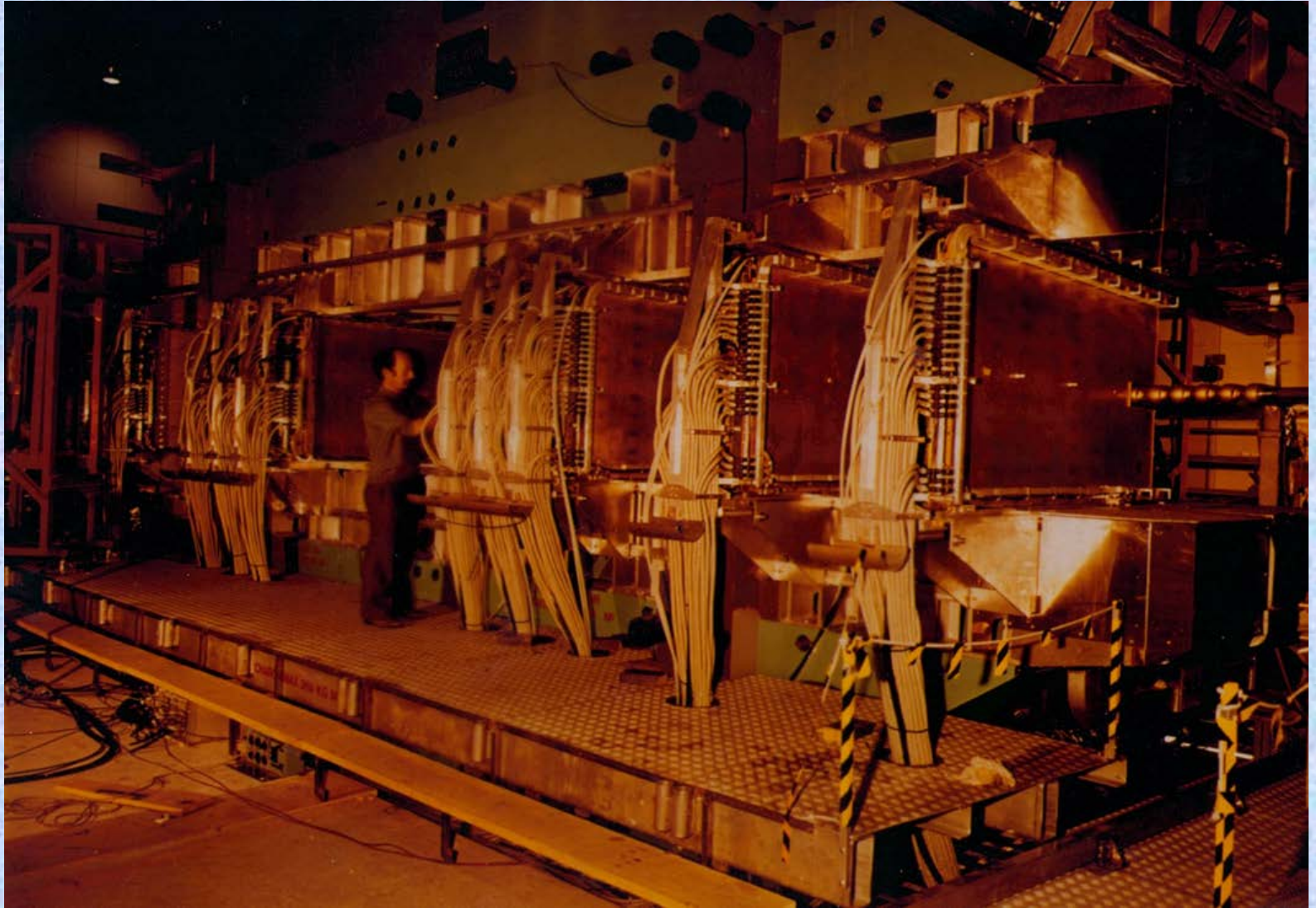
TWO-DIMENSIONAL MWPC READOUT CATHODE
INDUCED CHARGE (Charpak and Sauli, 1973)



Spatial resolution determined by: Signal / Noise Ratio
Typical (i.e. 'very good') values: $S \sim 20000 \text{ e}$; noise $\sim 1000 \text{ e}$
Space resolution $< 100 \mu\text{m}$

Resolution of MWPCs limited by wire spacing
better resolution \rightarrow shorter wire spacing \rightarrow more (and more) wires...

First Large Experiment with MWPCs

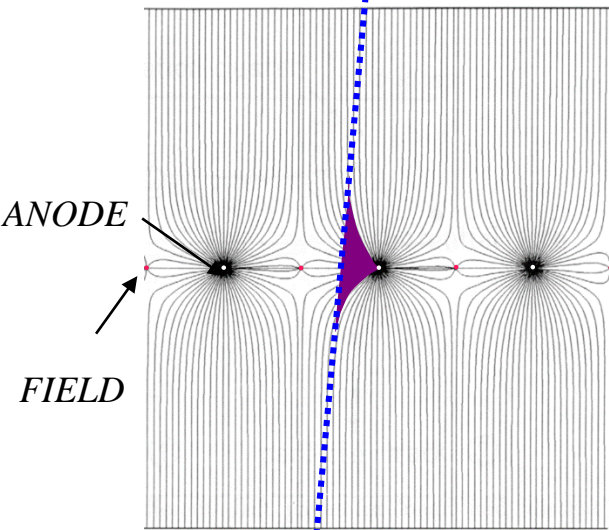


***1972-1983: SPLIT FIELD MAGNET DETECTOR
40 LARGE AREA MWPCs AT CERN ISR:***

Drift Chambers

FIRST DRIFT CHAMBER OPERATION (H. WALENTA ~ 1971)
 HIGH ACCURACY DRIFT CHAMBERS (Charpak-Breskin-Sauli ~ 1973-75)

THE ELECTRONS DRIFT TIME PROVIDES THE DISTANCE OF THE TRACK FROM THE ANODE:



Measure drift time t_D
 [need to know t_0 ; fast scintillator, beam timing]

Determine location of original ionization:

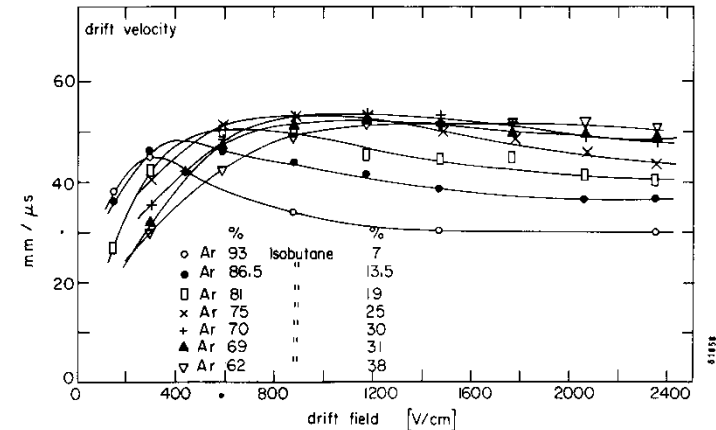
$$x = x_0 \pm v_D \cdot t_D$$

$$y = y_0 \pm v_D \cdot t_D$$

If drift velocity changes along path:

$$x = \int_0^{t_D} v_D dt$$

In any case:
 Need well-defined drift field ...

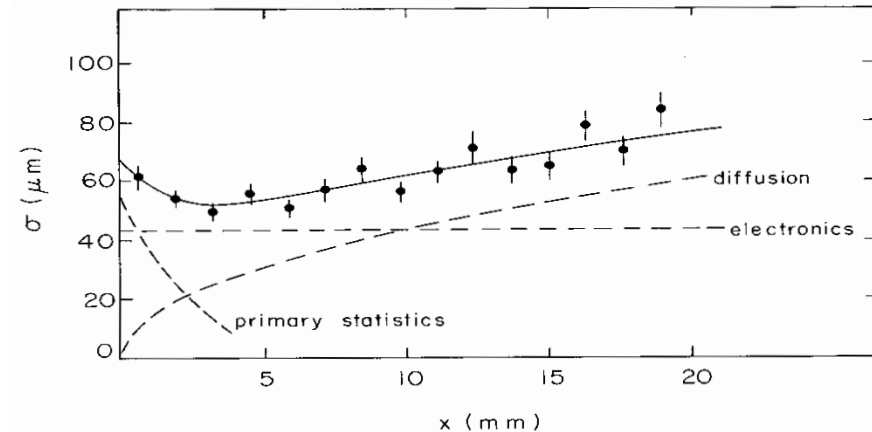


The spatial resolution is not limited to the cell size

$$\sigma_x^2 = \underbrace{\left(\frac{1}{64N^2} \right) \cdot \frac{1}{x^2}}_{1^{\text{st}} \text{ ionization statistics}} + \underbrace{\frac{2D}{v_d} \cdot x}_{\text{diffusion}} + \underbrace{\sigma_{\text{const}}^2}_{\text{electronics } \delta\text{-electrons}}$$

Factors affecting spatial resolution:

- Distribution of primary ionization
- Diffusion
- Readout electronics
- Electric field (gas amplification)
- Range of 'delta electrons'



Nobel Prize: W, Z - Discovery at UA1/UA2 (1983)

UA1 used the largest imaging drift chamber of its day
(5.8 m long, 2.3 m in diameter)

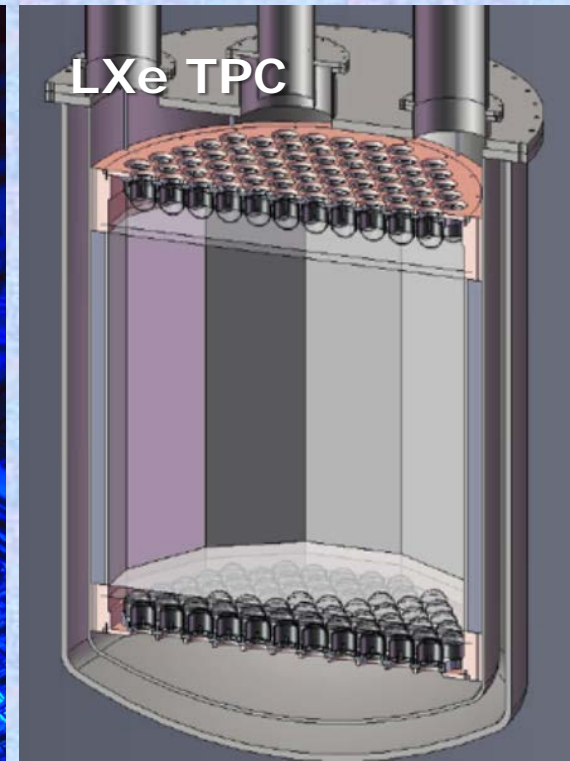
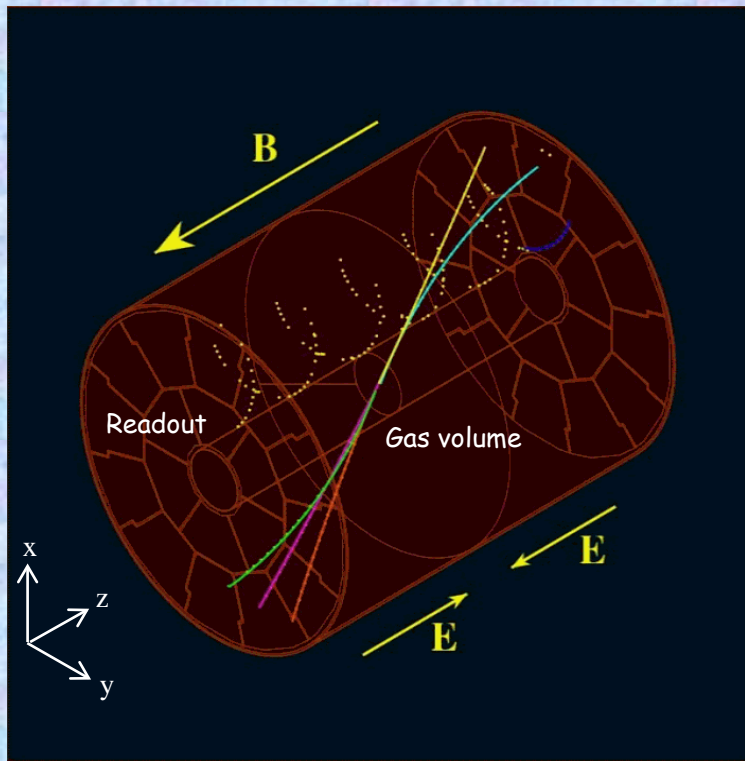
It can now be seen in the CERN
Microcosm Exhibition

Particle trajectories in the CERN-UA1
3D Wire Chamber
Discovery of W and Z bosons
C. Rubbia & S. Van der Meer Nobel 1984



Time Projection Chamber (TPC)

The TPC is a gas-filled cylindrical chamber with 1 or 2 endplates (D. Nygren, 1974)



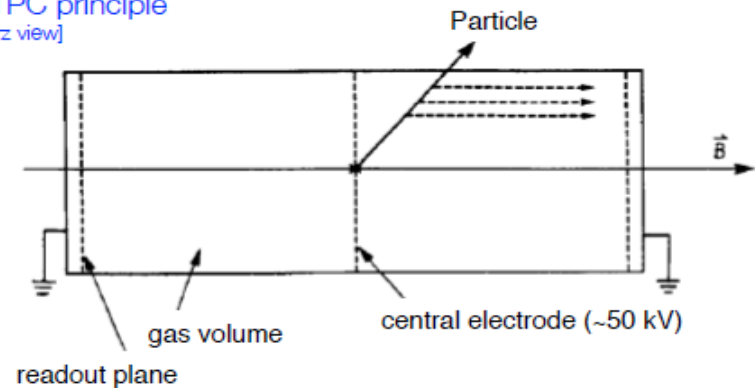
Separate two regions:

- Long drift along $z \sim 1-3$ m;
- Amplification at the end plate

Challenges:

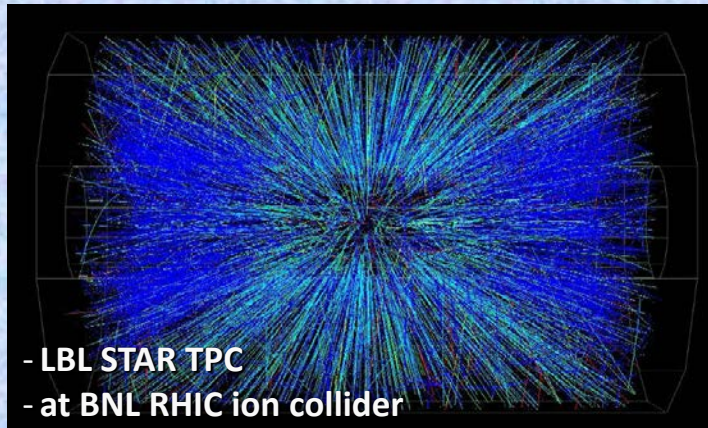
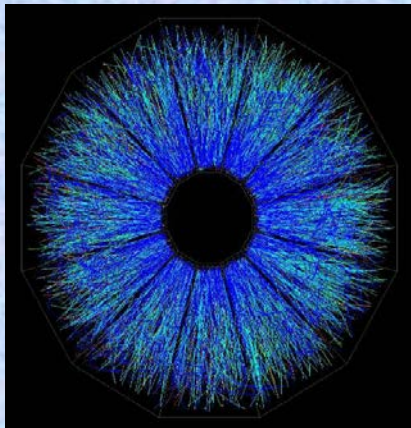
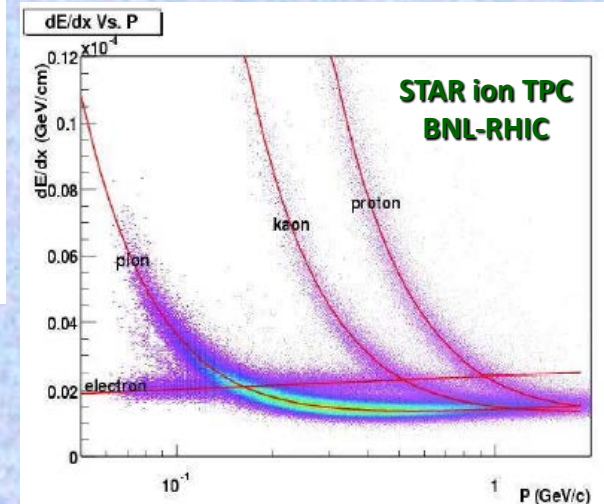
Long drift time; limited rate capability

TPC principle
[rz view]



TPC Characteristics

- Track point recorded in 3-D
(2-D channels in x-y) \times (1-D channel in $z = v_{\text{drift}} \times t_{\text{drift}}$)
- Particle identification by dE/dx
long ionization track, segmented in 100-200 measurements



	STAR	ALICE	ILC
Inner radius (cm)	50	85	32
Outer radius (cm)	200	250	170
Length (cm)	2 * 210	2 * 250	2 * 250
Charge collection	wire	wire	MPGD
Pad size (mm)	2.8 * 11.5 6.2 * 19.5	4 * 7.5 6*10(15)	2 * 6
Total # pads	140000	560000	1200000
Magnetic field [T]	0.5	0.5	4
Gas Mixture	Ar/CH4 (90:10)	Ne/CO2 (90:10)	Ar/CH4/CO2 (93:5:2)
Drift Field [V/cm]	135	400	230
Total drift time (μ s)	38	88	50
Diffusion σ_T (μ m/ \sqrt cm)	230	220	70
Diffusion σ_L (μ m/ \sqrt cm)	360	220	300
Resolution in $r\phi$ (μ m)	500-2000	300-2000	70-150
Resolution in r_z (μ m)	1000-3000	600-2000	500-800
dE/dx resolution [%]	7	7	< 5
Tracking efficiency[%]	80	95	98

Powerfull tool for:

- Lepton Colliders
- Modern heavy ion collisions
- Liquid and high pressure noble gases for neutrino and dark matter physics program

Muon Detectors

● Muon detectors are **tracking detectors** (e.g. wire chambers)

- they form the outer shell of the (LHC) detectors
- they are **not only sensitive to muons** (but to all charged particles)!
- just by “definition”: if a particle has reached the muon detector it's considered to be a muon
 - all other particles should have been absorbed in the calorimeters

● Challenge for muon detectors

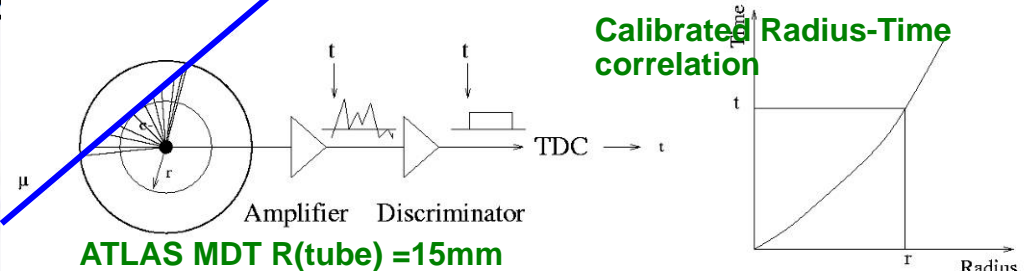
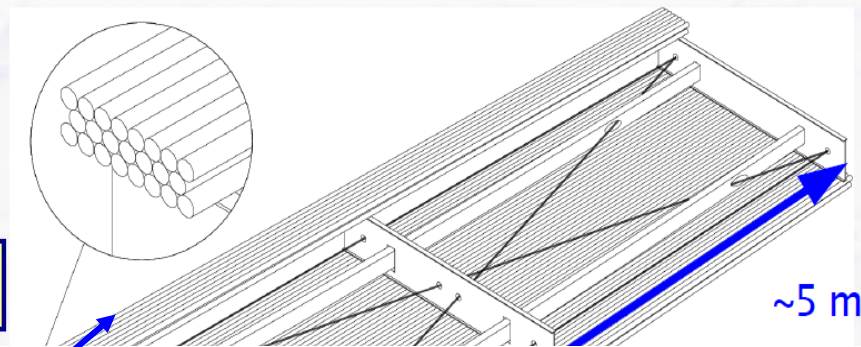
- large surface to cover (outer shell)
- keep mechanical positioning stable over time

● ATLAS

- 1200 chambers with 5500 m²
- also good knowledge of (inhomogeneous) magnetic field needed

ATLAS Muon Detector Elements

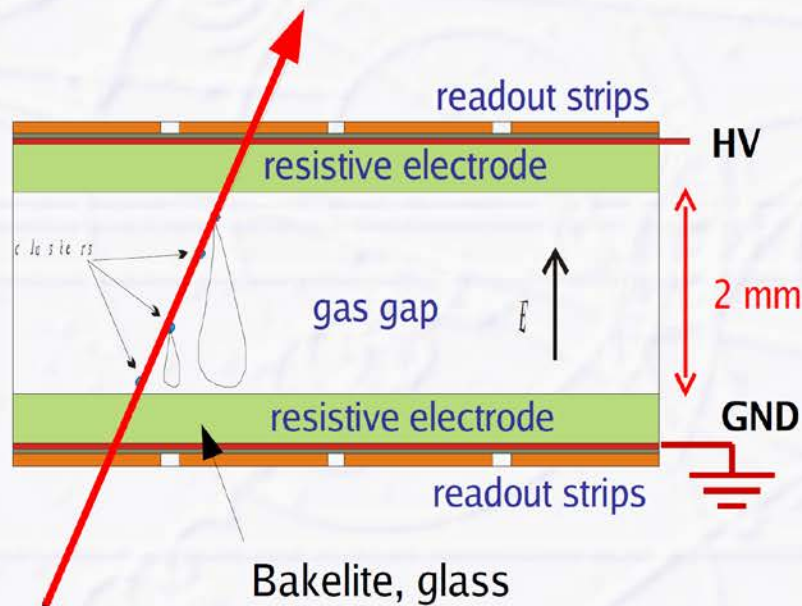
Aluminum tubes with central wire filled with 3 bar gas



Conceptual View of Resistive Plate Chambers (RPC)

There are also gaseous detectors without wires

- two resistive plates ($\sim 10^9 \Omega\text{cm}$) with a small gas gap (2 mm) and large high voltage (12 kV) on outside electrodes
- strong E-field: operation in “streamer mode”
 - gas avalanche already starting in gas gap (no wires involved)
 - developing of “streamers” (blob with lots of charge, almost like a spark)
 - signal on external read-out strips via influence (segmented for position resolution)
 - streamer/discharge is “self-quenching”: stops when near-by resistive electrodes are locally discharged (E-field breaks down)



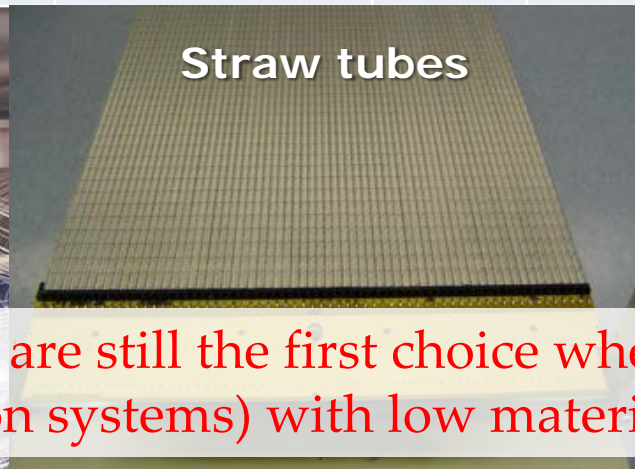
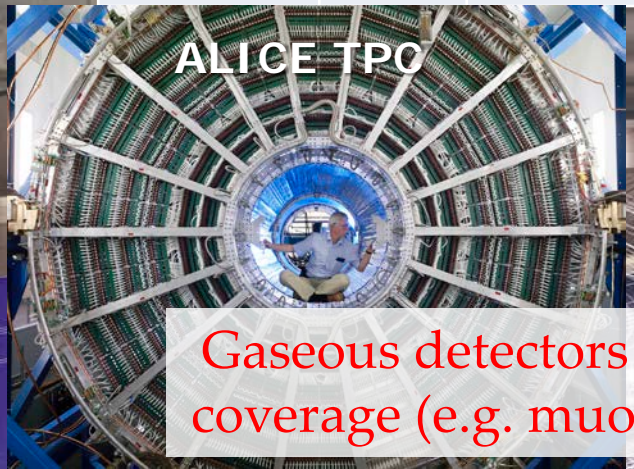
Advantages: simple device, good to cover large areas, VERY fast!!!

→ used as trigger devices in LHC experiments, time resolution $\sim 50 - 100$ ps

Disadvantages: Choice of resistive material + surface quality crucial, affects “dark” trigger rate

Gaseous Detectors in LHC Experiments

	Vertex	Inner Tracker	PID/ photo-det.	EM CALO	HAD CALO	MUON Track	MUON Trigger
ATLAS	-	TRD (straws)	-	-	-	MDT (drift tubes), CSC	RPC, TGC (thin gap chambers)
CMS	-	-	-	-	-	Drift tubes, CSC	RPC, CSC
----- TOTEM						----- GEM	----- GEM
LHCb	-	Straw Tubes	-	-	-	MWPC	MWPC, GEM
ALICE	-	TPC (MWPC)	TOF(MRPC), PMD, HPMID (RICH-pad chamber), TRD (MWPC)	-	-	Muon pad chambers	RPC



Gaseous detectors are still the first choice whenever the large-area coverage (e.g. muon systems) with low material budget is required

X-ray Imaging (Radiography)

Wire Chamber Radiography:

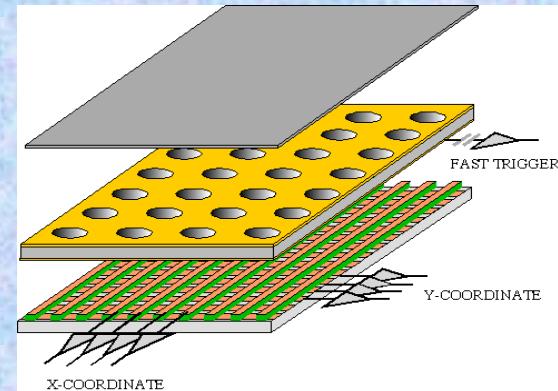


Position resolution ~ 250 μm

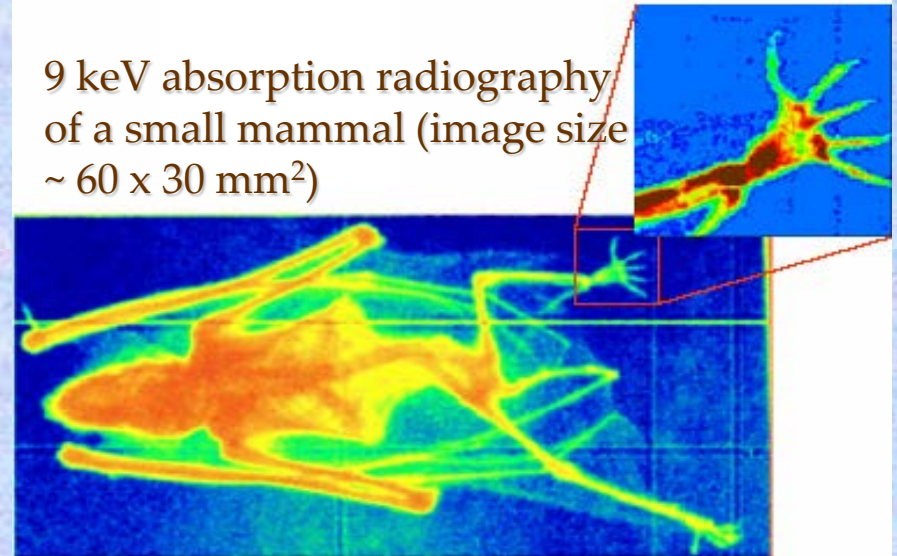
- A. Bressan et al, Nucl. Instr. and Meth. A 425(1999)254
- F. Sauli, Nucl. Instr. and Meth. A 461(2001)47
- G. Charpak, Eur. Phys. J. C 34, 77-83 (2004)
- F. Sauli, <http://www.cern.ch/GDD>

GEM for 2D Imaging:

Using the lower GEM signal, the readout can be self-triggered with energy discrimination:



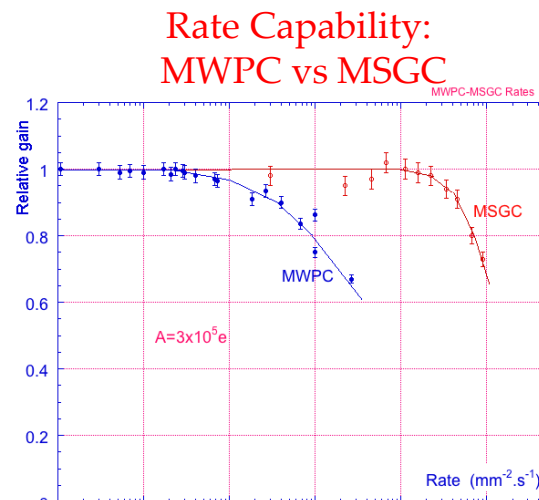
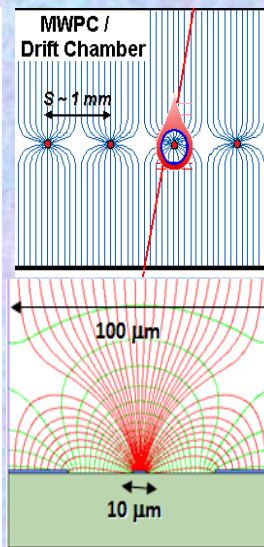
9 keV absorption radiography of a small mammal (image size ~ 60 x 30 mm²)



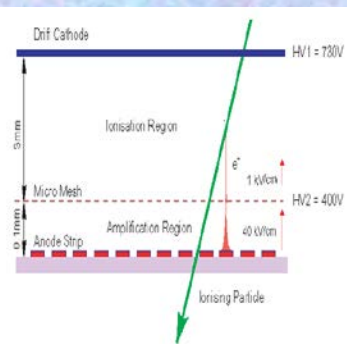
Position resolution ~ 100 μm
(limited by photoelectron range in the gas)

Micro-Pattern Gaseous Detector Technologies for Future Physics Projects

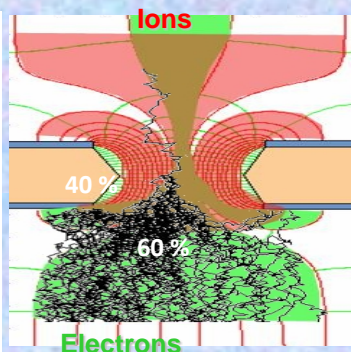
- Micromegas
- GEM
- Thick-GEM, Hole-Type and RETGEM
- MPDG with CMOS pixel ASICs ("InGrid")
- Micro-Pixel Chamber (μ PIC)



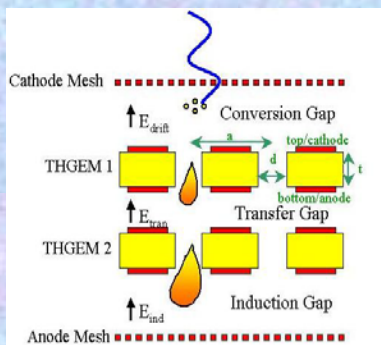
Micromegas



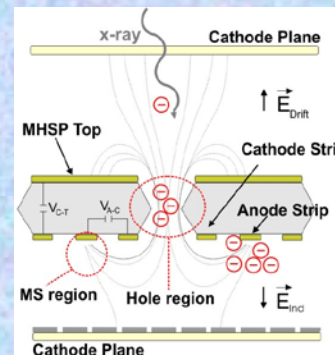
GEM



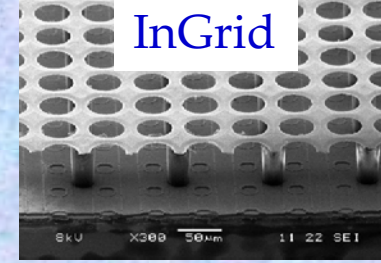
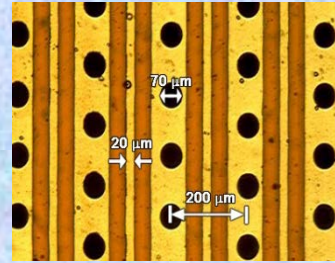
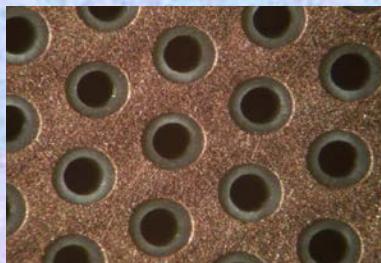
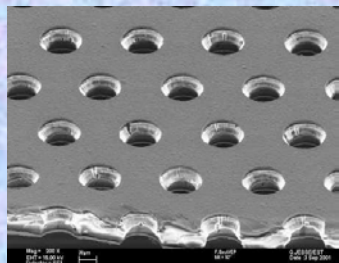
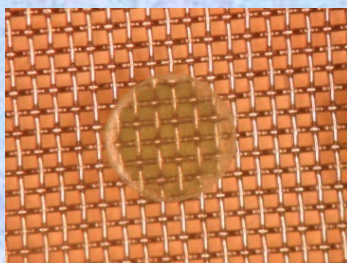
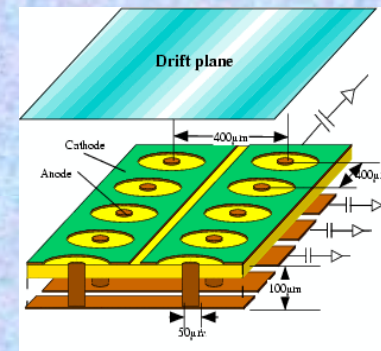
THGEM



MHSP

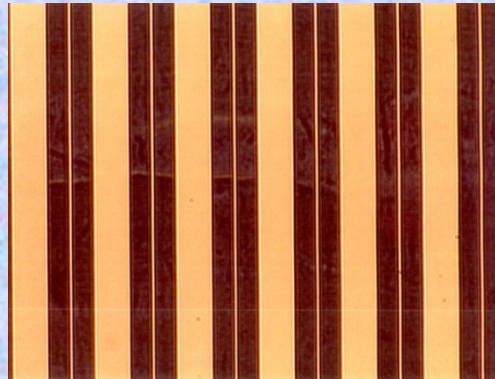
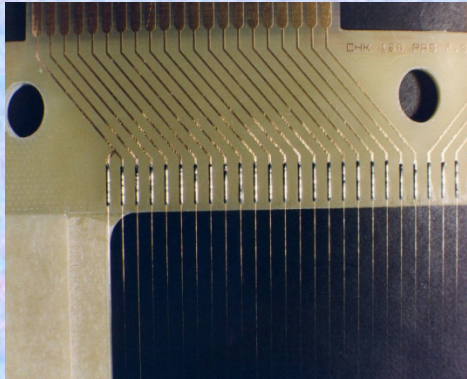


μ PIC

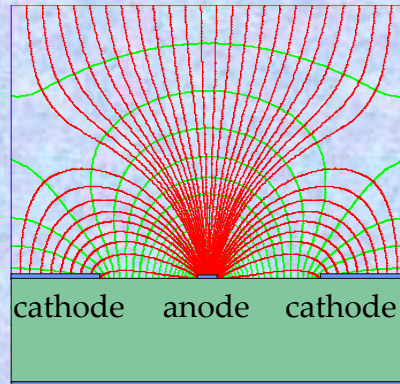
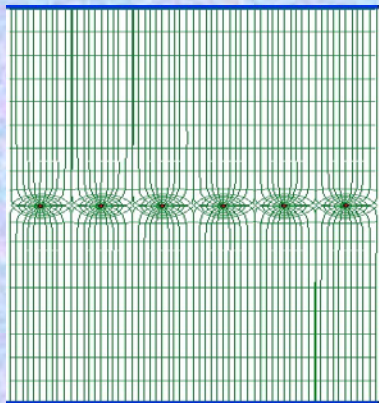
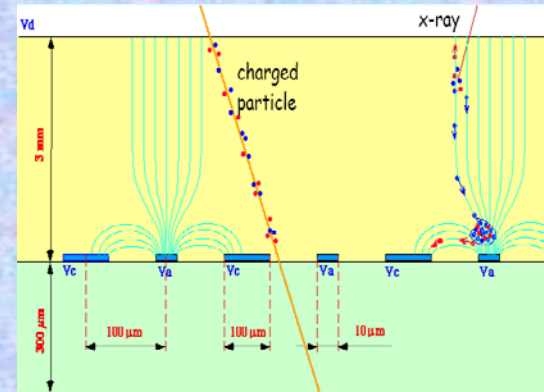


Micro-Strip Gas Chamber (MSGC)

MWPC



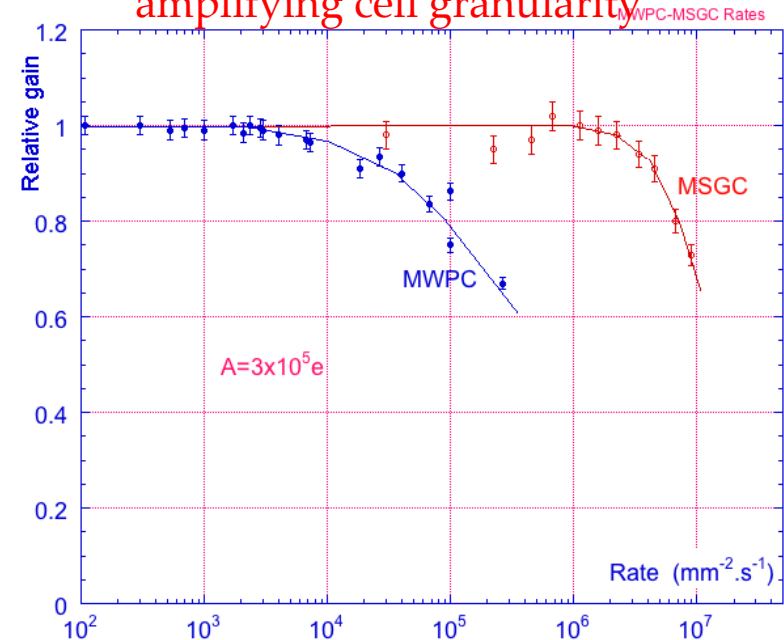
MSGC



Typical distance between wires limited to 1 mm due to mechanical and electrostatic forces

Typical distance between anodes 200 μm thanks to semiconductor etching technology

Rate capability limit due to space charge overcome by increased amplifying cell granularity



MSGC Discharge Problems

Discharge is very fast (~ns)
Difficult to predict or prevent

L-06

Do not copy

© W. Faidley - Weatherstock Inc.

MICRODISCHARGES

Owing to very small distance between anode and cathode the transition from proportional mode to streamer can be followed by spark, discharge, if the avalanche size exceeds RAETHER'S LIMIT
 $Q \sim 10^7 - 10^8$ electrons

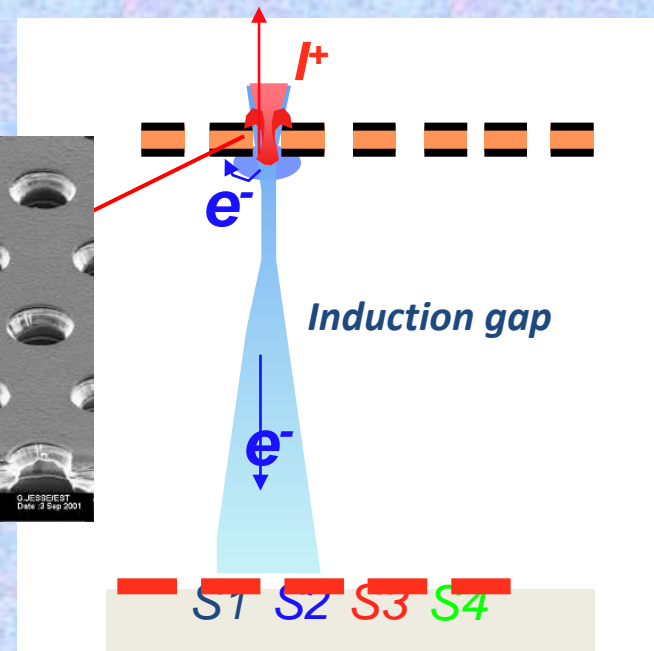
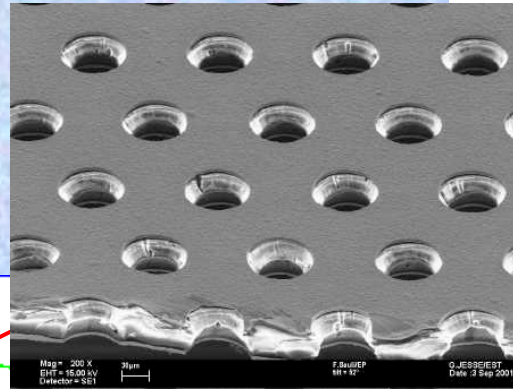
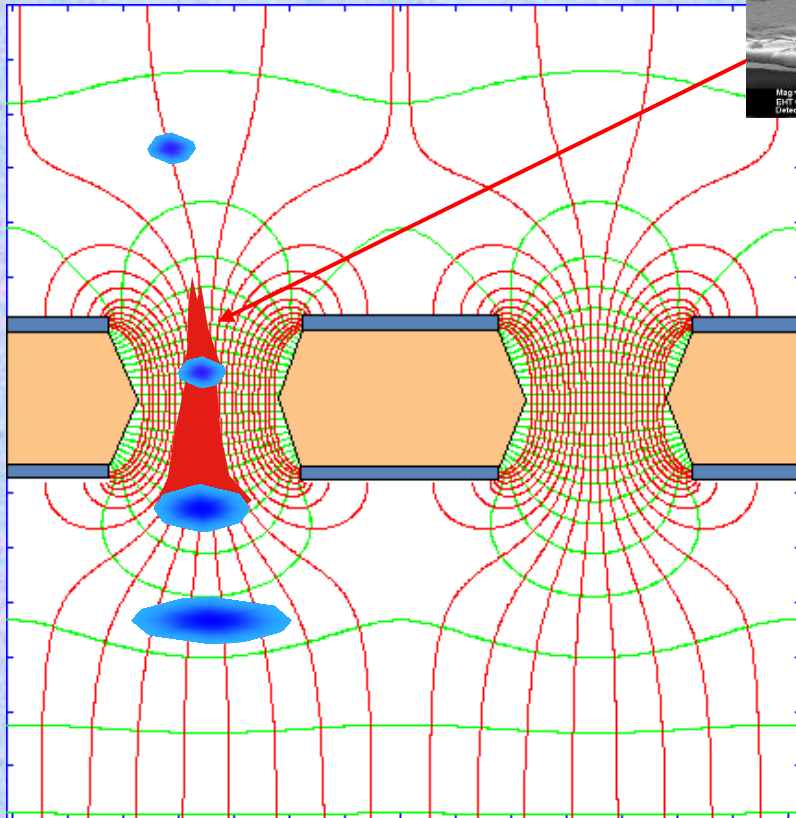
FULL BREAKDOWN

GEM (Gas Electron Multiplier)

Thin metal-coated polymer foil chemically pierced by a high density of holes

A difference of potentials of $\sim 500\text{V}$ is applied between the two GEM electrodes.

→ the primary electrons released by the ionizing particle, drift towards the holes where the high electric field triggers the electron multiplication process.



- Electrons are collected on patterned readout board.
- A fast signal can be detected on the lower GEM electrode for triggering or energy discrimination.
- All readout electrodes are at ground potential.

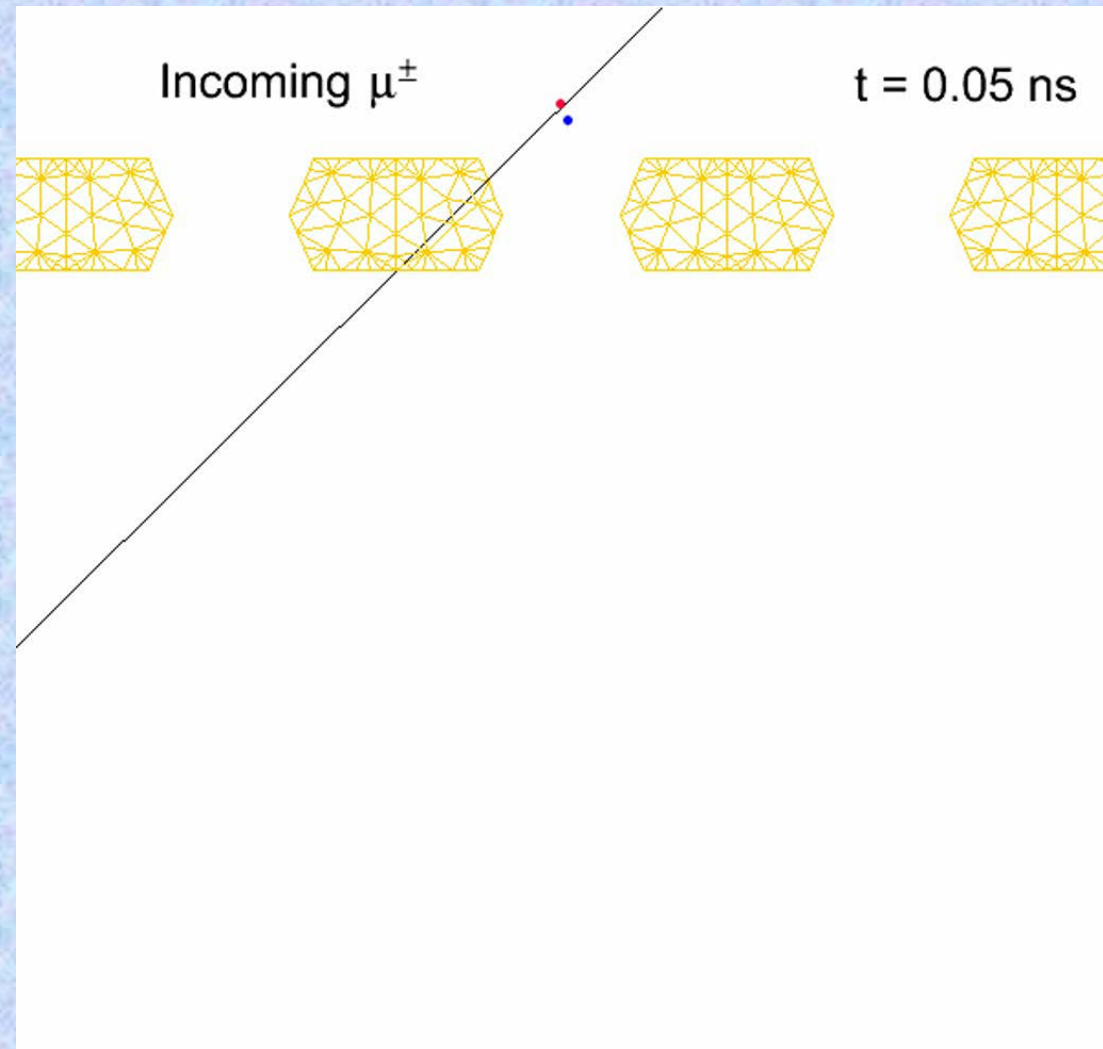
MPGD Simulation Tools (Avalanche Simulation in GEM)



Animation of the avalanche process
(monitor in ns-time electron/ion
drifting and multiplication in GEM):

electrons are blue, ions are red, the
GEM mesh is orange

- ANSYS: field model
- Magboltz 8.9.6: relevant cross sections of electron-matter interactions
- Garfield++: simulate electron avalanches

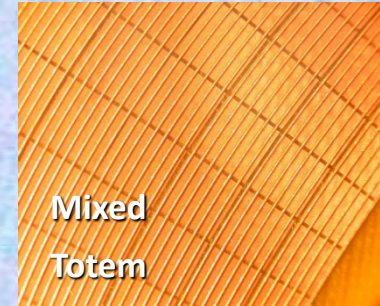
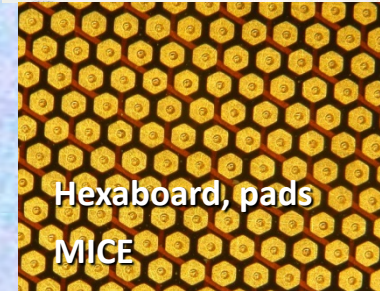
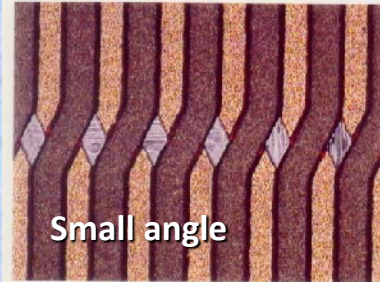
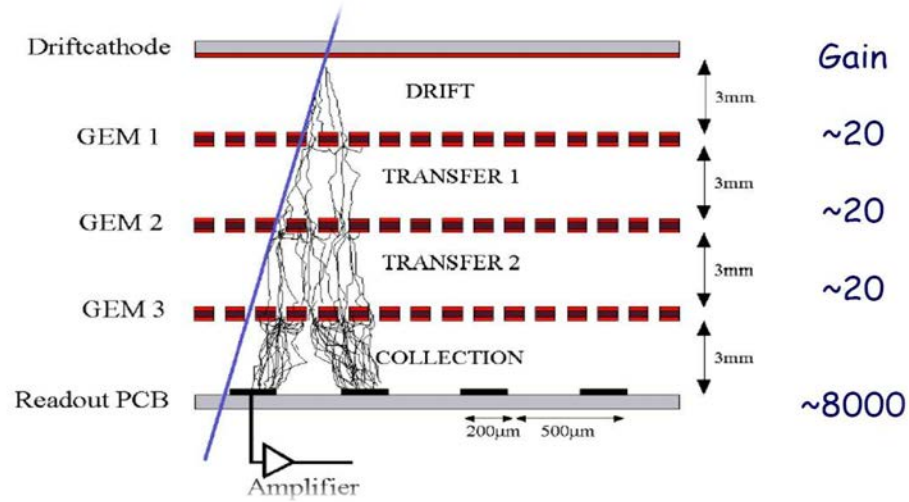


Gas Electron Multiplier (GEM)

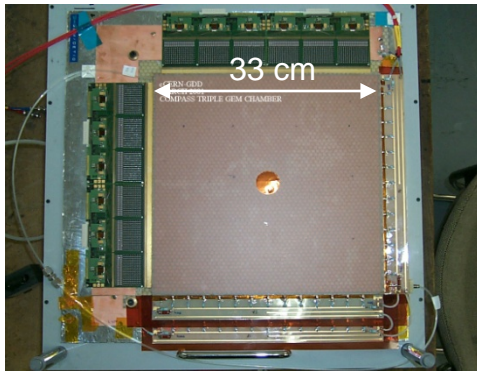
F. Sauli, NIM A386(1997) 531;
 F. Sauli, <http://www.cern.ch/GDD>



Full decoupling of amplification stage (GEM) and readout stage (PCB, anode)



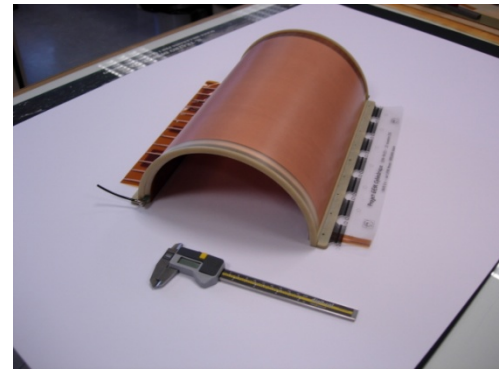
Amplification and readout structures can be optimized independently !



Compass



Totem



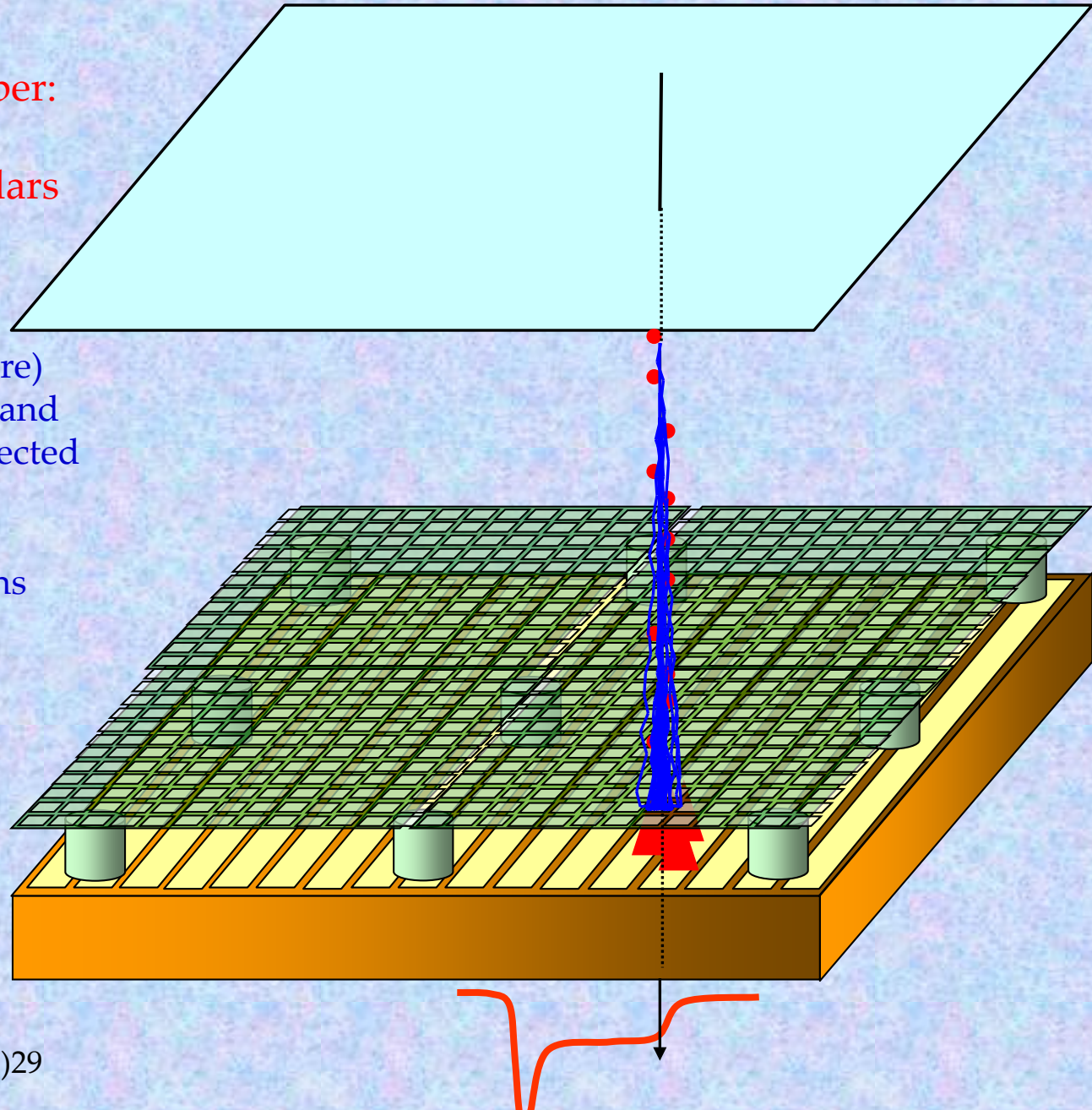
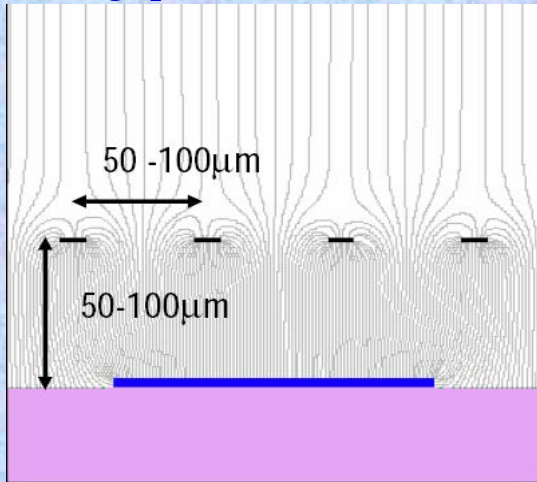
NA49-future

MICro MESH Gaseous Structure (MICROME GAS)

Micromesh Gaseous Chamber:
micromesh supported
by 50-100 μm insulating pillars

Multiplication (up to 10^5 or more)
takes place between the anode and
the mesh and the charge is collected
on the anode (one stage)

Small gap: fast collection of ions

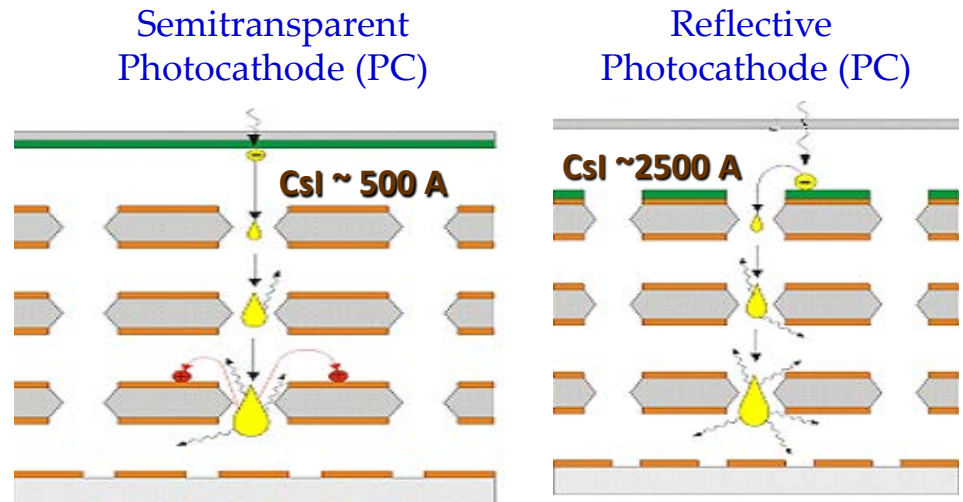


MPGD-Based Gaseous Photomultipliers (GPM)

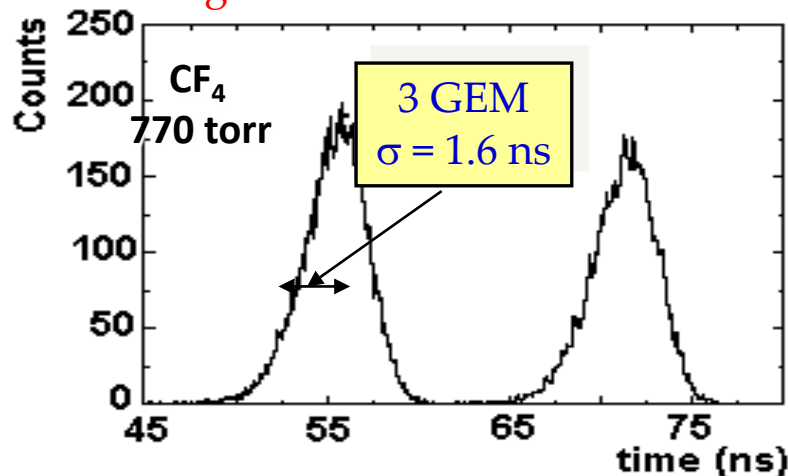
GEM Gaseous Photomultipliers (GEM+CsI photocathode) to detect single photoelectrons

Multi-GEM Gaseous Photomultipliers:

- ❖ Largely reduced photon feedback (can operate in pure noble gas & CF_4)
- ❖ Fast signals [ns] \rightarrow good timing
- ❖ Excellent localization response
- ❖ Able to operate at cryogenic T

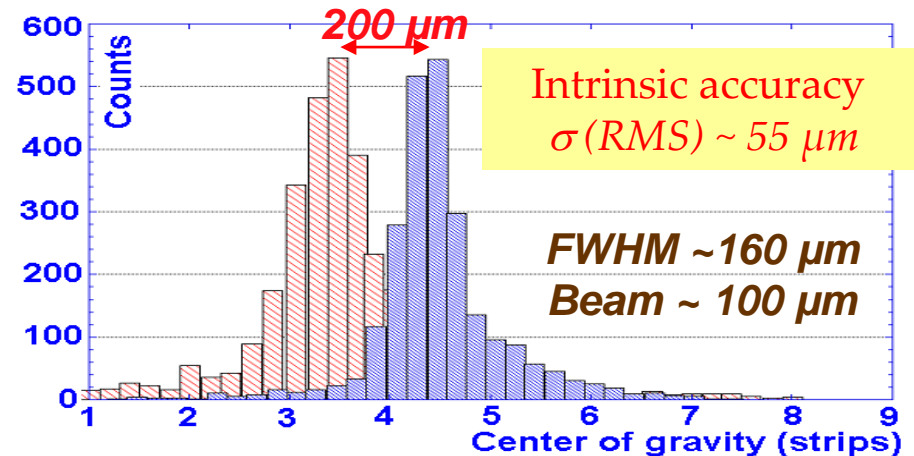


Single Photon Time Resolution:



Micromegas: $\sigma \sim 0.7$ ns with MIPs

Single Photon Position Accuracy:



X-ray Imaging (Radiography)

Wire Chamber Radiography:

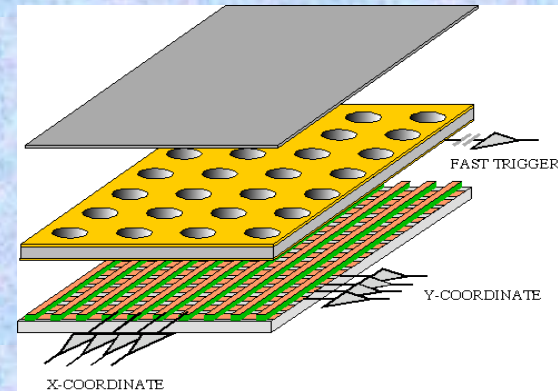


Position resolution ~ 250 μm

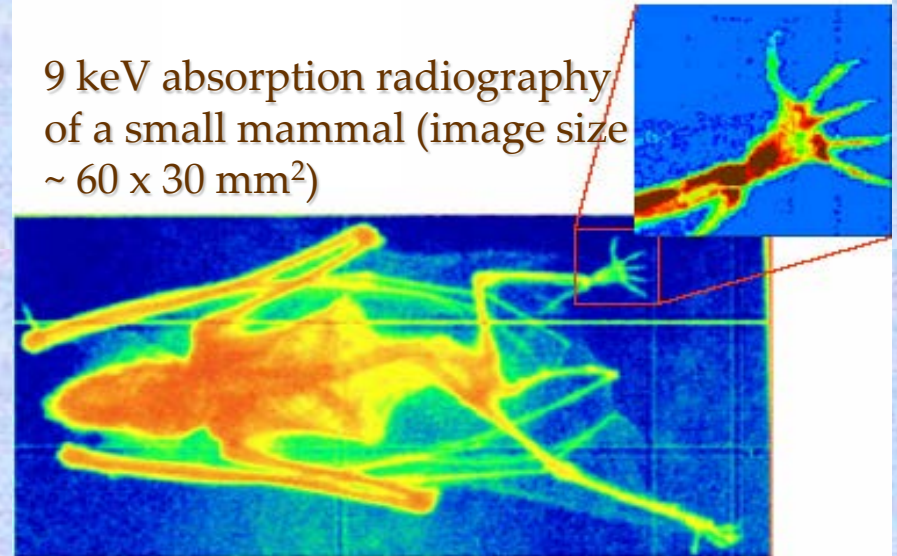
- A. Bressan et al, Nucl. Instr. and Meth. A 425(1999)254
- F. Sauli, Nucl. Instr. and Meth. A 461(2001)47
- G. Charpak, Eur. Phys. J. C 34, 77-83 (2004)
- F. Sauli, <http://www.cern.ch/GDD>

GEM for 2D Imaging:

Using the lower GEM signal, the readout can be self-triggered with energy discrimination:



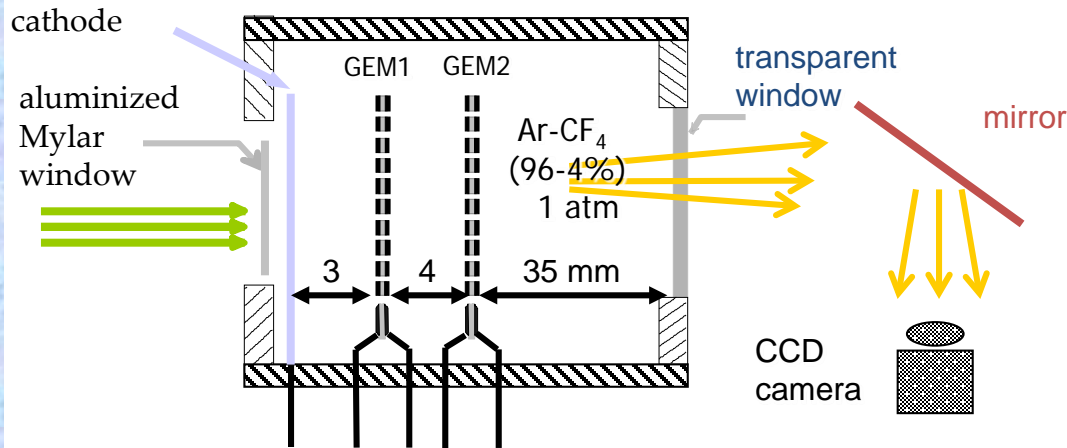
9 keV absorption radiography of a small mammal (image size ~ 60 x 30 mm²)



Position resolution ~ 100 μm
(limited by photoelectron range in the gas)

A Scintillating GEM for Dose Imaging in Radiotherapy

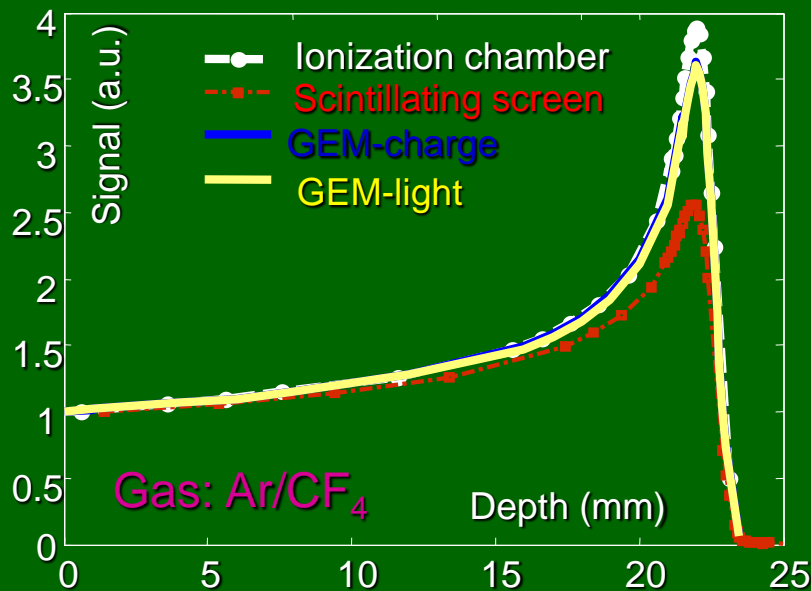
Scintillation light (optical) & charge Readout:



Light output for 138 MeV protons:

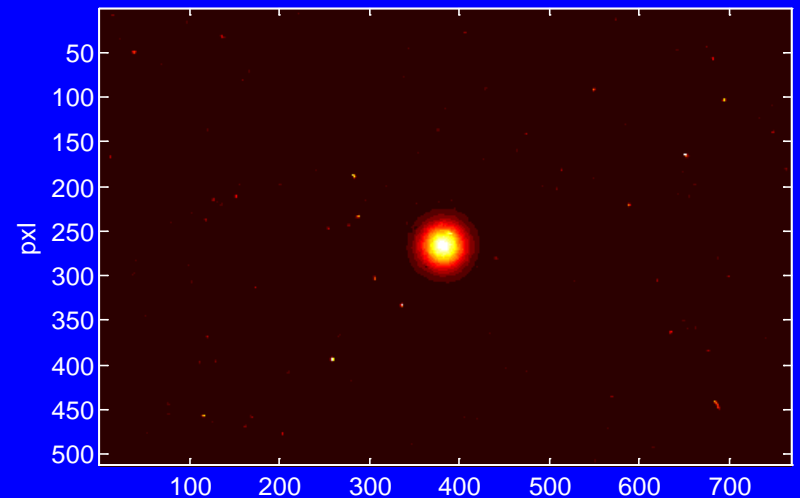
Scintillation type	Gas gain	Light signal (CCD) at 1Gy proton dose (ADU)
Screen (Gd ₂ O ₂ S:Tb)		2670
Ar/CO ₂ (90:10)	3000	270
Ar/CF ₄ (90:10)	1400	2350
Ar/CF ₄ (95:5)	1300	4000
Ar/CF ₄ (97,5:2,5)	770	2000

Bragg curve with 360 MeV a-beam



LIGHT SIGNAL FROM GEM:

(only 4% smaller than ionization chamber signal)



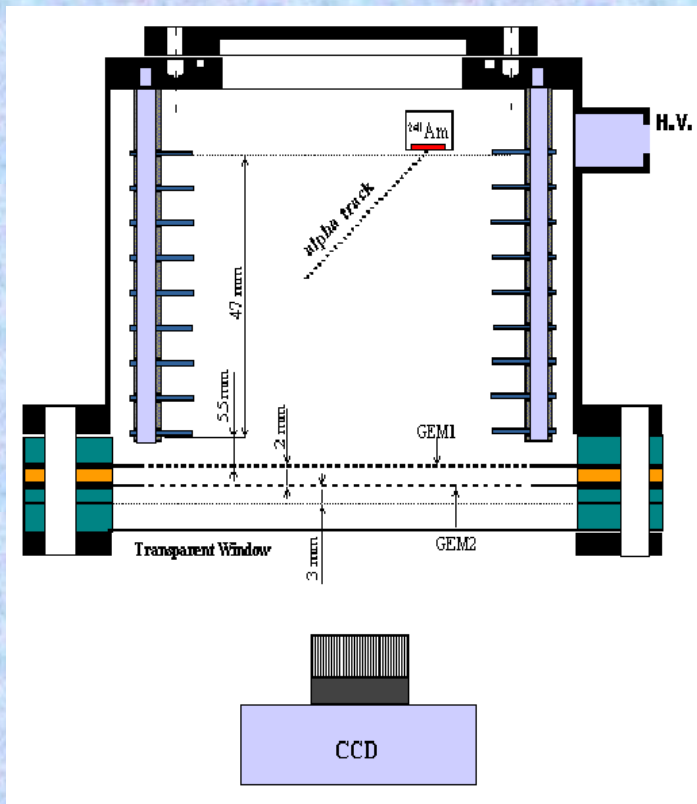
E. Sevaralli et al., Scintillating GEM for 2D Dosimetry in a-beam, submitted to IEEE TNS

S. Fetal et al., NIMA513 (2003) 42

Optical Imaging of a GEM Detector

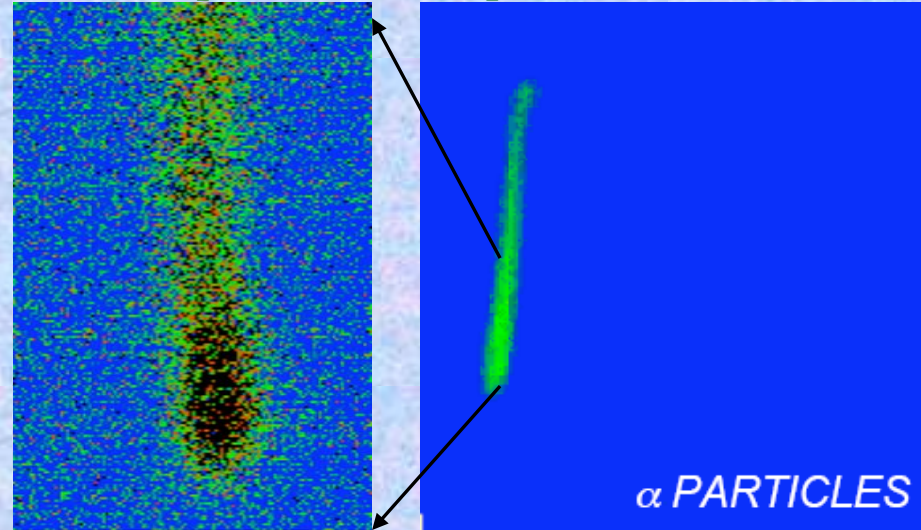
Scintillation light (optical readout) in a multiple GEM detector recorded by a CCD camera

Light yield is proportional to the amount of secondary (avalanche) electrons

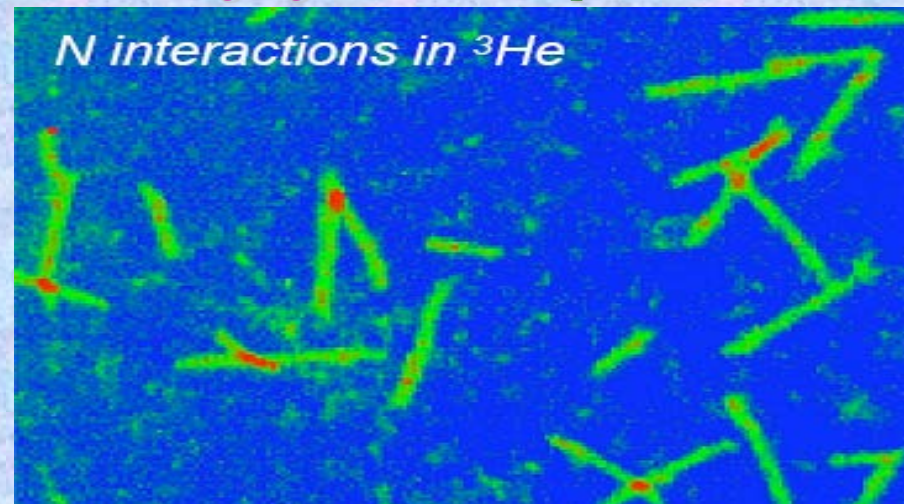


Bragg peak
for a-particles

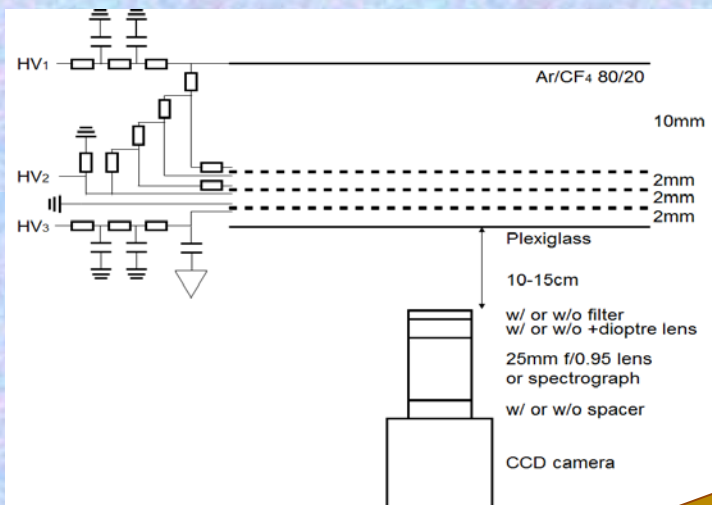
Scintillation image of
a-particle



Neutron Imaging: $3\text{He} + n \rightarrow p + 3\text{H} + 764 \text{ keV}$



MPGD Technologies for Imaging Applications: Optical Readout



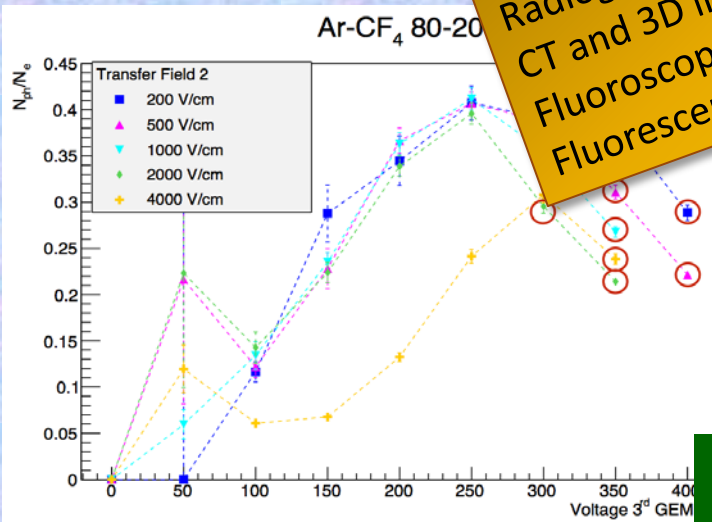
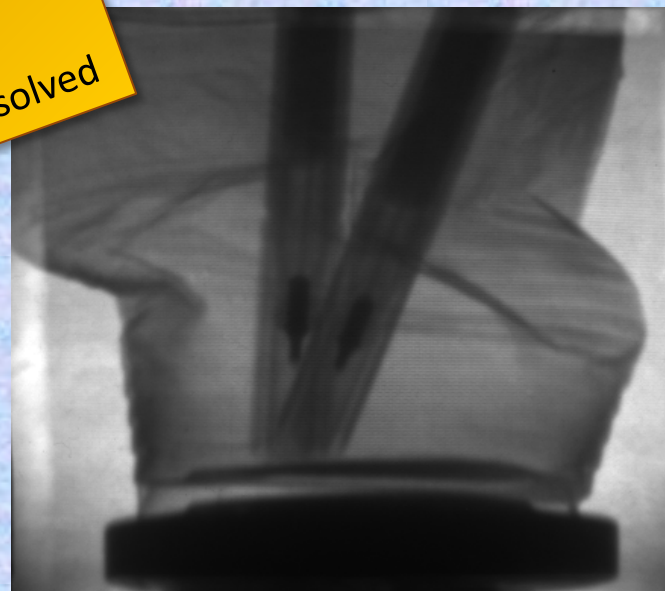
QImaging Retiga
 CCD: 2688
 ADC: 14b
 rate: 6.9fp
 read noise
 dark current
 trigger: exte

Potential Applications:
 Single events down to MIPs
 Radiography - imaging and energy resolved
 CT and 3D imaging
 Fluoroscopy
 Fluorescence - imaging and energy resolved

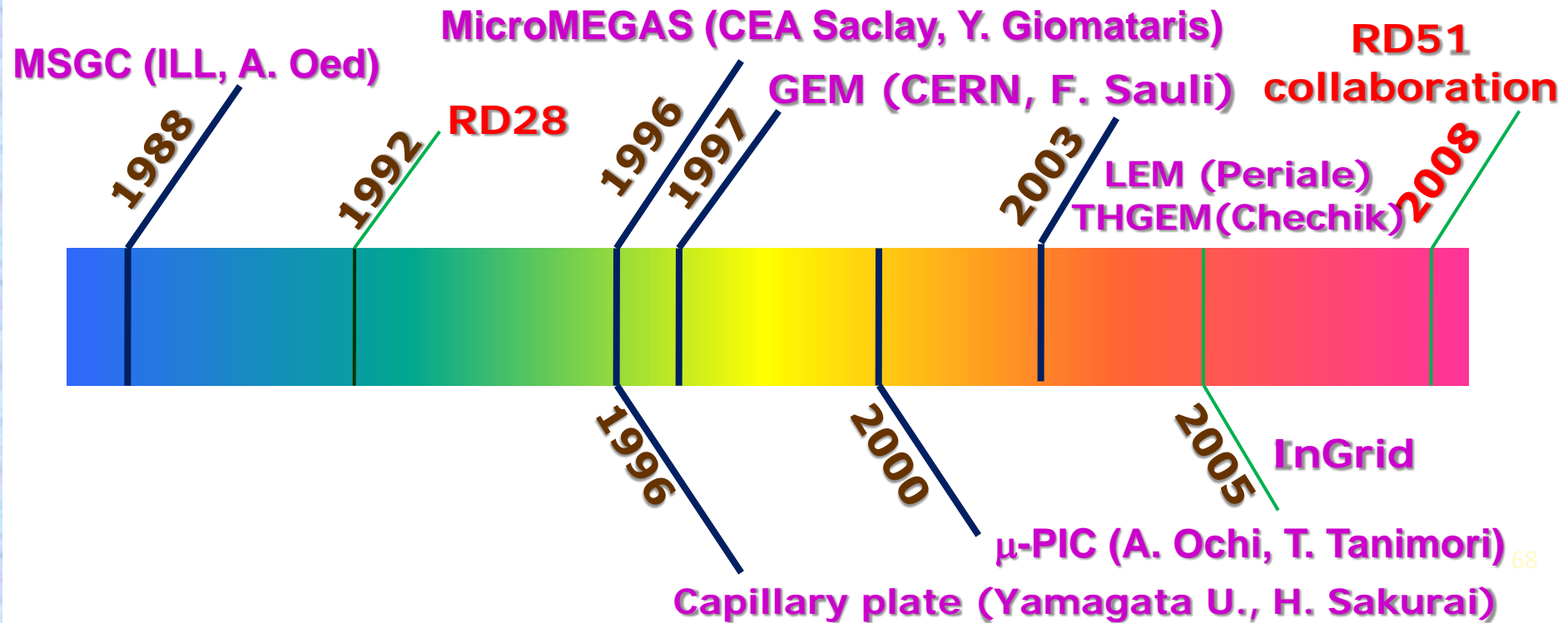
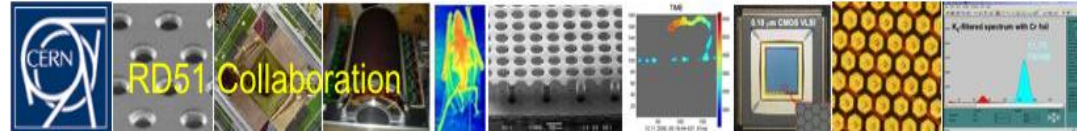
Fluoroscopy:



**CT and
 3 D Imaging:**

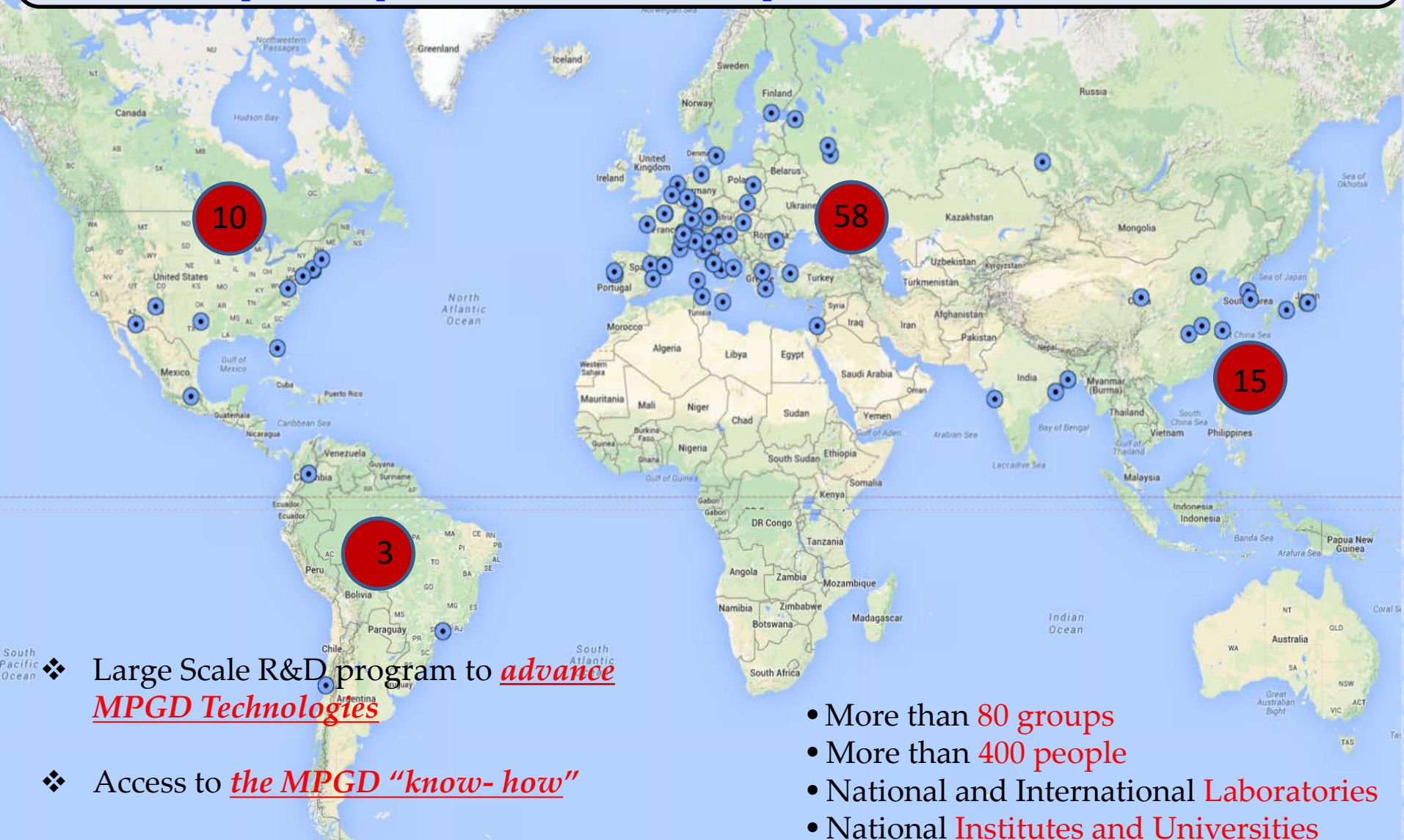
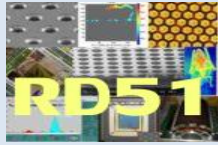


Historical Roadmap of the MPGD Technologies and RD51 Collaboration



- Many of the Micro-Pattern Gaseous Detector Technologies were introduced before the RD51 Collaboration was founded
- With more techniques becoming available (or affordable), new detection concepts are being introduced and the existing ones are substantially improved

The **main objective** is to advance **MPGD technological development** and associated electronic-readout systems, for applications in basic and applied research": <http://rd51-public.web.cern.ch/rd51-public>



- ❖ Large Scale R&D program to **advance** MPGD Technologies
- ❖ Access to the MPGD "know-how"
- ❖ Foster Industrial Production

- More than **80 groups**
- More than **400 people**
- National and International **Laboratories**
- National **Institutes and Universities**

The Rise of Micro-Pattern Gas Detector Technologies

Wire Chambers, TPC, RPC → MPGD (GEM, Micromegas) → InGrid (3D)

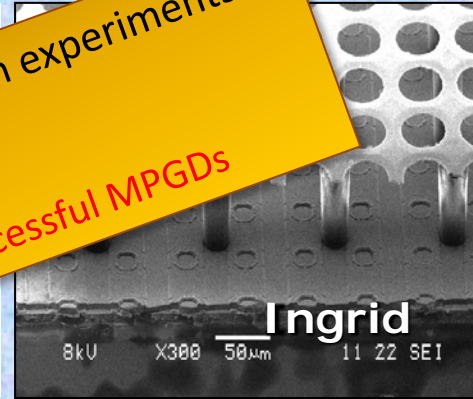
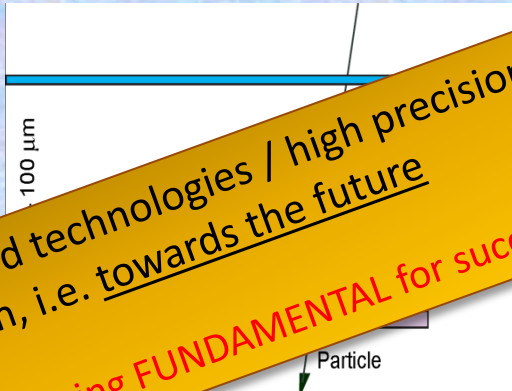
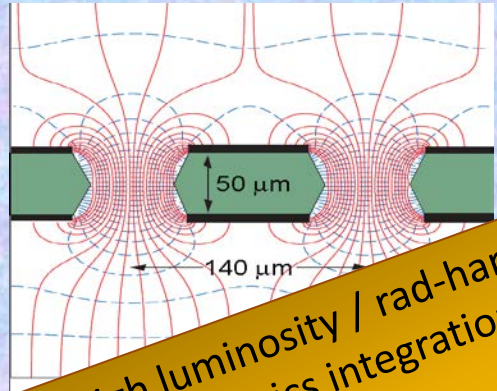
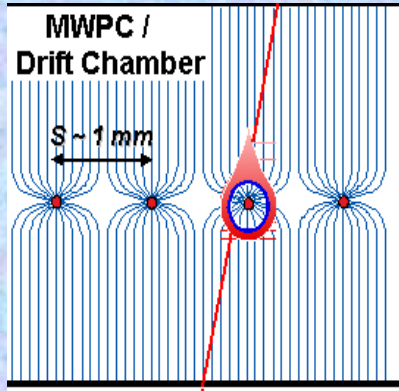
YESTERDAY:

INTEGRATION →

TODAY:

INTEGRATION →

FUTURE:

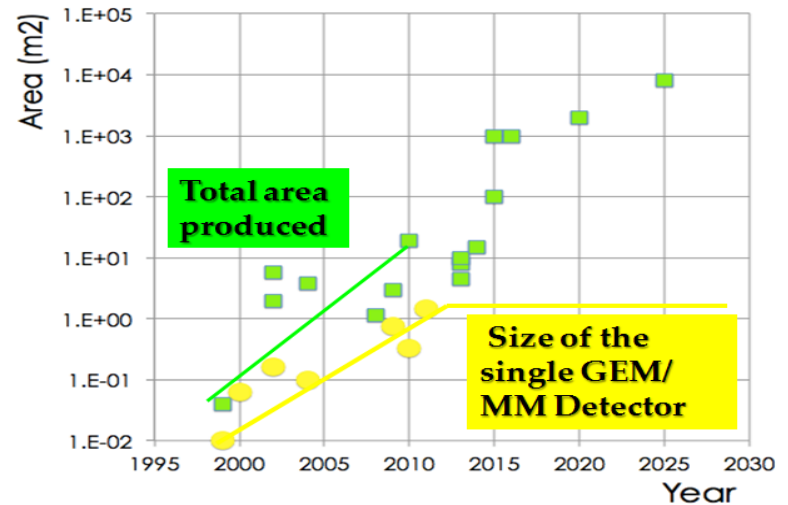


Moving towards high luminosity / rad-hard technologies / high precision experiments / ultimate detector-electronics integration, i.e. towards the future

Technological maturity and accurate engineering FUNDAMENTAL for successful MPGDs

MPGD Characteristic	Res MM	Res MM
Active Area (Size of sensitive area)	~0.5 m ²	~2 x 1 m ²
Large Scale	yes	yes
Radiation Hardness	Similar to Si-strip det.	Similar to Si-strip. det.
High-Rate Capability	~ 50 MHz/cm ²	Res MM: ~10 MHz/cm ²
Spatial resolution	<~30 μm ang. dep.: μTPC	<~30 μm ang. dep.: μTPC
Tracking efficiency	99%	98%
Timing Resolution	~3-5 ns (MIP) & CF ₄ <1-2 ns (UV - 1 ph.e)	3-5 ns (MIP) & CF ₄ 0.2-0.5 ns (UV-1 ph.e)

Advances in photolithography → Large Area MPGDs (~ m² unit size)



Tracking

Momentum measurement

Multiple scattering

Bethe-Bloch formula
/ Landau tails

Ionization of gases

Wire chambers

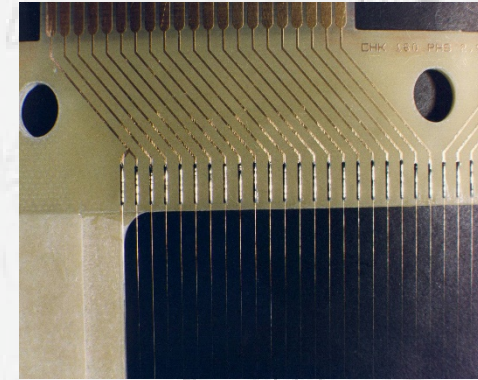
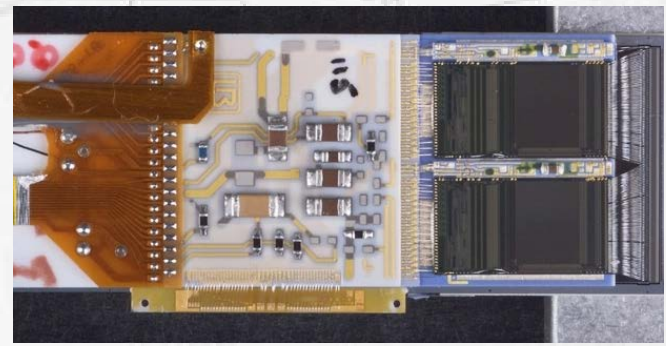
Drift and diffusion in gases

Drift chambers

Micro gas detectors

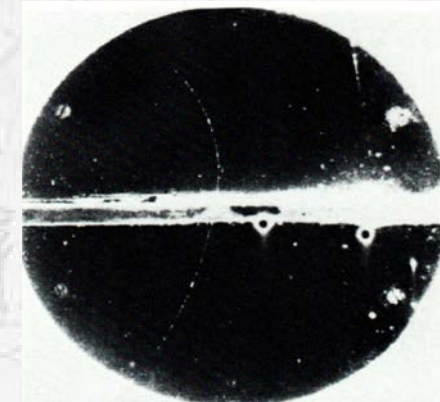
Silicon as a detection medium

Silicon detectors strips/pixels

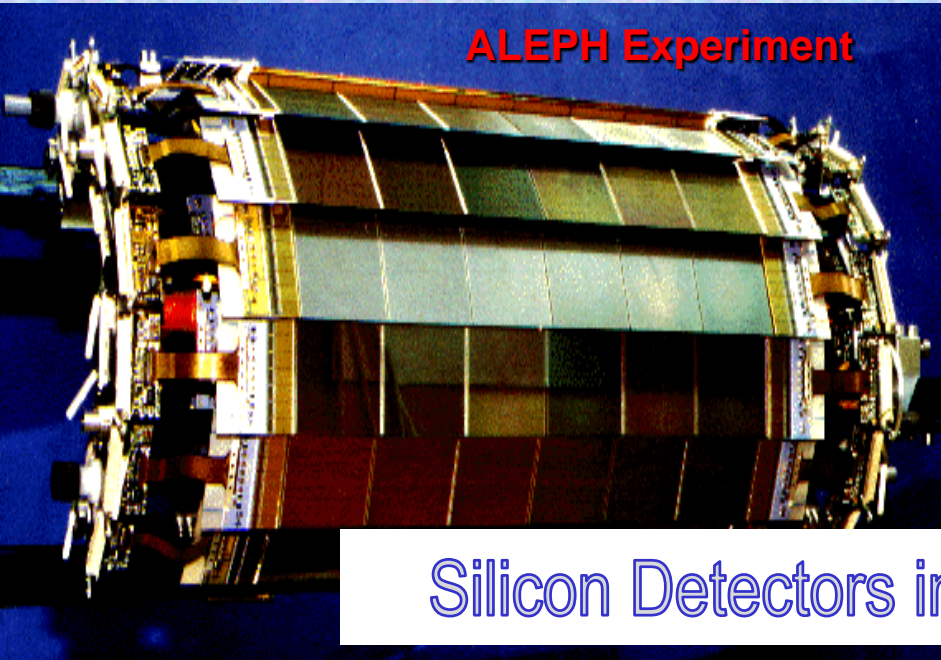


Tracking Detectors

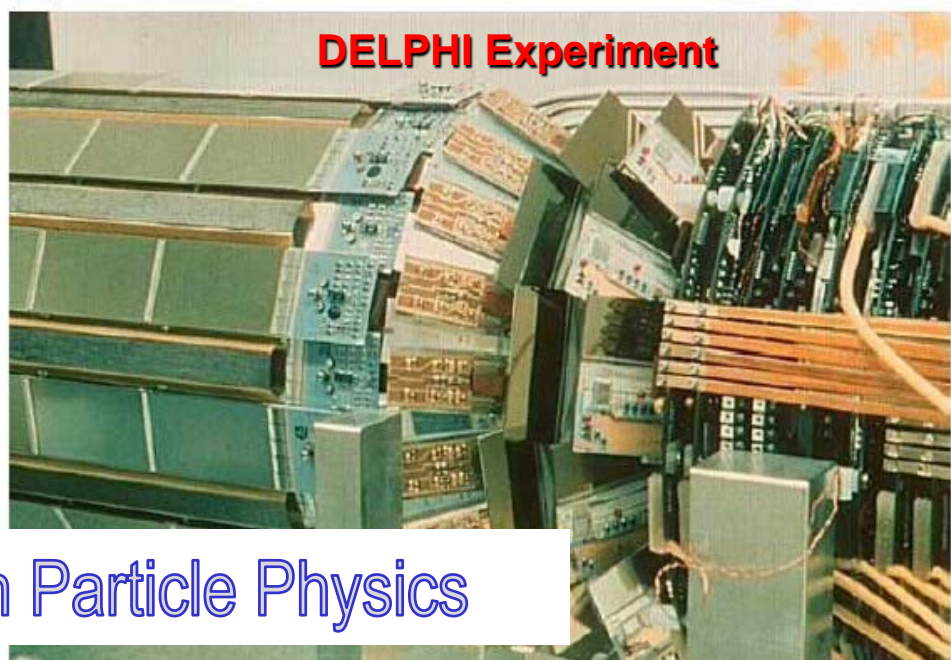
- “Classic” Detectors (historical touch...)
- Momentum Measurements
- Gaseous Chambers
- Silicon Detectors



ALEPH Experiment

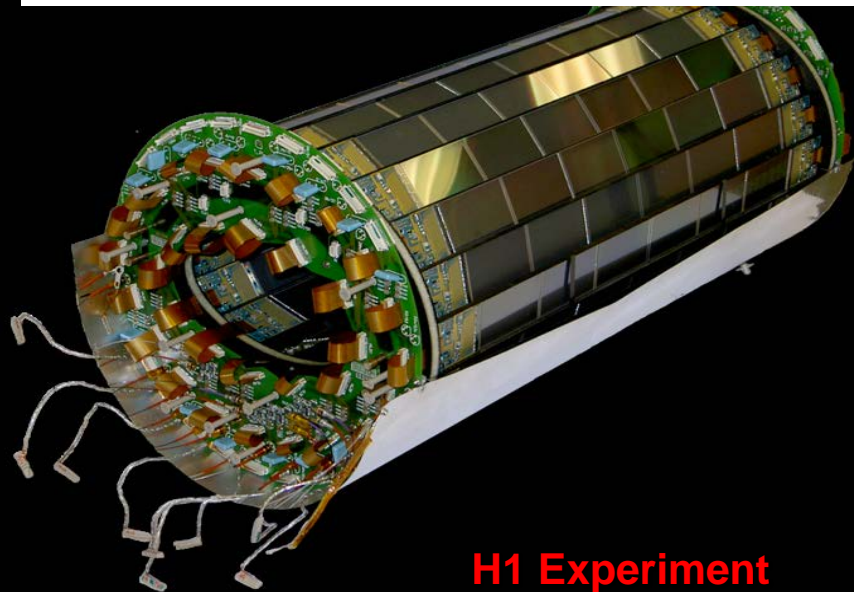


DELPHI Experiment

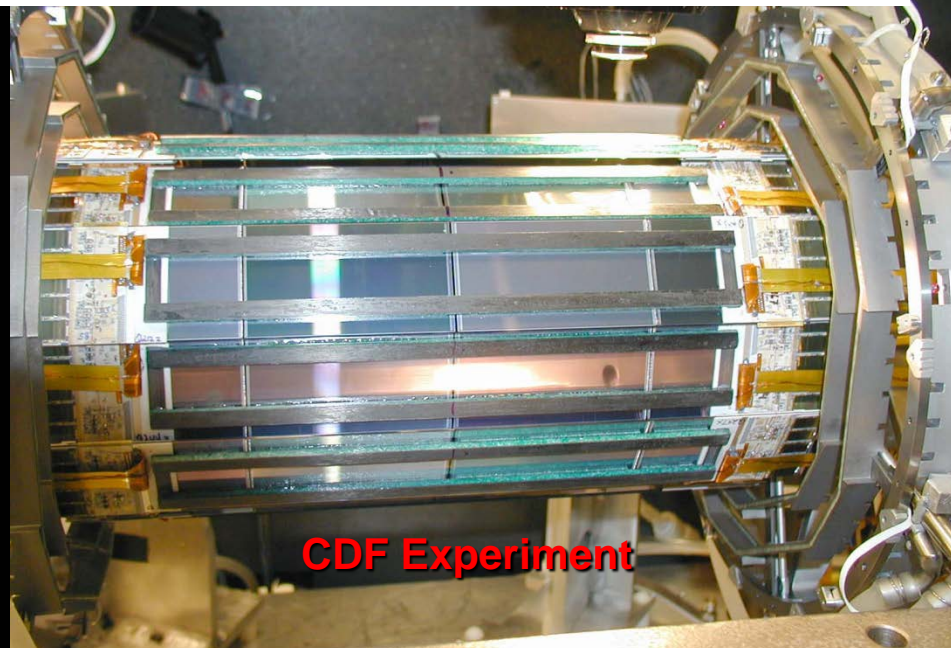


Silicon Detectors in Particle Physics

Strip and hybrid pixel detectors are mature technologies employed in almost every experiment in high energy physics.



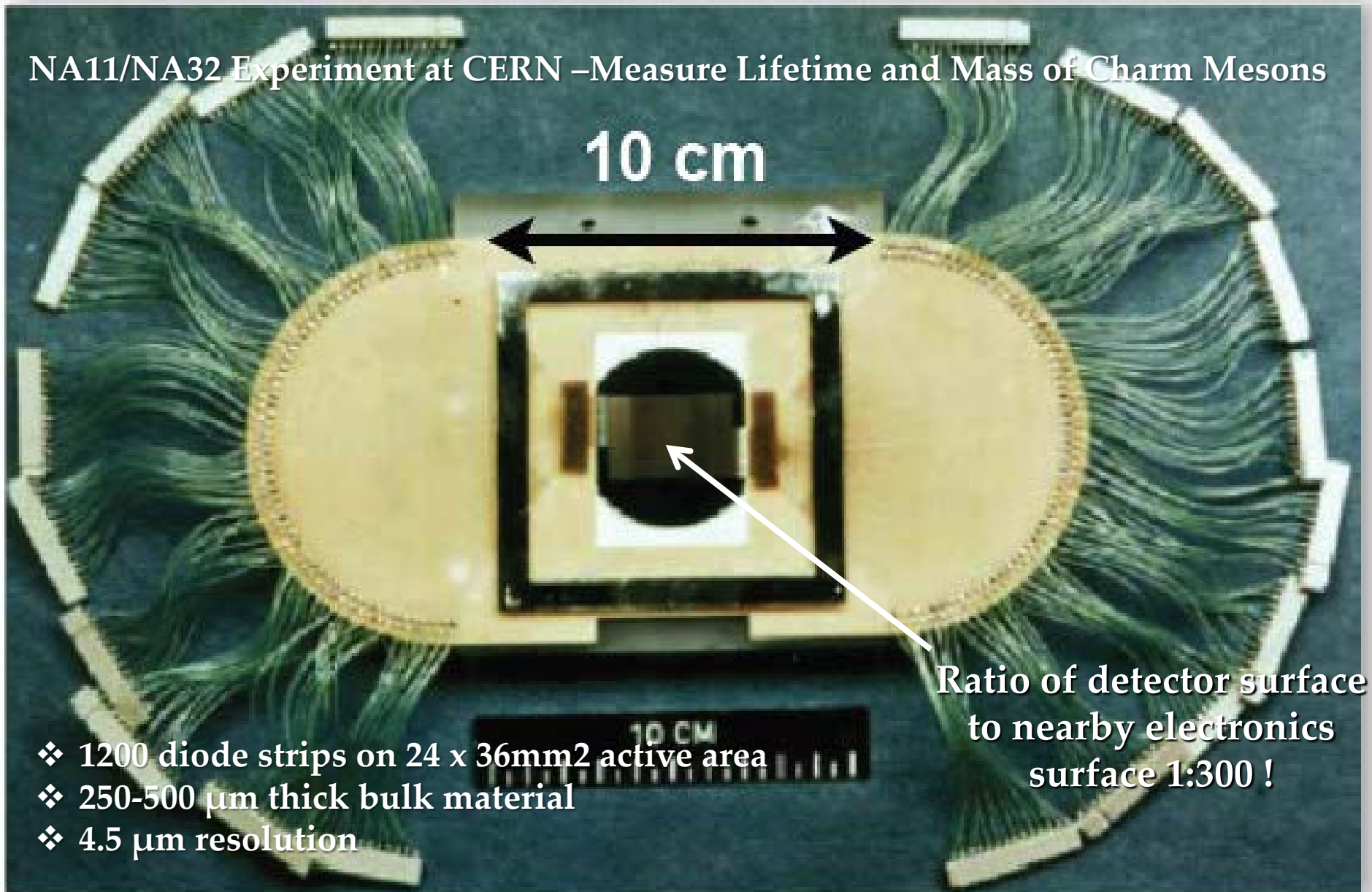
H1 Experiment



CDF Experiment

1983: First Silicon Strip Detector in HEP

NA11/NA32 Experiment at CERN – Measure Lifetime and Mass of Charm Mesons



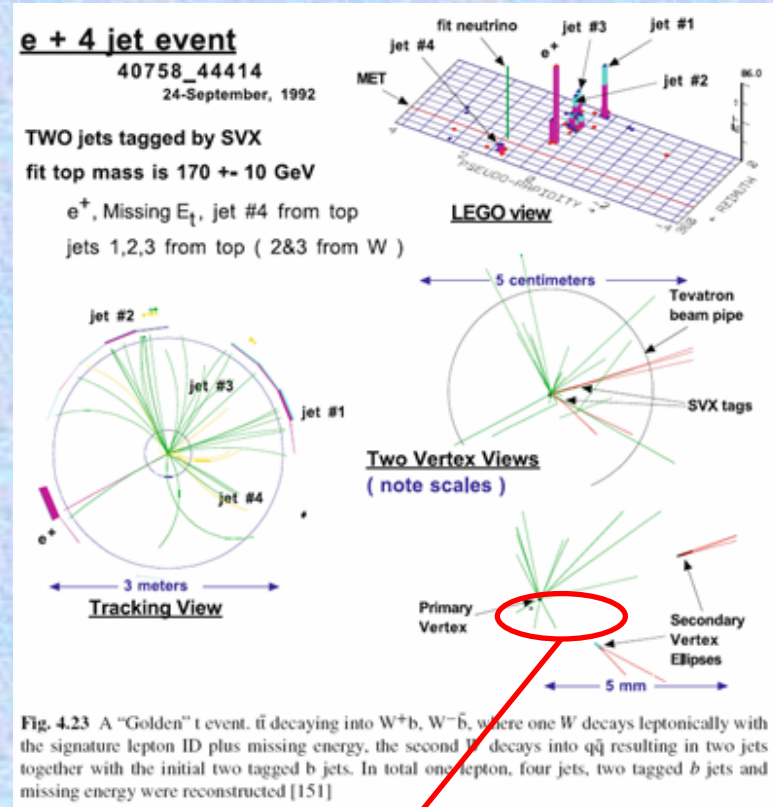
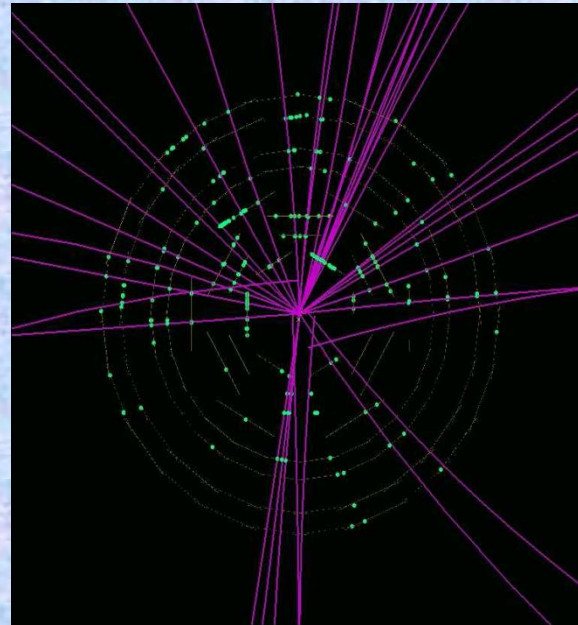
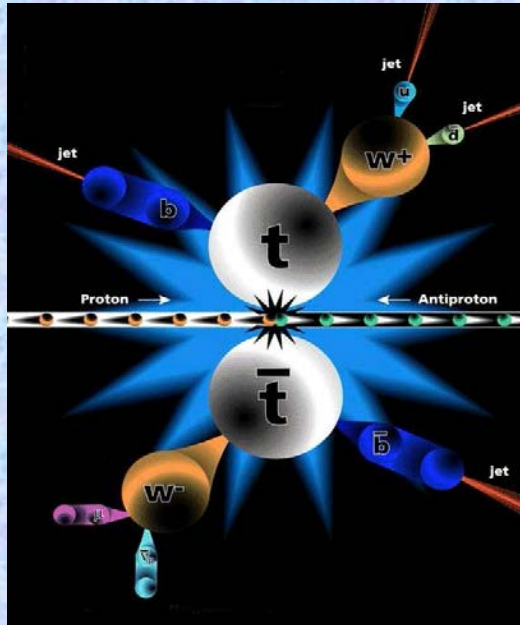
Ratio of detector surface
to nearby electronics
surface 1:300 !

- ❖ 1200 diode strips on 24 x 36mm² active area
- ❖ 250-500 μm thick bulk material
- ❖ 4.5 μm resolution

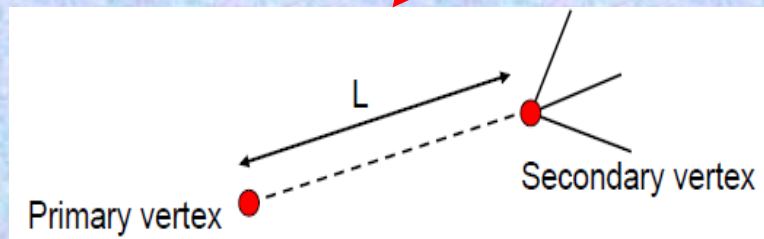
Why Silicon Detectors – Discovery of Top Quark Discovery at Tevatron (1995)

1980's: The post era of the *Z* and *W* discovery, after the observation of Jets at UA1 and UA2 at CERN – “To proceed with high energy particle physics, one has to tag the flavour of the quarks!”

Top Quark Production at Tevatron ($t\bar{t} \rightarrow bW\bar{b}W$):



b -jet identification is crucial,
making use of 1.5 ps b lifetime:
→ flight distance few 100 μm
→ need hit precision $\sim 10 \mu\text{m}$

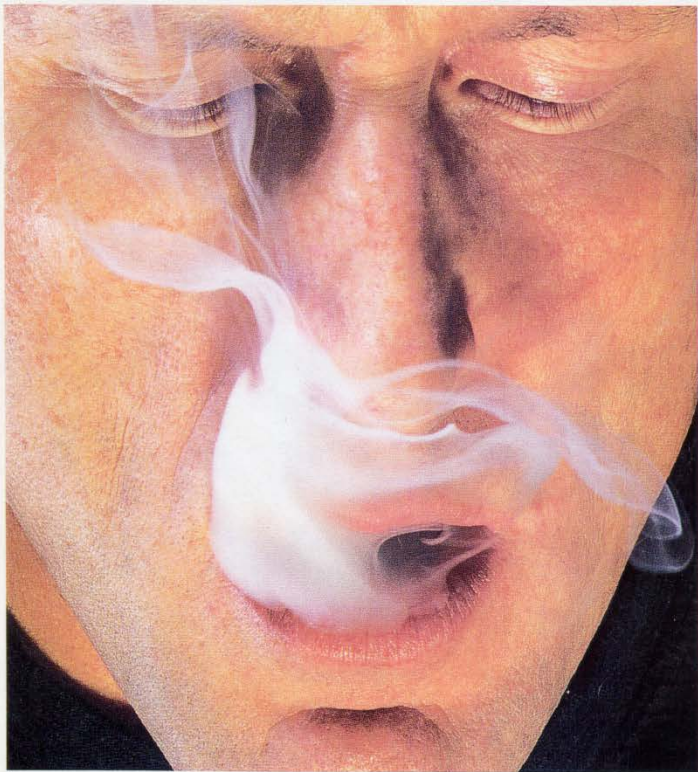


SCIENTIFIC AMERICAN

MAY 1995

\$3.95
U.K. £2.75

What found the top quark.
Archaeology in peril.
The Niels Bohr mysteries.



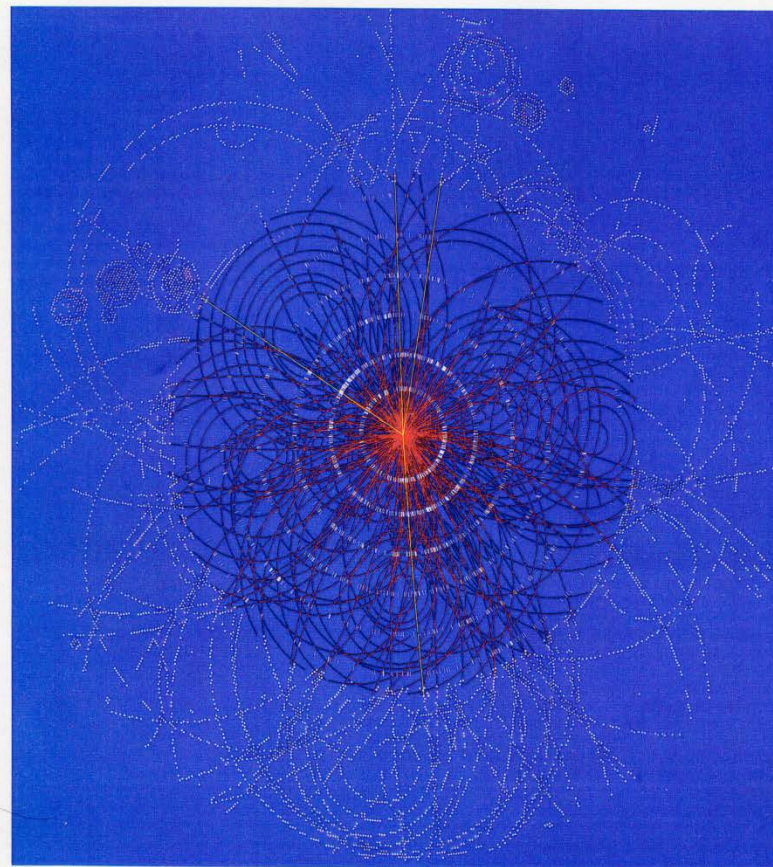
*Clouds of tobacco smoke continue
their spread, despite warnings.*



The Silicon Microstrip Detector

*Produced with the same tools used to create integrated
circuits, these detectors recently helped to find the top quark
and are central to other crucial experiments*

by Alan M. Litke and Andreas S. Schwarz

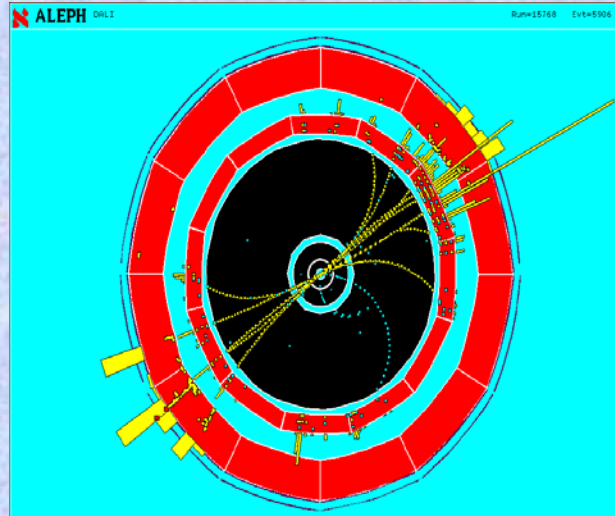


Silicon Detectors has transformed the way we look at particles

1950-1970: Pre-Silicon Era-
photo of ionization trails

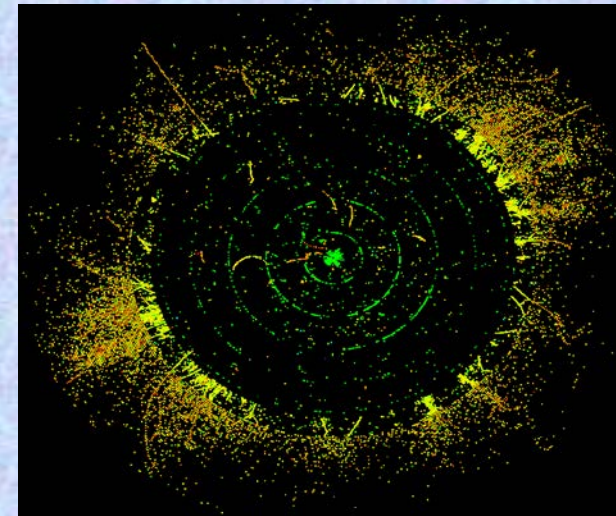


1990: Si-vertex detector
& gaseous tracking (TPC)



2010s: SiD concept for ILC

- Si vertexing
- Si tracking
- Si calorimetry



It might look like we are actually **seeing less** now,
but we can see **a lot more** than in pre-silicon era !

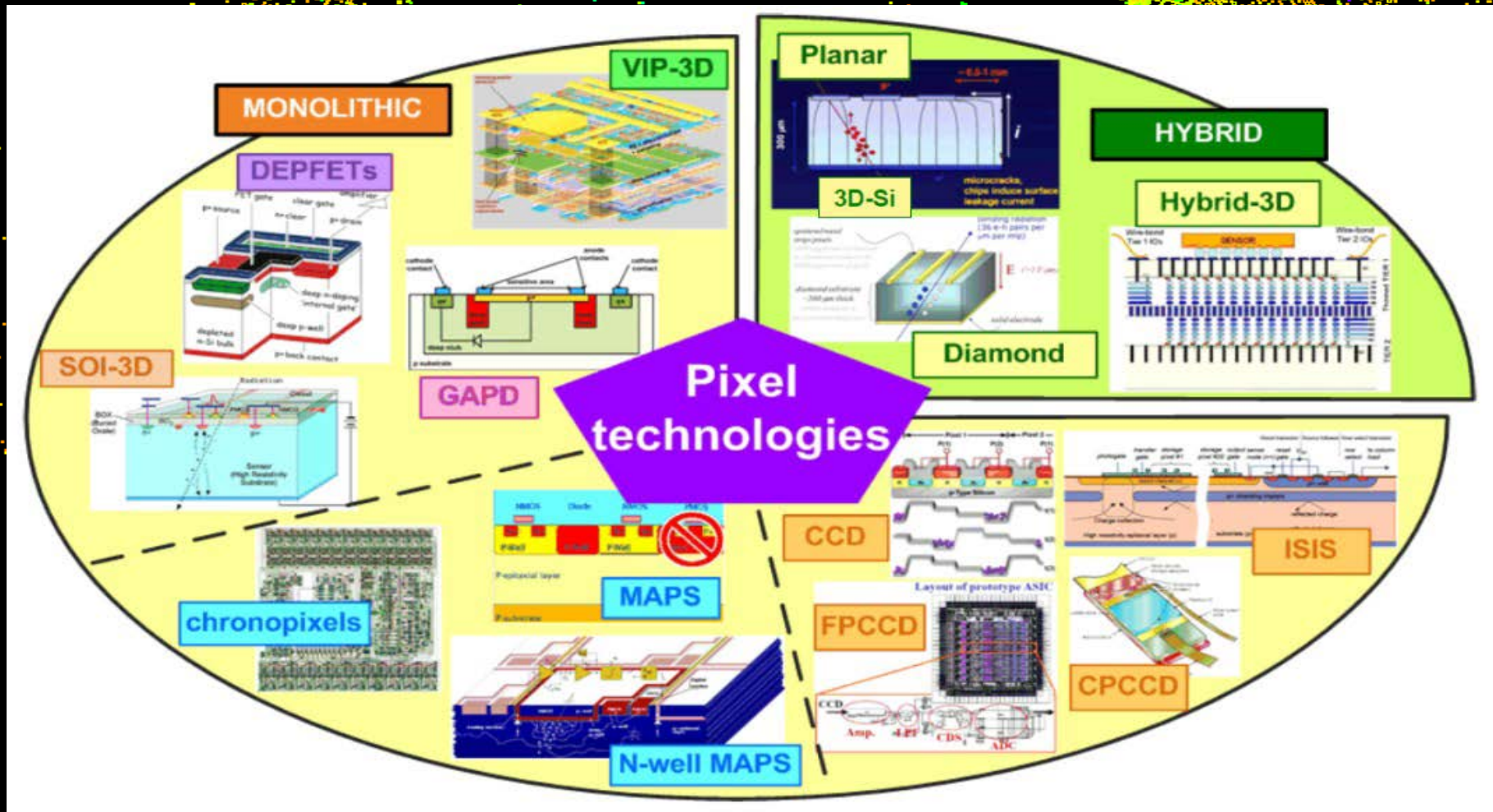
From Microelectronics to Nanoelectronics:

Detectors are more and more based on semi-conductor technology
→ from vertex elements (20 μm feature size) to Si-calorimetry (ILC)

Why are Silicon Detectors such a Success ?

Enormous benefit (compared to gaseous detectors):

- Huge technological advances of silicon technology in the IT industry
- Pattern and structure are industry standard



Why Silicon for Tracking Detectors

- Low ionisation energy (few eV per e-hole pair) compared to gas detectors (20-40 eV per e-ion pair) or scintillators (400-1000 eV to create a photon)
- A condensed medium is obligatory for precision < 10 microns (diffusion of electron cloud in gaseous detectors \sim tens of microns)
- Silicon band gap of 1.1 eV is 'just right'. Silicon delivers ~ 80 electron-hole pairs per micron of track, but kT at room temperature is only 0.026 eV, so dark current generation is modest

Property		Si	Ge	GaAs	Diamant
Z		14	32	31/33	6
A		28.1	72.6	144.6	12.0
Band gap	[eV]	1.12	0.66	1.42	5.5
radiation length X_0	[cm]	9.4	2.3	2.3	18.8
mean energy to generate eh pair	[eV]	3.6	2.9	4.1	~ 13
mean E-loss dE/dx	[MeV/cm]	3.9	7.5	7.7	3.8
mean signal produced	[$e^-/\mu\text{m}$]	110	260	173	~ 50
intrinsic charge carrier concentration n_i	[cm^{-3}]	$1.5 \cdot 10^{10}$	$2.4 \cdot 10^{13}$	$1.8 \cdot 10^6$	$< 10^3$
electron mobility	[cm^2/Vs]	1500	3900	8500	1800
hole mobility	[cm^2/Vs]	450	1900	400	1200

The pn junction (diode): basic principles

A pn junction consists of n and p doped substrates:

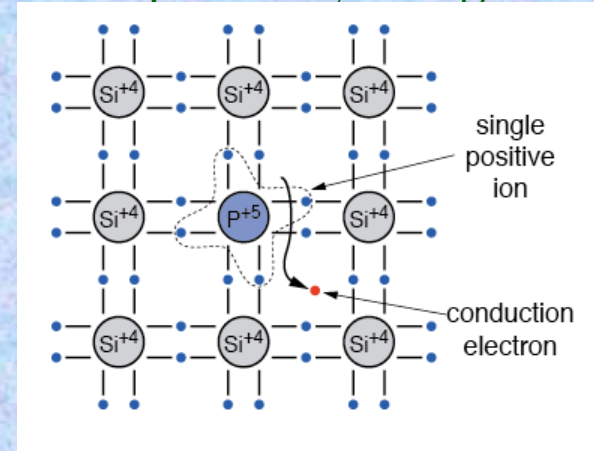
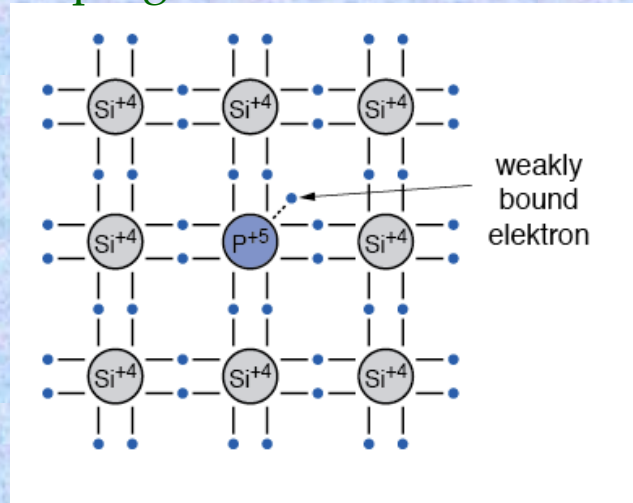
- Doping is the replacement of a small number of atoms in the lattice by atoms of neighboring columns from the atomic table (with one valence electron more or less compared to the basic material). Typical doping concentrations for Si detectors are $\approx 10^{12}$ atoms/cm³ (10^{14} und 10^{18} atoms/cm³ for CMOS elements).
- These doping atoms create energy levels within the band gap and therefore alter the conductivity.
- An undoped semiconductor is called an intrinsic semiconductor
- A doped semiconductor is called an extrinsic semiconductor.
- In an intrinsic semiconductor for each conduction electron there exists the corresponding hole. In extrinsic semiconductors there is a surplus of electrons or holes.

Basic Solid State Physics: n-doping

Doping with element 5 atom (e.g. P, As, Sb). The 5th electron is weakly bound

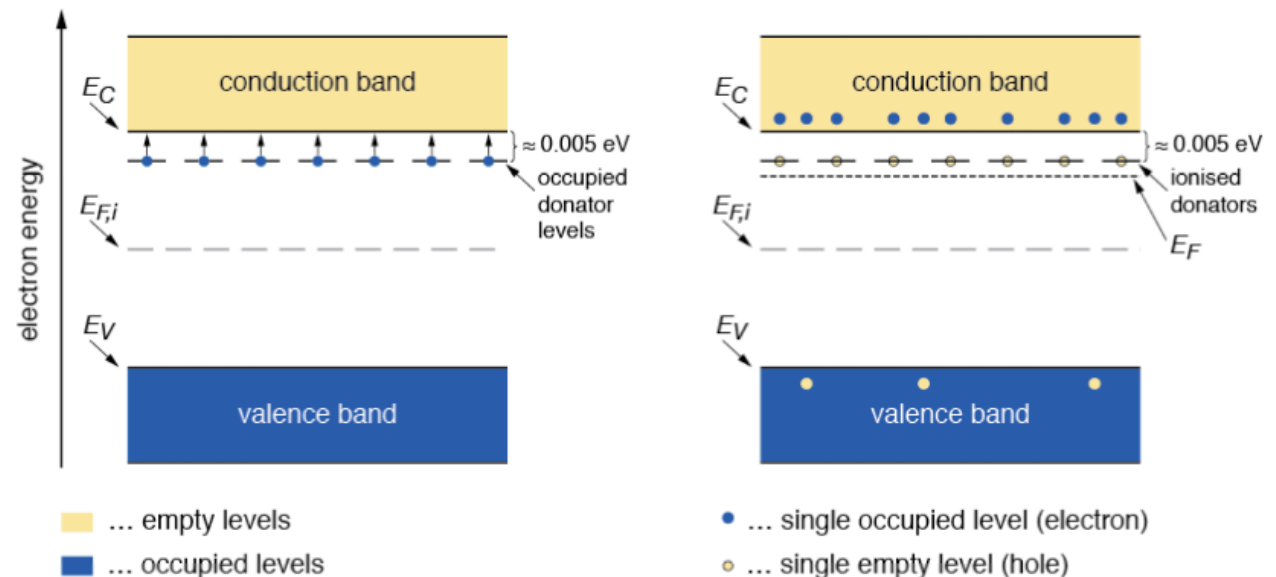
The doping atom is called donor

The released conduction electron leaves positively charged ion



- The energy level of the donor is close to the edge of the conduction band.

- At room T most electrons are raised to the conduction band. The fermi level E_F moves up.

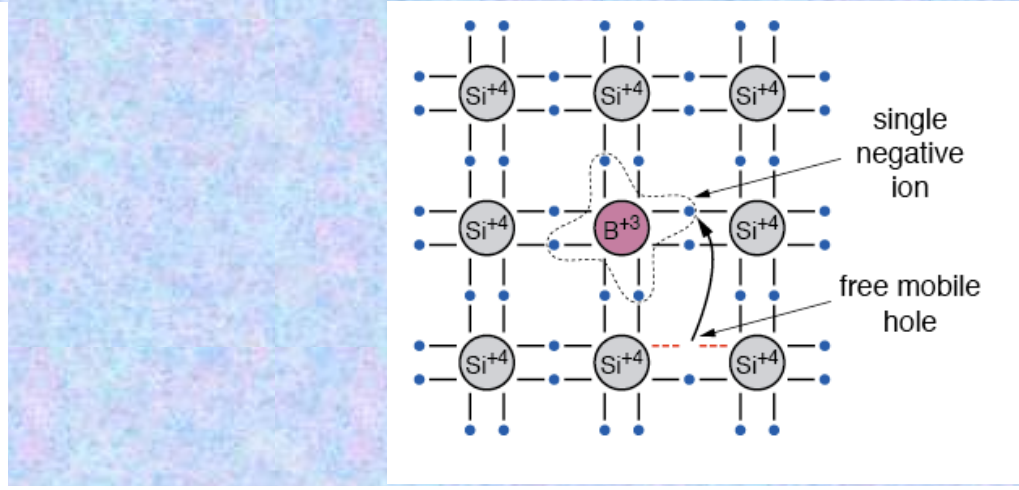
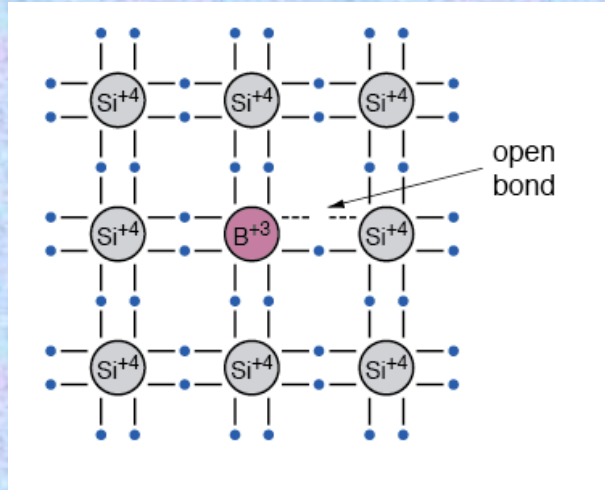


Basic Solid State Physics: p-doping

Doping with element 3 atom (e.g. B, Ga, In). One valence bond remains open. This bond attracts electrons from neighboring atoms.

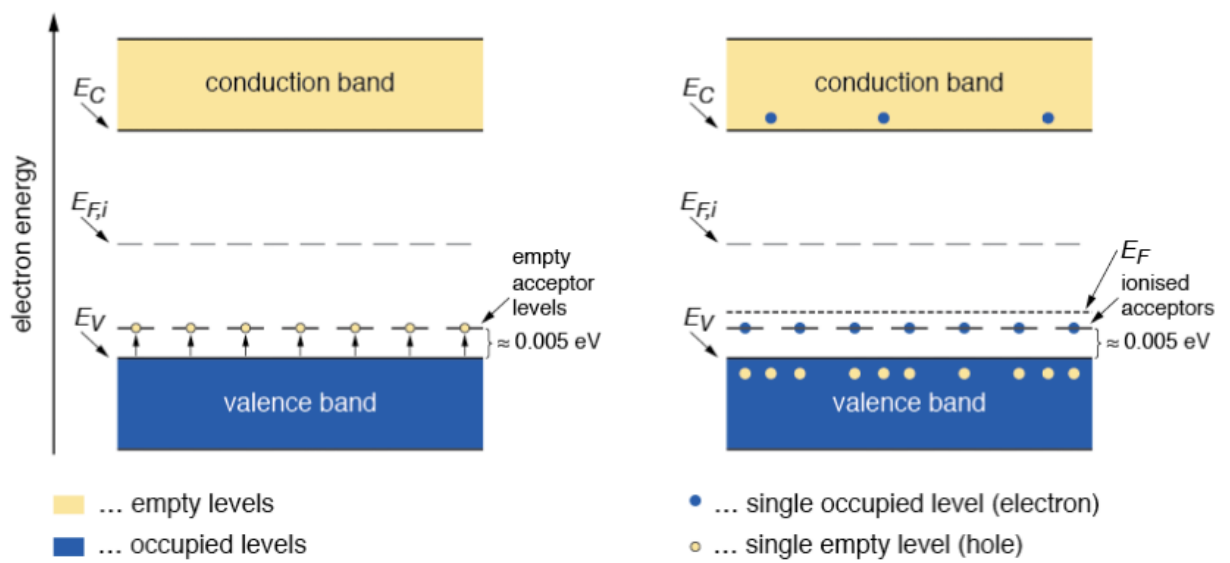
The doping atom is called acceptor

The acceptor atom is negatively charged



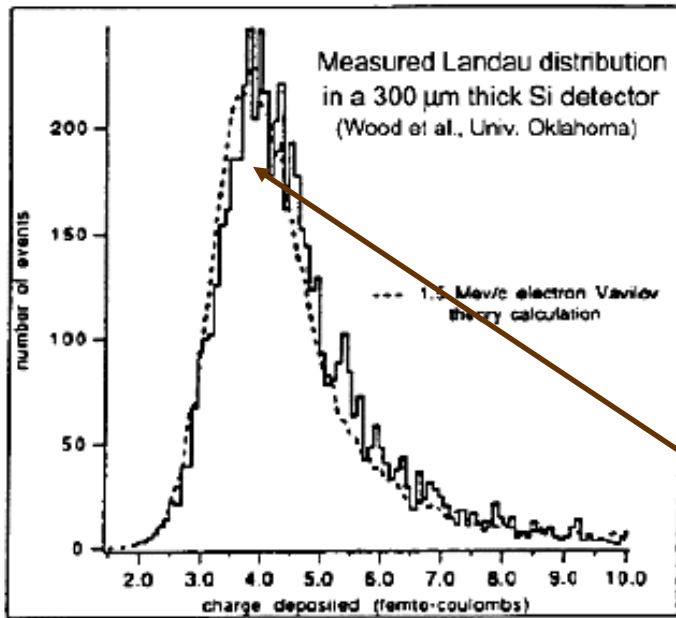
- The energy level of the acceptor is close to the edge of the valence band.

- At room T most levels are occupied by electrons leaving holes in the valence band. The fermi level E_F moves down.



Intrinsic Semiconductors: Signal Formation

Let's take a piece a Si and wait for a passing of charged ionizing particle



Signal of a MIP in d=300 μm Si-detector:

$$\frac{dE/dx \cdot d}{I_0} = \frac{3.87 \text{ eV/cm} \cdot 0.03 \text{ cm}}{3.62 \text{ eV}} \sim 3 \cdot 10^4 \text{ (e/h pairs)}$$

- Fluctuations give the famous Landau distribution → the most probable value is 0.7 of the peak
- The most probable value is 22000 e/h pairs

Intrinsic charge carrier in Si (in d = 300 μm & area A = 1 cm²) at T = 300 K:

$$n_i \cdot d \cdot A = 1.45 \cdot 10^{10} \text{ cm}^{-2} \cdot 0.03 \text{ cm} \cdot 1 \text{ cm}^2 \sim 4.35 \cdot 10^8 \text{ e/h pairs}$$

Number of thermal charge carriers (at room temperature) are four orders of magnitude larger than signal !!!

→ Cool the solid-state detectots (n_i at 77K $\sim 10^{-20}$) → complicated

→ Deplete the volume from free charge carriers & to register MIP signal

→ pn Junction

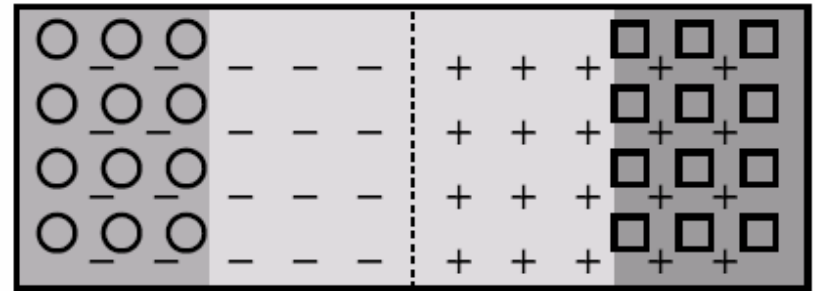
The pn-Junction

Now, for the magic part → we can construct pn junction

- When brought together to form a junction, the majority diffuse carriers across the junction.
- The migration leaves a region of net charge of opposite sign on each side, called the space-charge region or **depletion region**.
- The electric field set up in the region prevents further migration of carriers.

electrons drift towards p-side, holes towards n-side
buildup of a potential

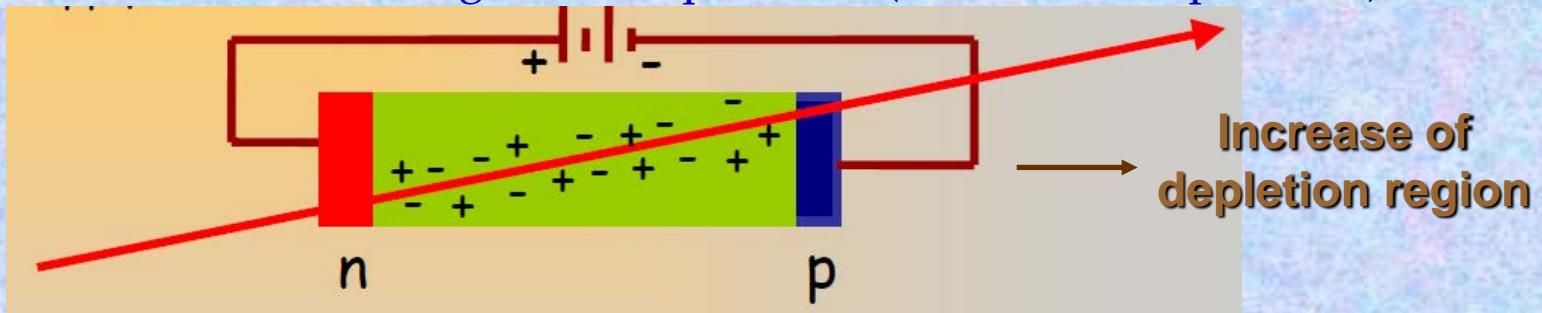
p-type region n-type region



depletion zone

○ hole □ electron - acceptor ion + donor ion

The depleted part is very nice, but very small → apply external voltage in the same direction as generated potential (reverse bias operation)



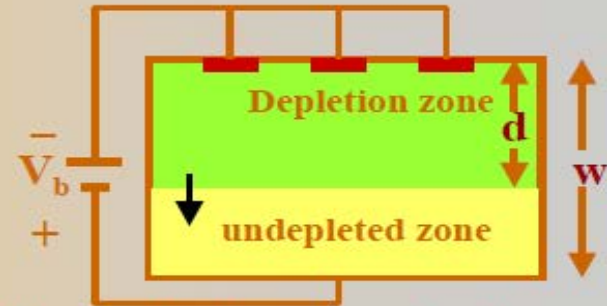
The depletion zone can be used as detector, since it contains an electric field (and is depleted of free charges).

Properties of the Depletion Zone

- Depletion width is a function of the bulk resistivity, charge carrier mobility μ and the magnitude of the reverse bias voltage V_b :

$$d = \sqrt{2\varepsilon\rho\mu V_b}$$

where $\rho = 1/q\mu N$ for doped material and N is the doping concentration (q is always the charge of the electron)



- The voltage needed to completely deplete a device of thickness d is called the depletion voltage, V_d

$$V_d = w^2 / (2\varepsilon\rho\mu)$$

Effective doping concentration $N_a = 10^{15} \text{ cm}^{-3}$ in p+ region and $N_d = 10^{12} \text{ cm}^{-3}$ in n bulk.

Without external voltage:

$$d_p = 0.02 \mu\text{m}$$

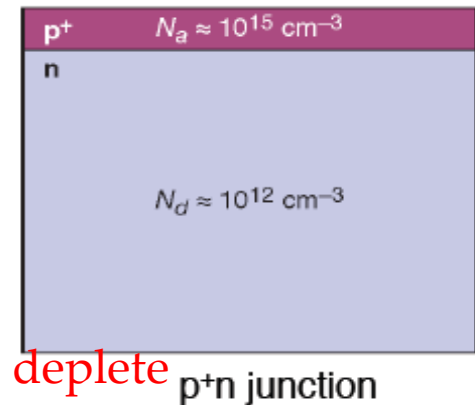
$$d_n = 23 \mu\text{m}$$

Applying a reverse bias voltage of 100 V:

$$d_p = 0.4 \mu\text{m}$$

$$d_n = 363 \mu\text{m}$$

100 V is enough to deplete
~ 300 μm Si-detector

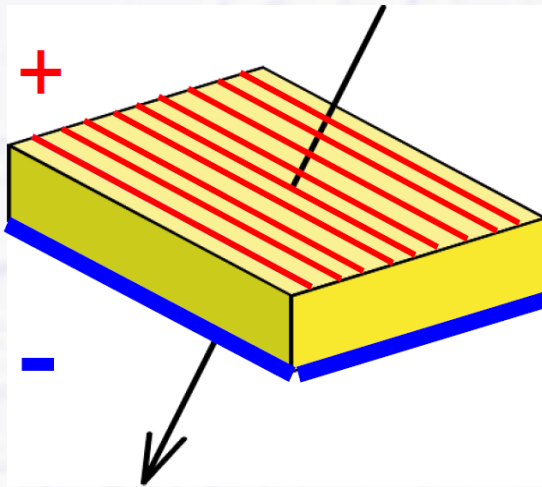


Silicon Tracking Detector

- Now take a large Si crystal, e.g. $10 \times 10 \text{ cm}^2$, $300 \mu\text{m}$ thick

make bottom layer p-type

and subdivide the top n-type layer into many strips with small spacing

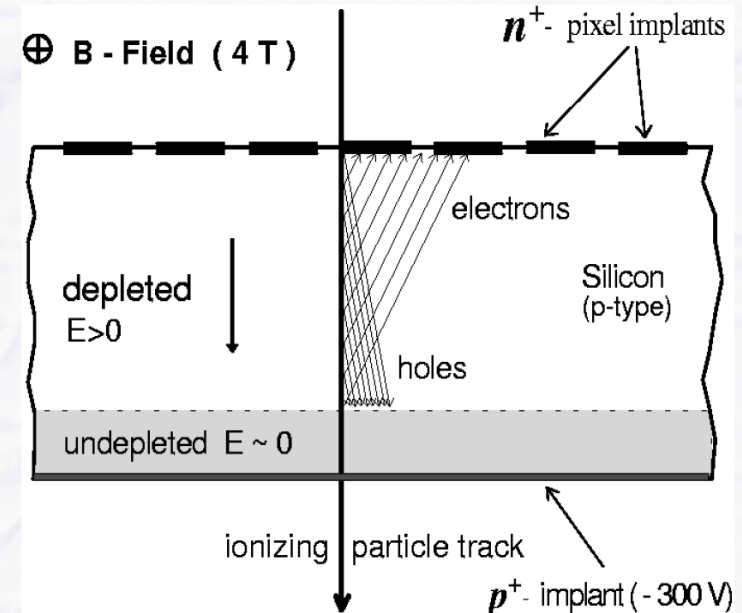


many diodes next to each other (like MWPC at wire chambers) with position information

- Advantage compared to wire/gas detectors

→ strip density (pitch) can be rather high (e.g. $\sim 20 \mu\text{m}$)

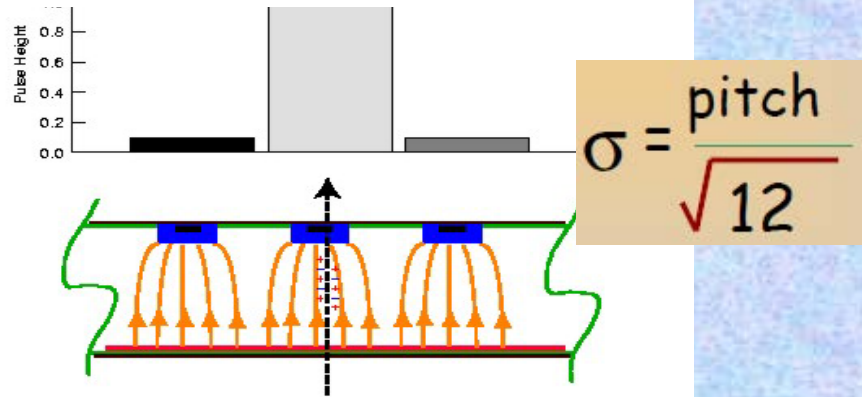
- high position accuracy
- but also many electronics channels needed



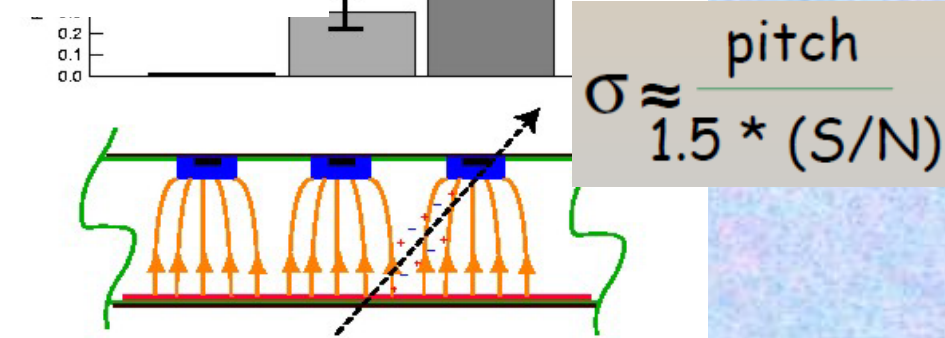
Silicon Microstrip Detector: Spatial Resolution

Resolution \rightarrow difference between reconstructed position and true position

For one strip cluster:



For two strip clusters:

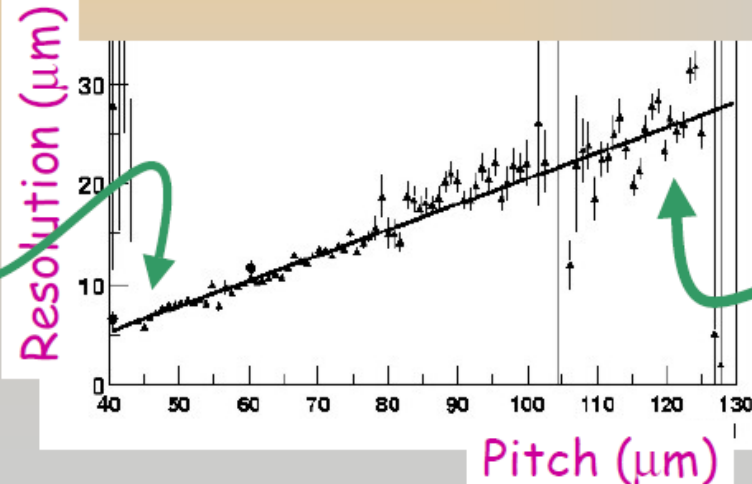


In real life, position resolution is degraded by many factors

- relationship of strip pitch and diffusion width (typically 25-150 μm and 5-10 μm)
- Statistical fluctuations on the energy deposition

Typical values of 300 μm thick sensor with $S/N \sim 20$:

Here charge sharing dominates



Here single strips dominate

Detector Characteristics: Leakage Current (IV curves)

Silicon detector is operated with reverse bias \rightarrow the leakage current is dominated by thermally generated e/h pairs. Due to the applied field they can not recombine and are separated.

Measure IV curve to check maximum long-term stability of the sensor and maximum V_{bias} :

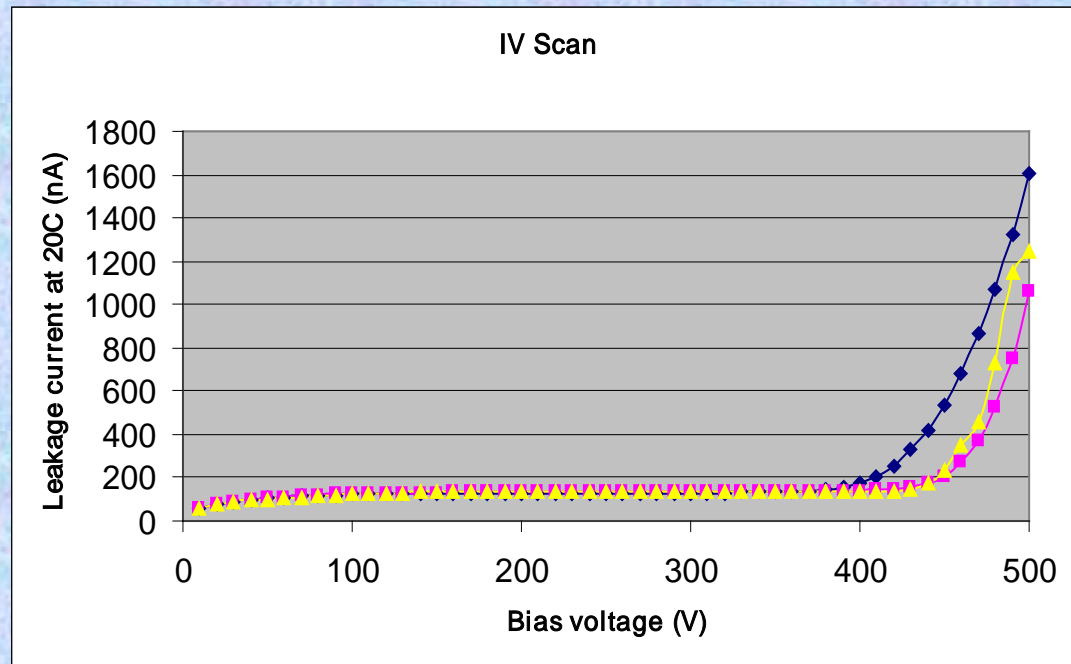
If V_{bias} too large, get high currents (breakdown):

Zener breakdown

- Tunnelling from occupied state in p side valence band to n side conduction band

Avalanche breakdown

- Carriers from leakage current get so much kinetic energy that due to collisions new free carriers are generated



Silicon Microstrip Detector: Signal to Noise Ratio

- Example of noise

- Some typical values for LEP silicon strip modules (OPAL):
 - $ENC = 500 + 15 \cdot C_d$
 - Typical strip capacitance is about 1.5pF/cm, strip length of 18cm so $C_d=27\text{pF}$

so ENC = 900e. Remember S=22500e

$$\Rightarrow S/N \approx 25/1$$

- Some typical values for LHC silicon strip modules

- $ENC = 425 + 64 \cdot C_d$
- Typical strip capacitance is about 1.2pF/cm, strip length of 12cm so $C_d=14\text{pF}$

so ENC = 1300e

$$\Rightarrow S/N \approx 17/1$$

Capacitive term is much worse for LHC in large part due to very fast shaping time needed (bunch crossing of 25ns vs 22μs for LEP)

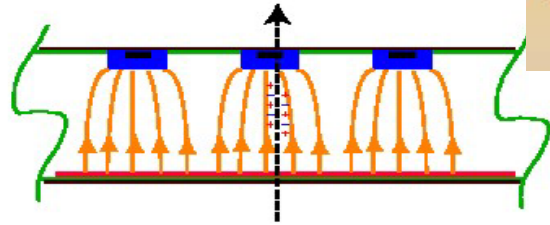
Silicon Microstrip Detector: Spatial Resolution

Resolution \rightarrow difference between reconstructed position and true position

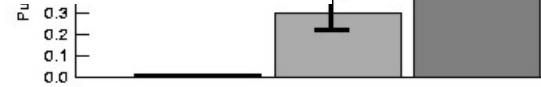
For one strip cluster:



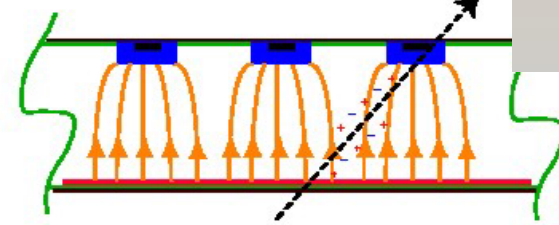
$$\sigma = \frac{\text{pitch}}{\sqrt{12}}$$



For two strip clusters:



$$\sigma \approx \frac{\text{pitch}}{1.5 * (S/N)}$$

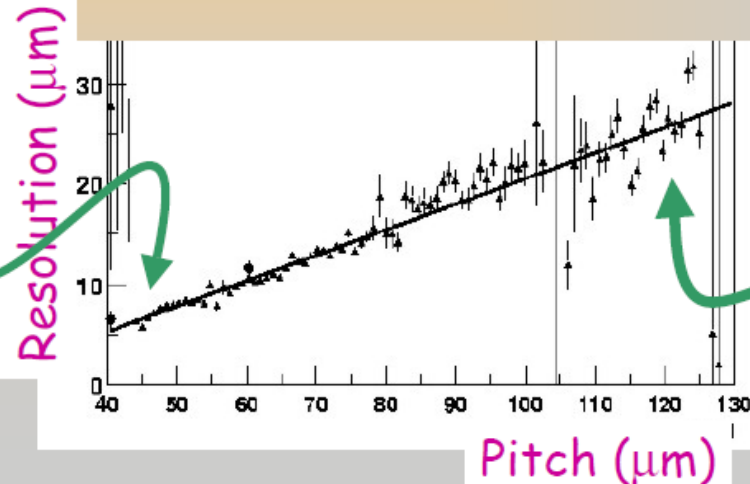


In real life, position resolution is degraded by many factors

- relationship of strip pitch and diffusion width (typically 25-150 μm and 5-10 μm)
- Statistical fluctuations on the energy deposition

Typical values of 300 μm thick sensor with $S/N \sim 20$:

Here charge sharing dominates



Here single strips dominate

Silicon Detectors: Radiation Damage

● Solid state detectors suffer from radiation damage

→ lots of R&D effort was spent over the past years to understand and to develop radiation-hard Si-detectors that can survive 10 LHC years

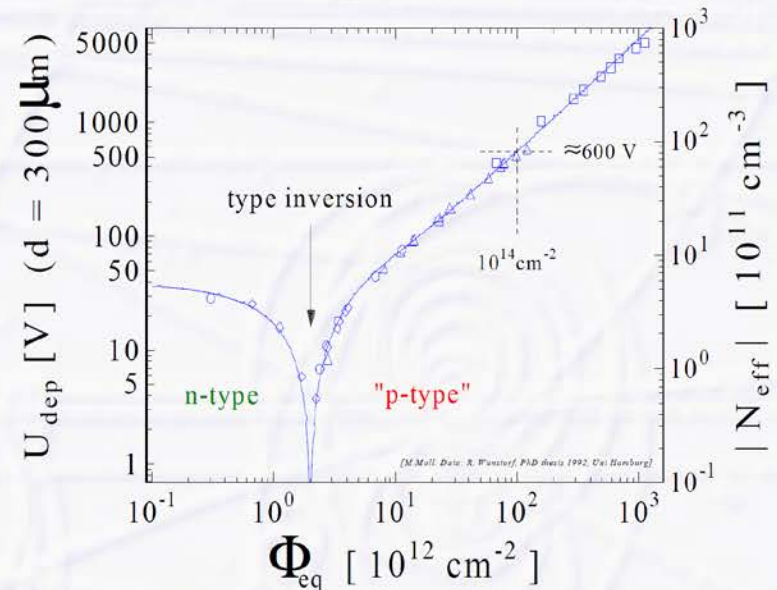
● Two general types of radiation damage

→ **bulk (crystal) damage** (mainly by nuclear interactions of protons/neutrons)

- change of depletion voltage
 - up to “type inversion”
n-type material becomes p-type material
- increase of leakage current
 - higher noise, more cooling needed
- decrease of charge collection efficiency
 - less signal

→ **surface damage**

- accumulation of positive ions on surface insulating structures (oxides)
 - higher noise, breakdown



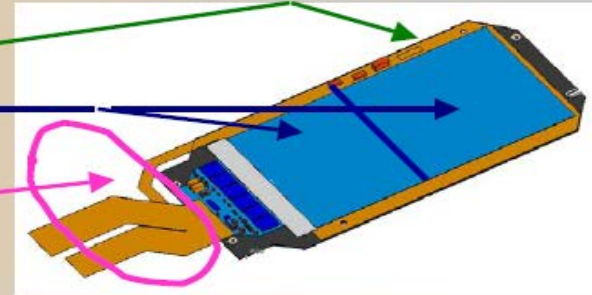
“Type inversion”: n-type material changes to p-type material after a certain accumulated radiation dose

From Si-sensor to a Full Detector Module

“Module” → the basic building block of a silicon tracking detector

- Modular design: try to make identical sub-units. Units consist of:

- mechanical support structure
- sensors
- front-end electronics and signal routing (connectivity)



Frame of carbon fiber

Micro-bonding

Front-end hybrid



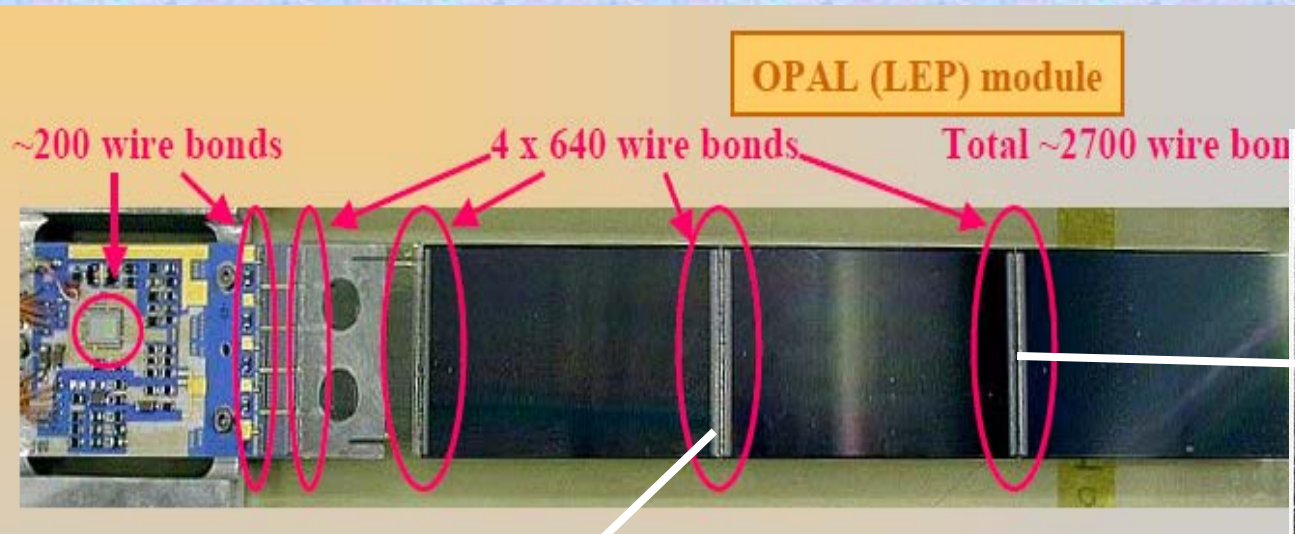
Sensors

Kapton & filter circuit

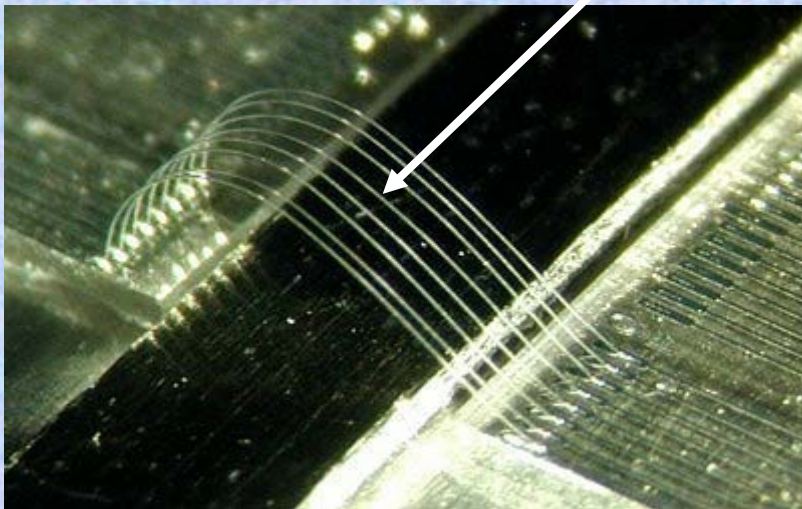
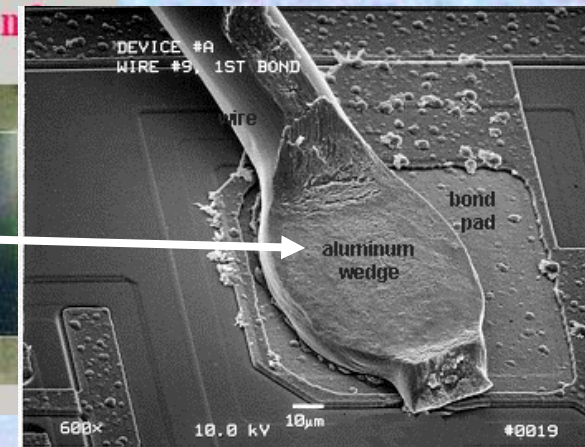
Pitch adapter (glass)

Front-End electronics and connectivity: Wire bonding

Wire bonding – A “mature” technology (has been around for 40 years) → the standard method for connecting sensors to each other and to the front-end chips.



SEM Image of bond “foot”:



- Uses ultrasonic power to vibrate needle-like tool on top of wire (17-25 µm Al wire). Friction welds wire to metalized substrate underneath.
- Heavily used in industry (PC processors) but not with such thin wire or small pitch.

Si-Detector Electronics and Si-Pixels

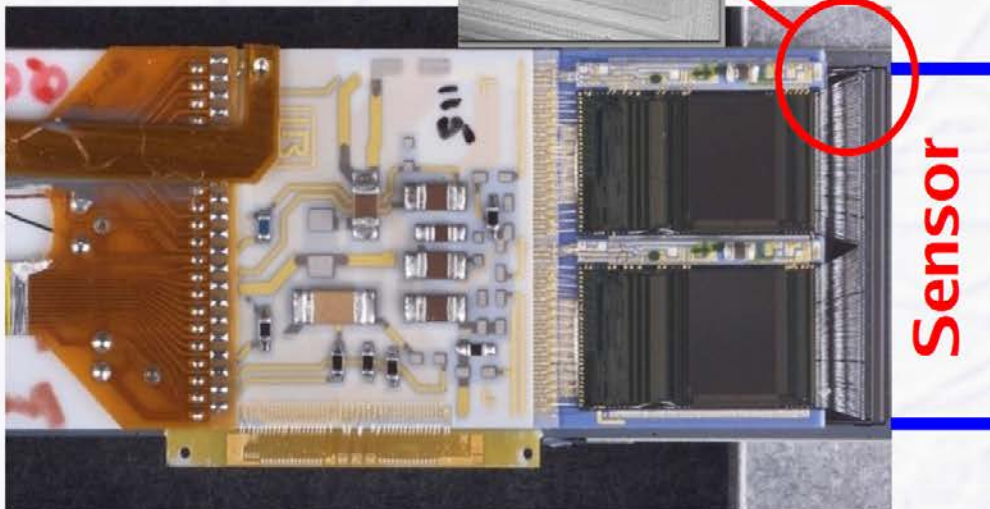
- Silicon detectors have a large number of electronics channels, $\sim 10^7$ each for ATLAS and CMS Si trackers

- requires highly integrated chips for amplification, shaping, zero suppression (only information of strips with signals is read-out) and multiplexing (put all strip signals on a few cables only)

→ electronics is directly connected to the sensor (the “multi-diode”) via wire bonds

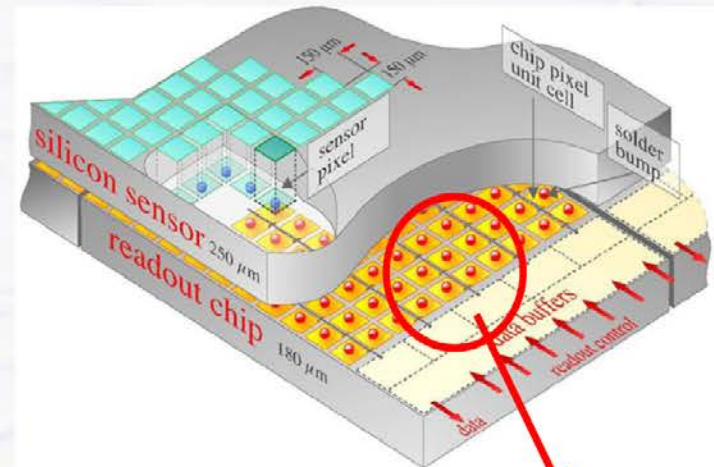


wire bonds

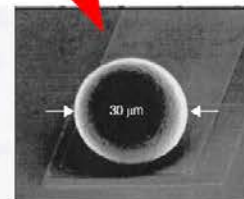


Sensor

Si-strip detectors provide only 1 coordinate, Pixel detectors are 2D detectors



Pixel detector need “bump” bonding and have even more channels, $\sim 10^8 - 10^9$



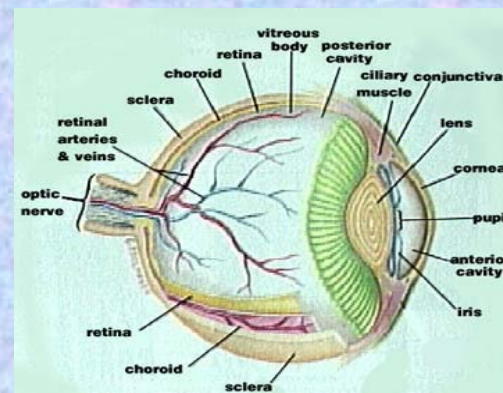
From Si-microstrip to Pixel Detector

Instead of strips measuring one dimension, have a matrix of points measuring two dimensions

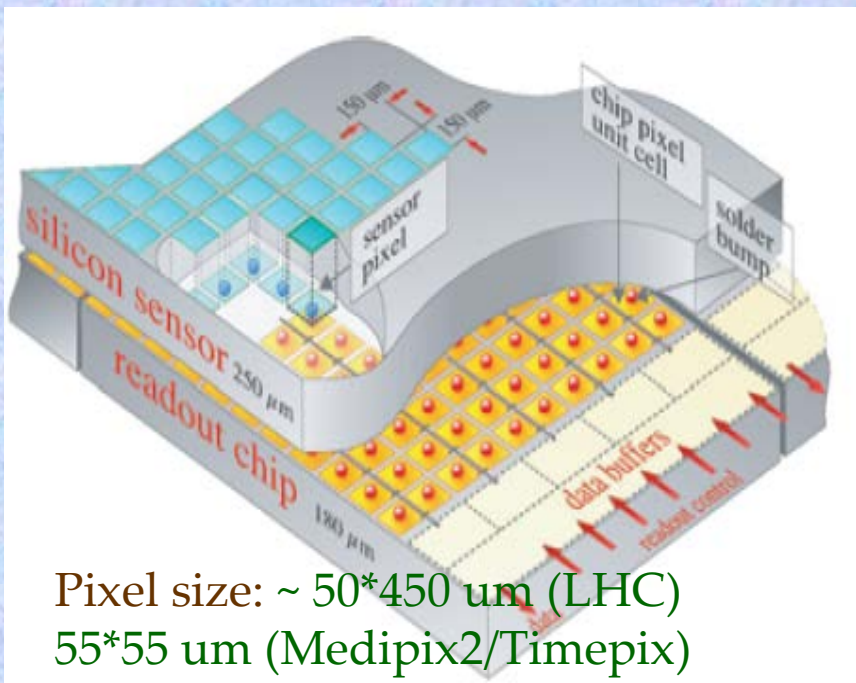
as used
In this



and in this



Two dimensional array (each electronic channel mounted directly on its pixel)



Pixel size: ~ 50*450 μm (LHC)
55*55 μm (Medipix2/Timepix)

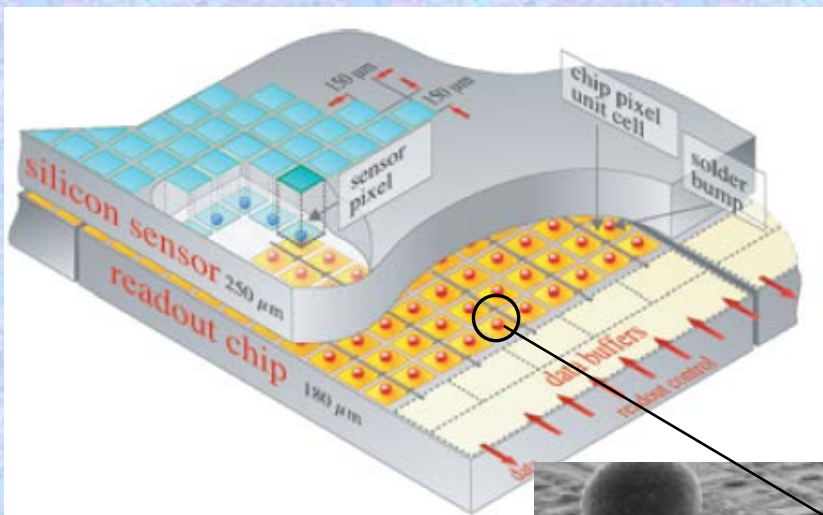
Sensor is just like a strip sensor but with the p+ implants further subdivided into tiny squares

- Biasing, depletion works in the same way
- Low leakage current: ~1pA/pixel
- Low detector capacitance (~1fF/pixel): S/N ~ 150/1
- “Radiation hard” due to large S/N margin

Hybrid Pixel Detector

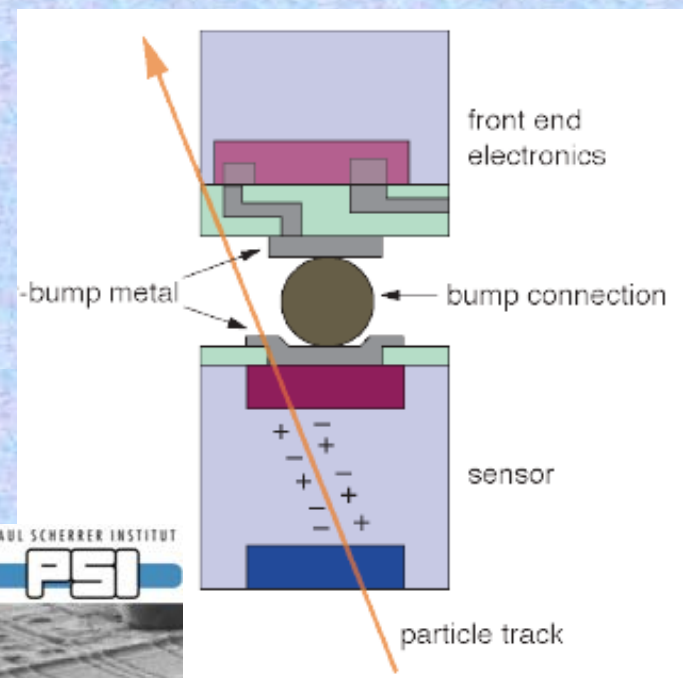
"Flip-chip" pixel detector:

On top of Si detector, below the readout chip, bump bonds make electrical connection for each pixel



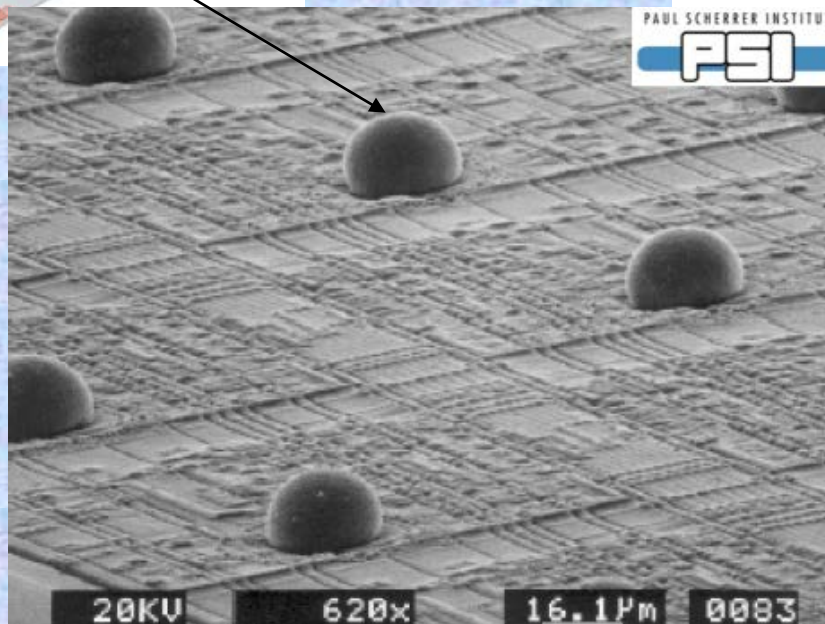
Details of the bump-bond connection:

Bottom is the detector, on top the readout chip



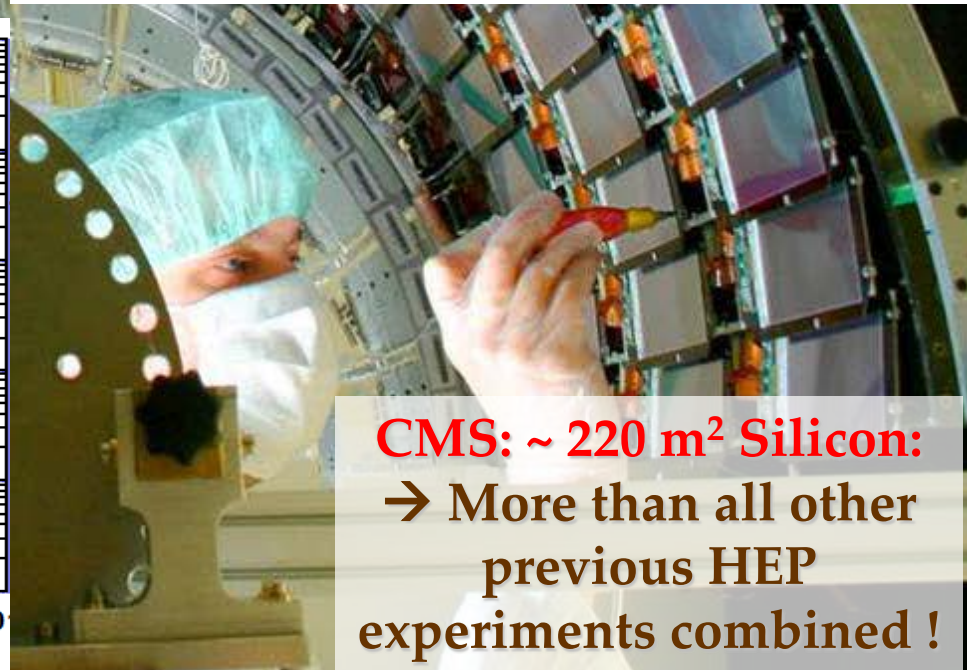
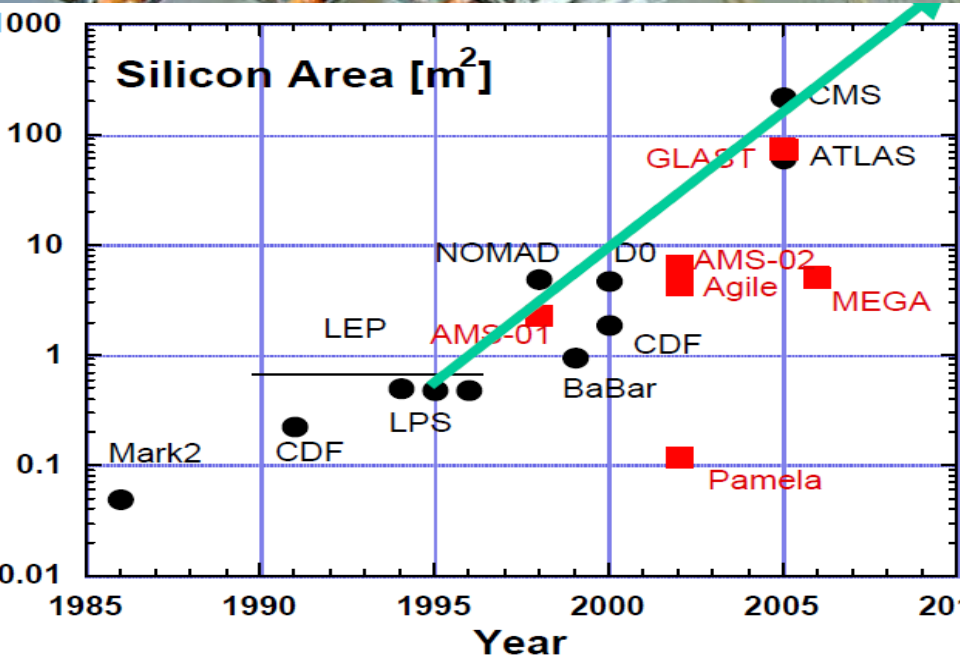
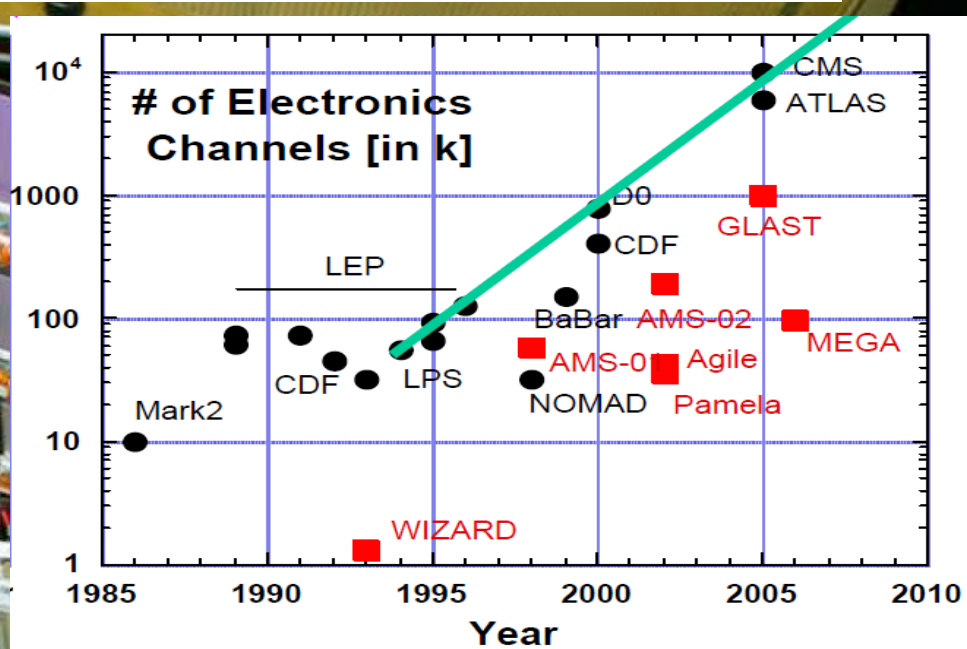
Bonds:

- 50 μm pitch
- PbSn or In
- 6-20 μm high
- ~ 3000/chip
- ~ 50000/module



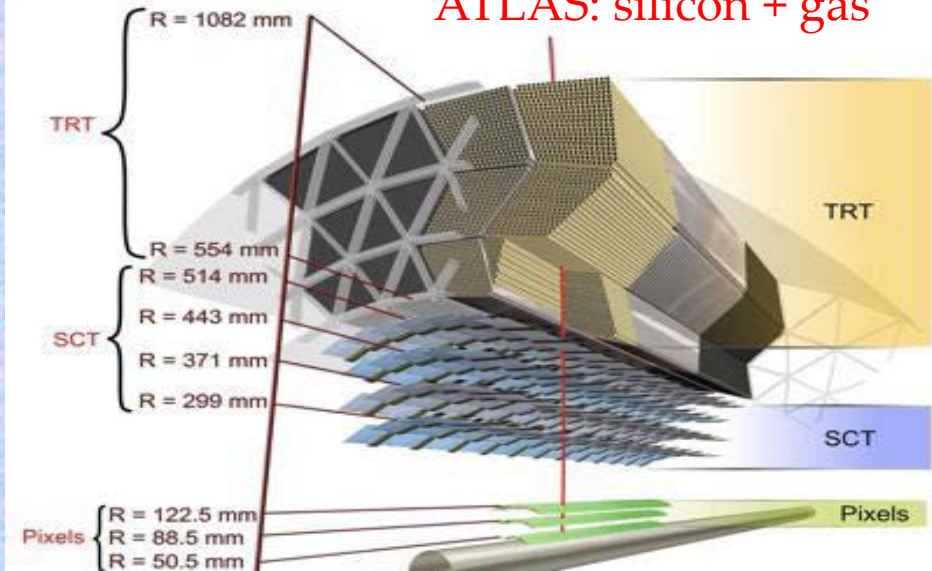
Bump-bond failure rate (CMS) ~ 10⁻⁴

Silicon Detectors in Particle Physics: Evolution of Scale

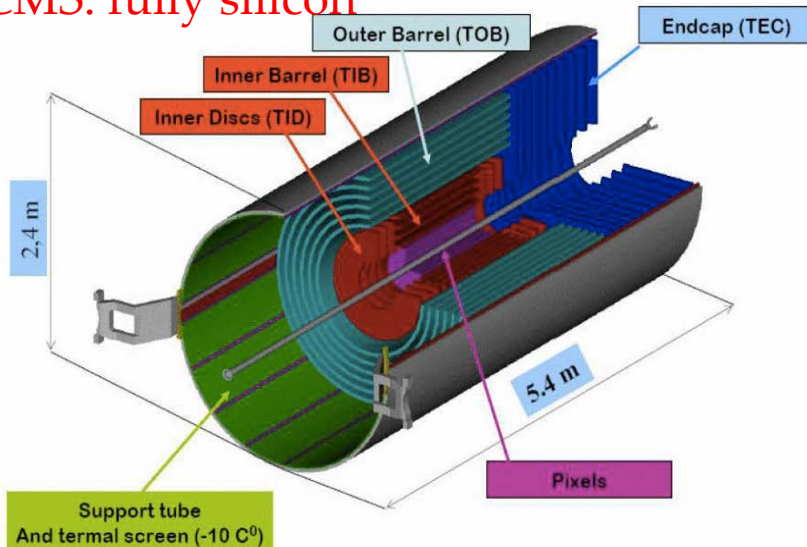


Tracking Systems

ATLAS: silicon + gas



CMS: fully silicon

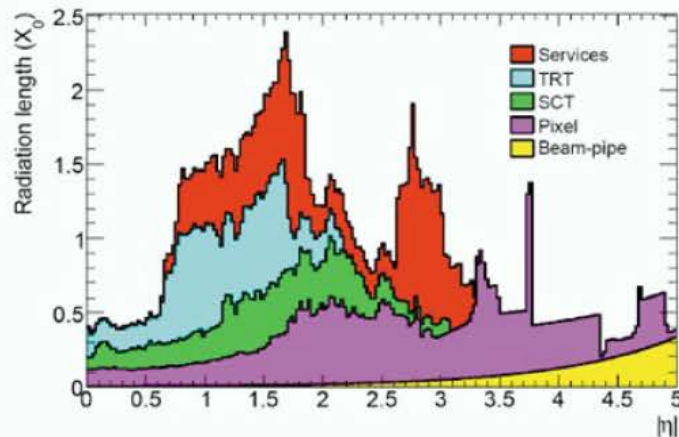


	ATLAS	CMS
Magnetic field (T)	2	4
Pixels:		
#hits	3	3
resolution (μm)	≈ 10	≈ 10
radius inner/outer	5.1/12.3	4.4/10.2
pixel size (μm^2)	50x400	100x150
channels	80 M	66 M
Silicon Microstrips:		
#hits	8	14
strip pitch (μm)	80	80/120
radius inner/outer (cm)	30/60	20/107
channels	6.2 M	9.6 M
Straw Tube Tracker		
#hits	35	
radius inner/outer (cm)	60/107	
cell size/strip pitch	4mm	
channels	0.35 M	

Material Budget

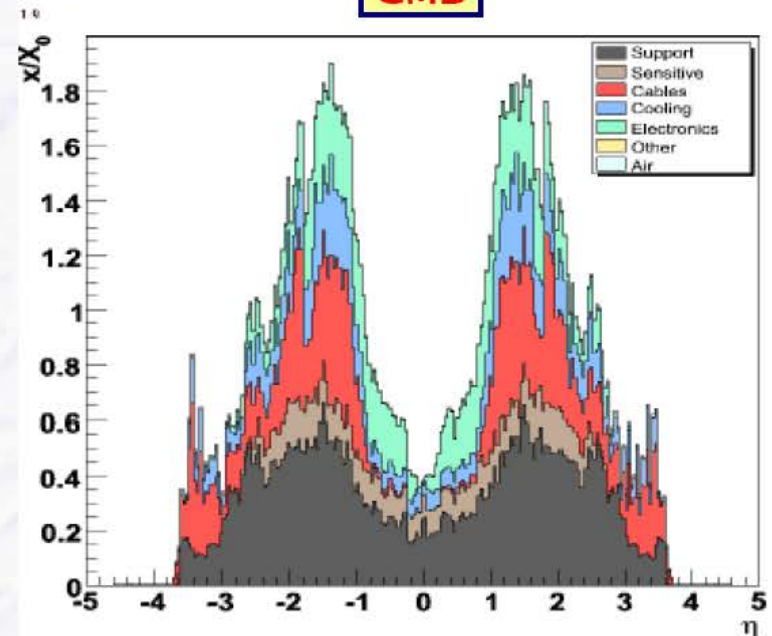
- **Tracking Detectors should be light-weighted and thin**
 - multiple scattering by material degrades resolution at low momenta
 - unwanted photon conversions in front of calorimeters
 - material often very inhomogeneous (in particular Si detectors)
- **Power & cooling adds most of the material**
 - not the Si sensor material

ATLAS



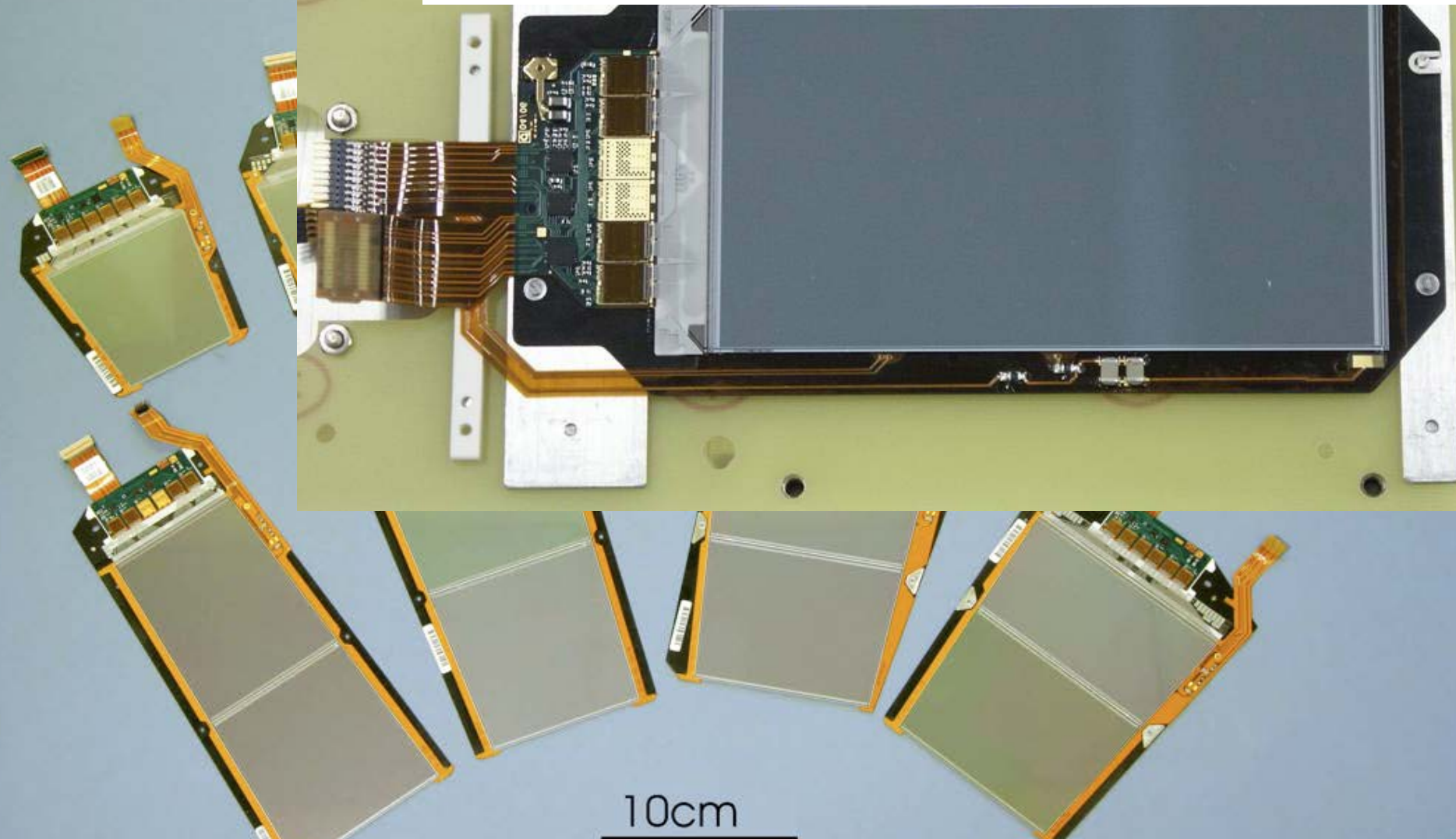
$ \eta $	radiation length	interaction length
< 1	$\sim 0.2 X_0$	$\sim 0.05 \lambda$
< 3.3	$\lesssim 0.5 X_0$	$\lesssim 0.2 \lambda$

CMS



The CMS Silicon Strip Module Examples

2D measurement → two singled-sided sensors are glued back-to-back with stereo angle using a robot (tolerances are few μm)

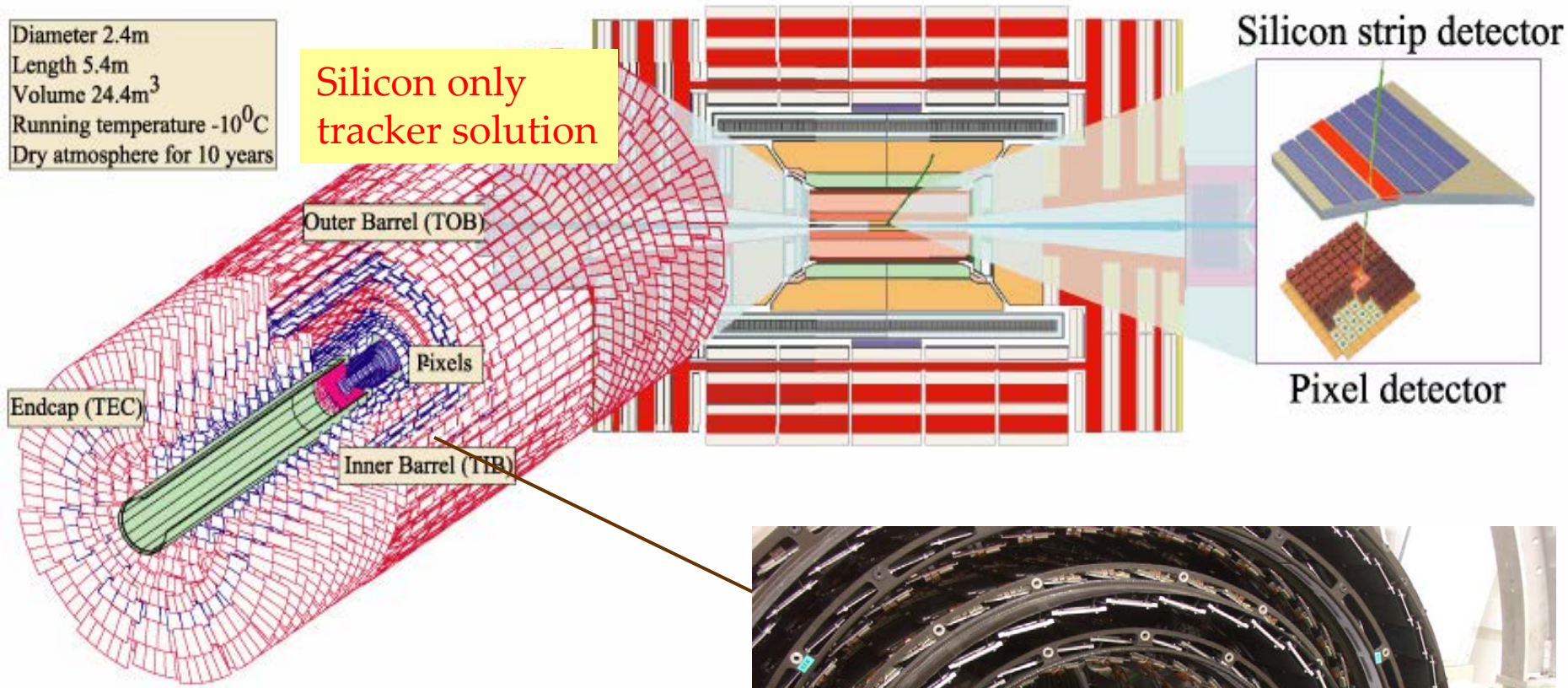


27 mechanical different modules + 2 types of alignment modules

The CMS Tracker: Pixels and Strips

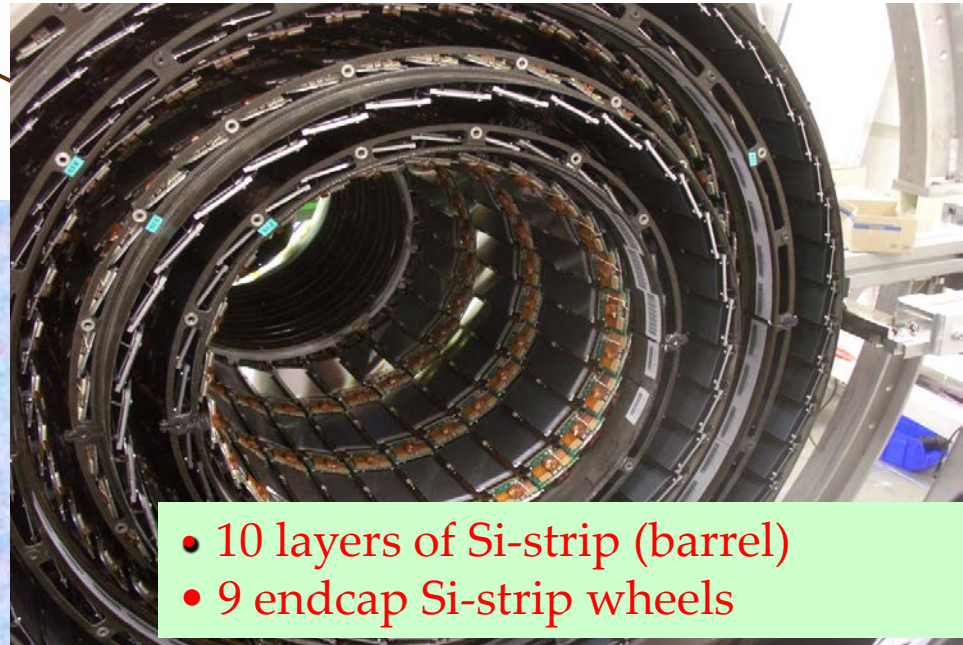
Diameter 2.4m
Length 5.4m
Volume 24.4m³
Running temperature -10⁰C
Dry atmosphere for 10 years

Silicon only
tracker solution



Silicon Strip Detectors: 220 m²

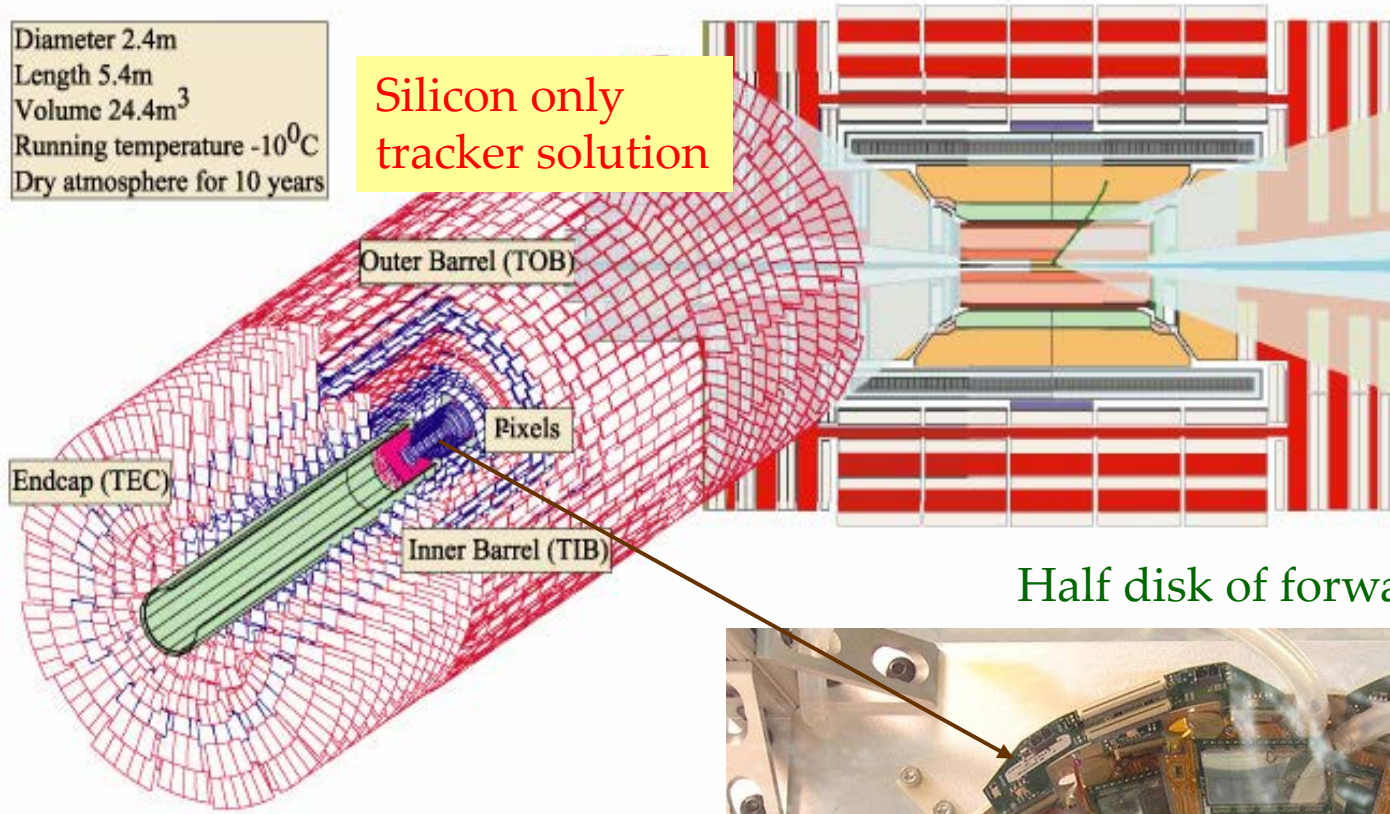
- 25000 silicon sensors
- 10 M strips = electronic ch.
- 75376 readout chips
- 26.000.000 bonds
- 37.000 analog optical links



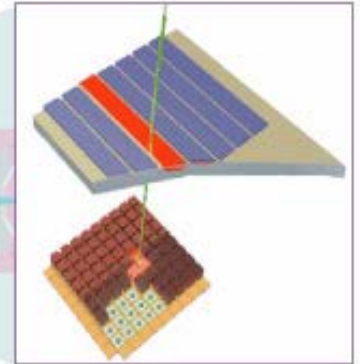
The CMS Tracker: Pixels and Strips

Diameter 2.4m
Length 5.4m
Volume 24.4m³
Running temperature -10⁰C
Dry atmosphere for 10 years

Silicon only
tracker solution



Silicon strip detector



Pixel detector

Half disk of forward pixels:

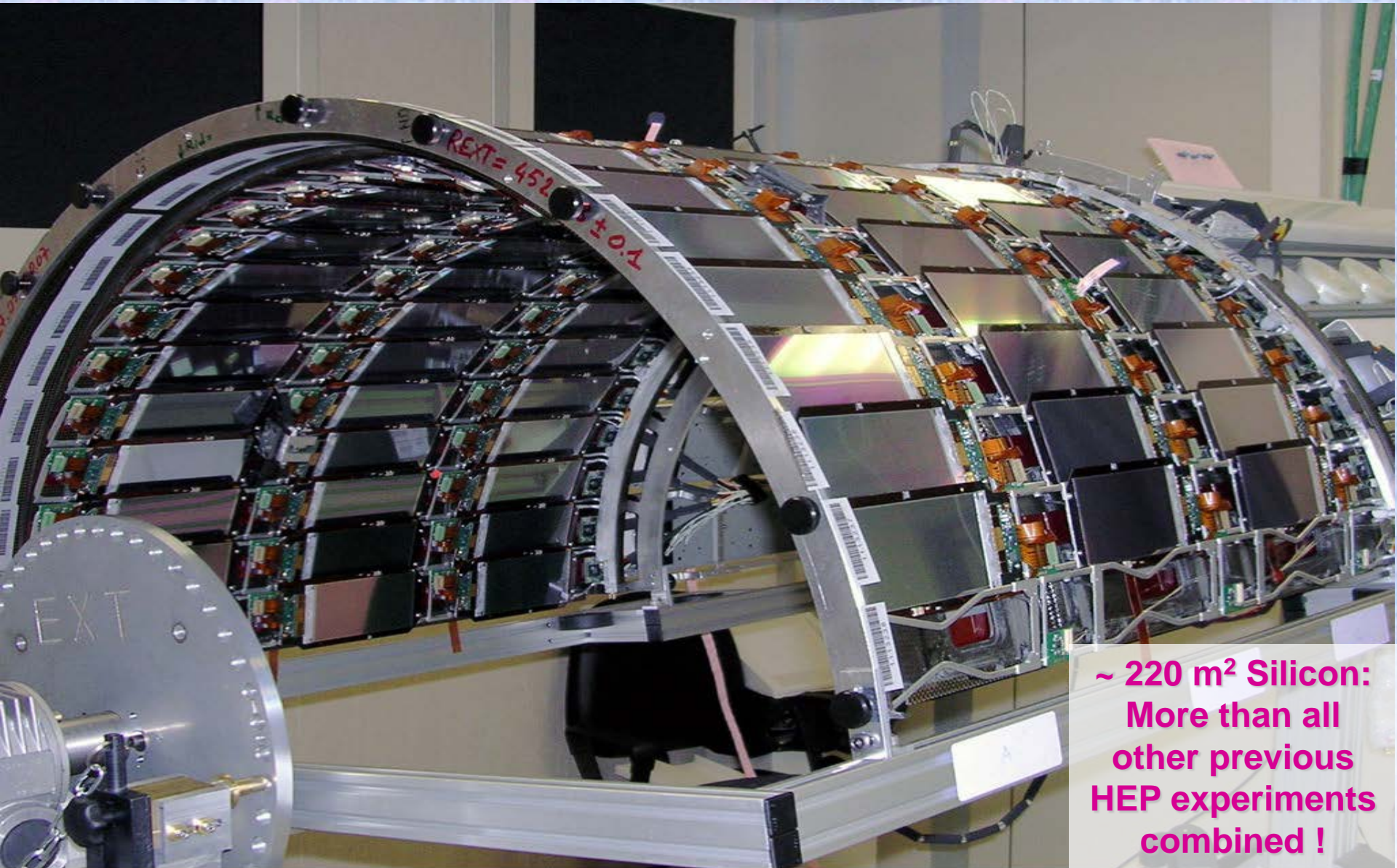


Pixel Detector: ~ m²

- 3 layers of pixels
- 1440 pixel modules
- 66 M pixel =
electronic channels

The CMS Inner Central Detector (Barrel)

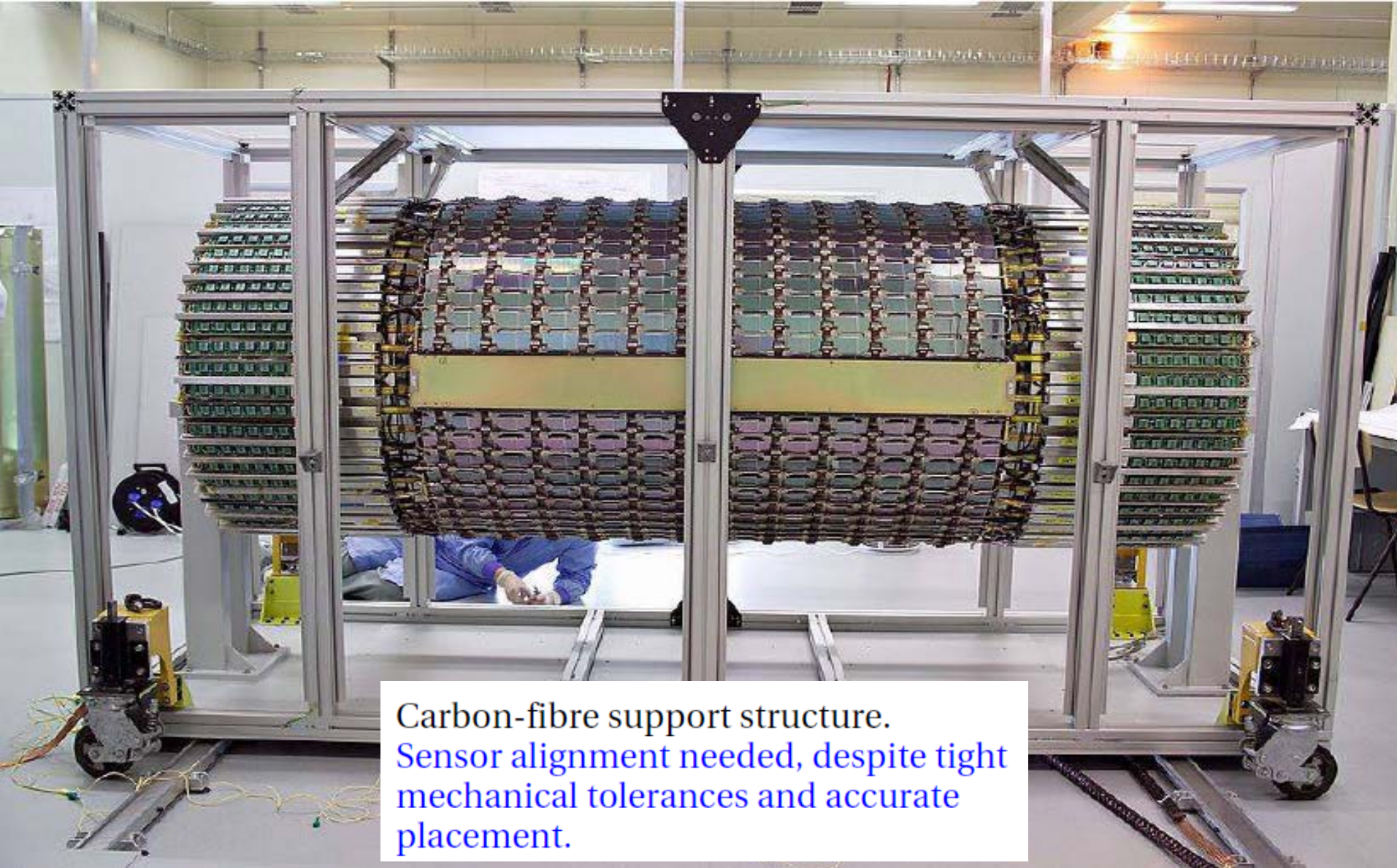
The most critical parts are the sensors, ASICs and system engineering (mechanics, power, cooling, assembly, etc) and integration



~ 220 m² Silicon:
More than all
other previous
HEP experiments
combined !

The ATLAS Inner Central Tracker (Barrel)

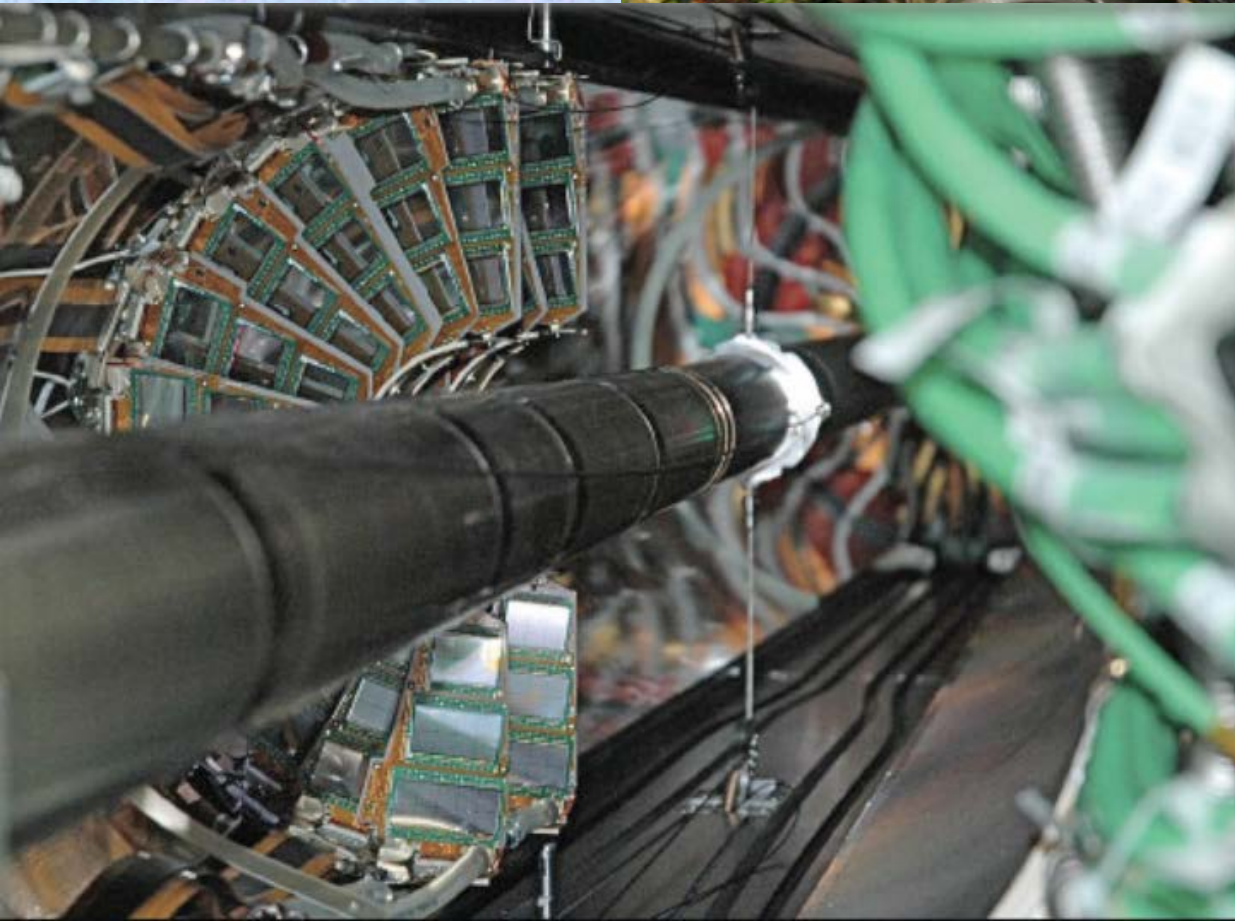
The most critical parts are the sensors, ASICs and system engineering (mechanics, power, cooling, assembly, etc) and integration



Carbon-fibre support structure.
Sensor alignment needed, despite tight mechanical tolerances and accurate placement.

The CMS Inner Tracker: Pixel Insertion

Barrel pixel



Forward pixel

Silicon Detectors has transformed the way we looked at particles

Detectors are more and more based on semi-conductor technology

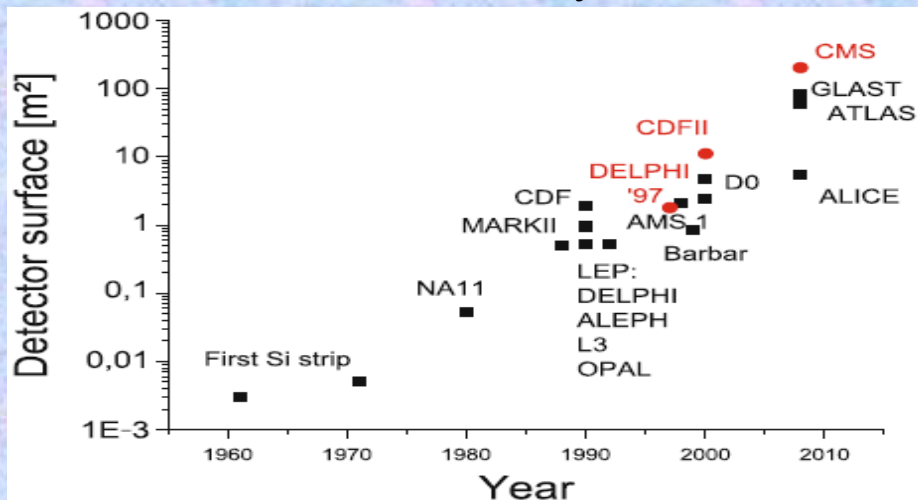
→ from vertex elements (20 μm feature size) to Si-calorimetry (ILC/CLIC)

Silicon surface:

ATLAS and CMS need to exchange Si-trackers during LS3 (2022/23) due to radiation effects: **400 m²**

CMS ECAL/HCAL Endcap: **600 m² ?**

ILD/SiD ECAL: **2500 (1200) m²**



HL-LHC Tracker Upgrades R&D: (Higher granularity / radiation hardness)

Upgrades	Area	Baseline sensor type
ALICE ITS	12 m ²	CMOS
LHCb VELO	0.15 m ²	tbd
LHCb UT	5 m ²	n-in-p
ATLAS Strips	193 m ²	n-in-p
CMS Strips	218 m ²	n-in-p
ATLAS Pixels	8.2 m ²	tbd
CMS Pixels	4.6 m ²	tbd

ILC / CLIC Oriented Pixel Sensor R&D:

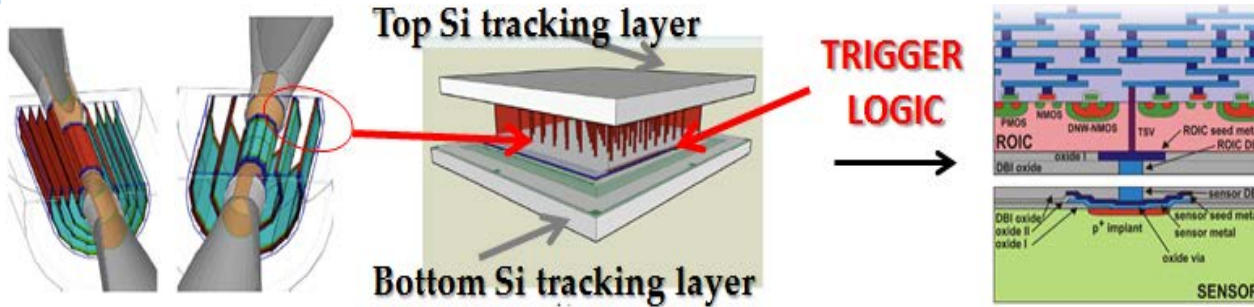
Wide range of technologies (ILD/SiD/CLIC):

- CMOS MAPS, DEPFET, SOI, FP-CCDs, thin-Si/Timepix, Chronopix, 3D integration
- Very light-weight supports → no liquid cooling to achieve material budget goals
- Low power consumption crucial: power-pulsing of readout electronics

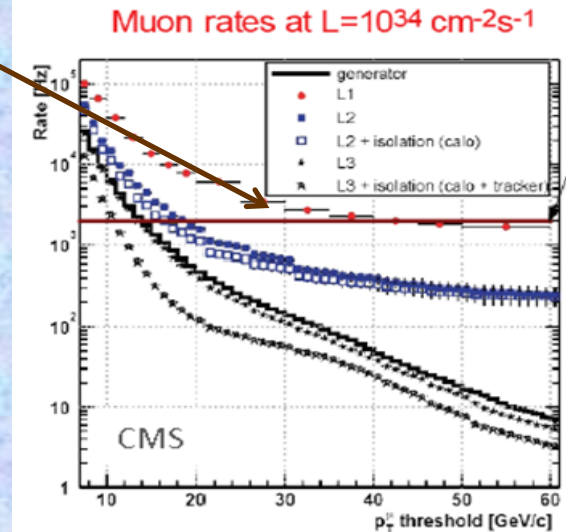
Day After Tomorrow: 3D-Vertically Integrated Systems

Track-Trigger Concept for High Luminosity-LHC: Integration of Functionality

Trigger @ L1: the path to fully exploit CMOS potential



Key technology: Through Silicon Via (TSV) → trigger logic, power, cooling inside the integrated chip layers



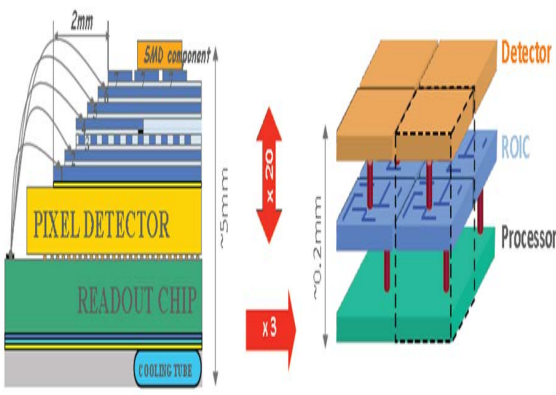
❖ Vertically Integrated 3D Si-sensor (initiated by ILC R&D)
→ multiple thin Si-processing layers, implementing analog and digital signal processing, stacked on top of sensor layer

❖ 3D-IT expected to be very beneficial for CMOS sensors: Combine different fabrication processes → choose the best ones for each tier/application

❖ Split signal collection and processing on different tiers

ALICE Pixel

3-D Pixel

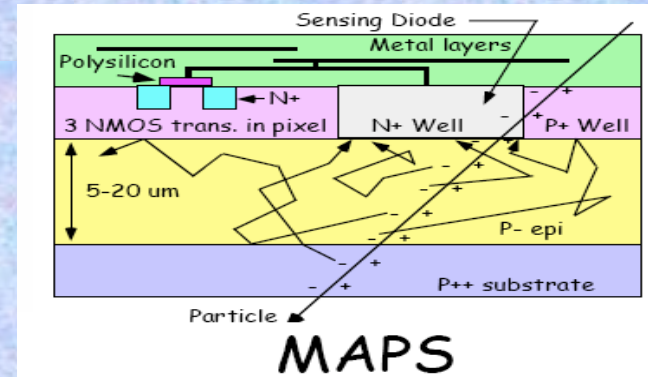
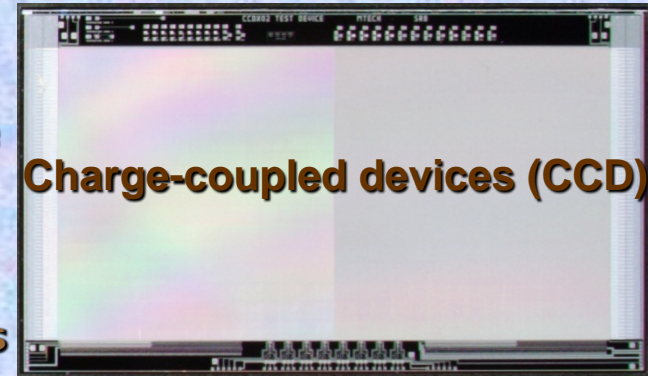


Advanced Concepts in Silicon Tracking

Several alternative pixel technologies & readout architecture under development:

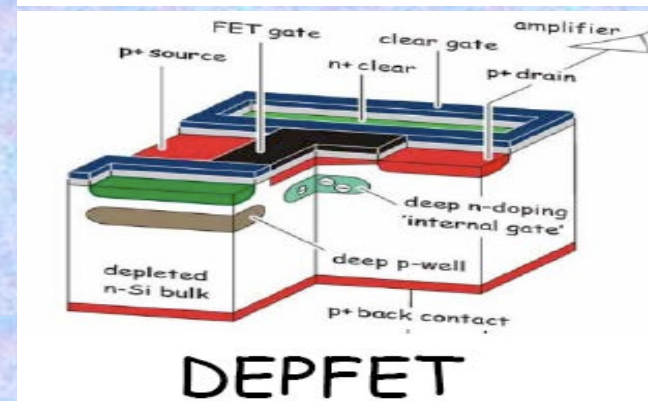
- Charged Coupled Devices (CCD)
- Silicon Drift Detectors
- Silicon Photo Multiplier (SiPM)
- Hybrid Active Pixels (HAPS)
- Monolithic Active Pixels (MAPS)
- Depleted Field Effect detectors (DEPFET)
- Silicon On Insulator (SOI)
- 3D pillar silicon sensors
- 3D vertically integrated systems

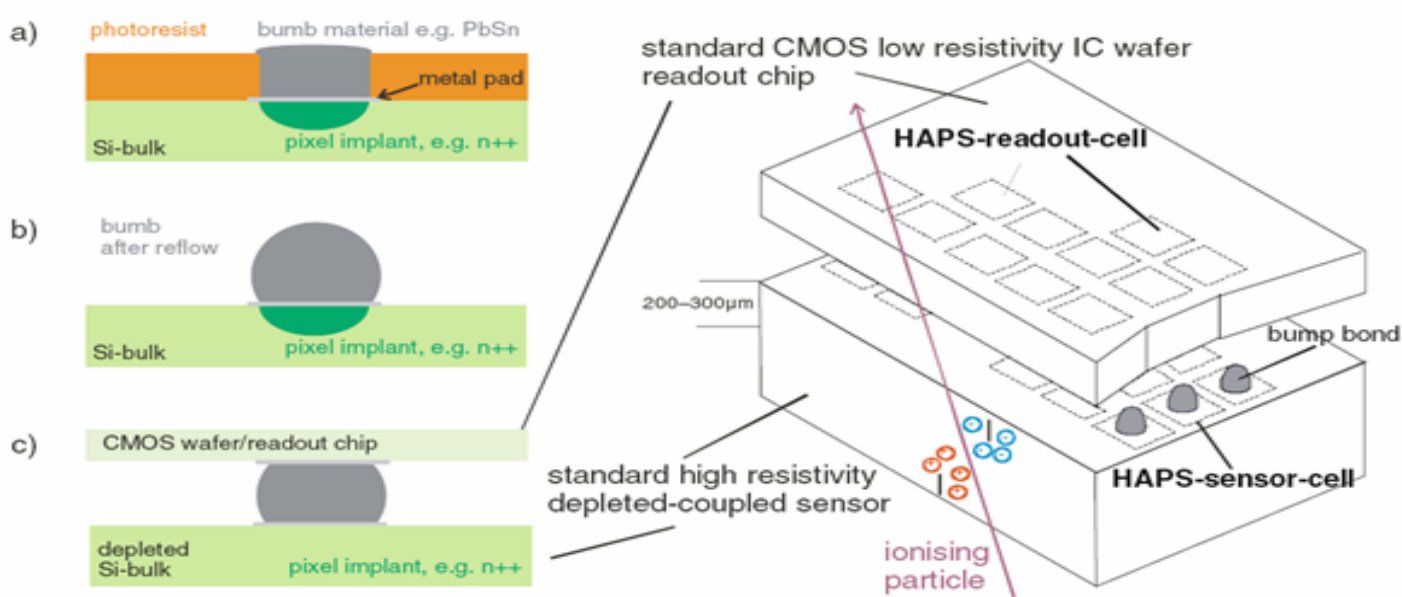
Some of these concepts described in backup transparencies



Motivation to develop new pixel systems:

- Decrease fabrication cost of pixel detector
- Develop thinner pixel systems
- Develop more radiation
- New interconnect methods (3D, bonding and vias)
- Easy fabrication of large area devices





HAPS
(Hybrid
Active
Pixels)

Fig. 1.63 Scheme of a *Hybrid Active Pixel Sensor* (HAPS). A HAPS is a sandwich of a silicon sensor and a standard CMOS readout chip. The sensor is of the high resistivity-depleted DC-coupled type processed as described in Sect. 1.8.2. The readout chip is realized in standard CMOS technology on a low-resistivity wafer, the same size as the sensor, and its readout cells are distributed in the same “pixellated” way as the sensor pixels. The merging is realized via so-called “bump bonding” or “flip-chip-bonding”. After preparing the pads with a dedicated under-bump metallization a further lithography step opens holes on each pad to place the bump metal (a), e.g. Cu or In. After removing/etching the photoresist the metal undergoes another temperature step, the so-called reflow to form balls of metal (b). The chip is then “flipped”, aligned and pressed onto the sensor, warmed up for reflow, connecting sensor channels to readout cells (c)

Used in DELPHI,
ALICE, ATLAS; CMS

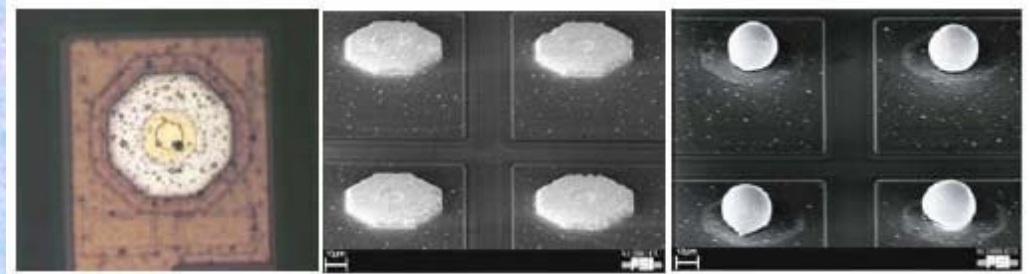
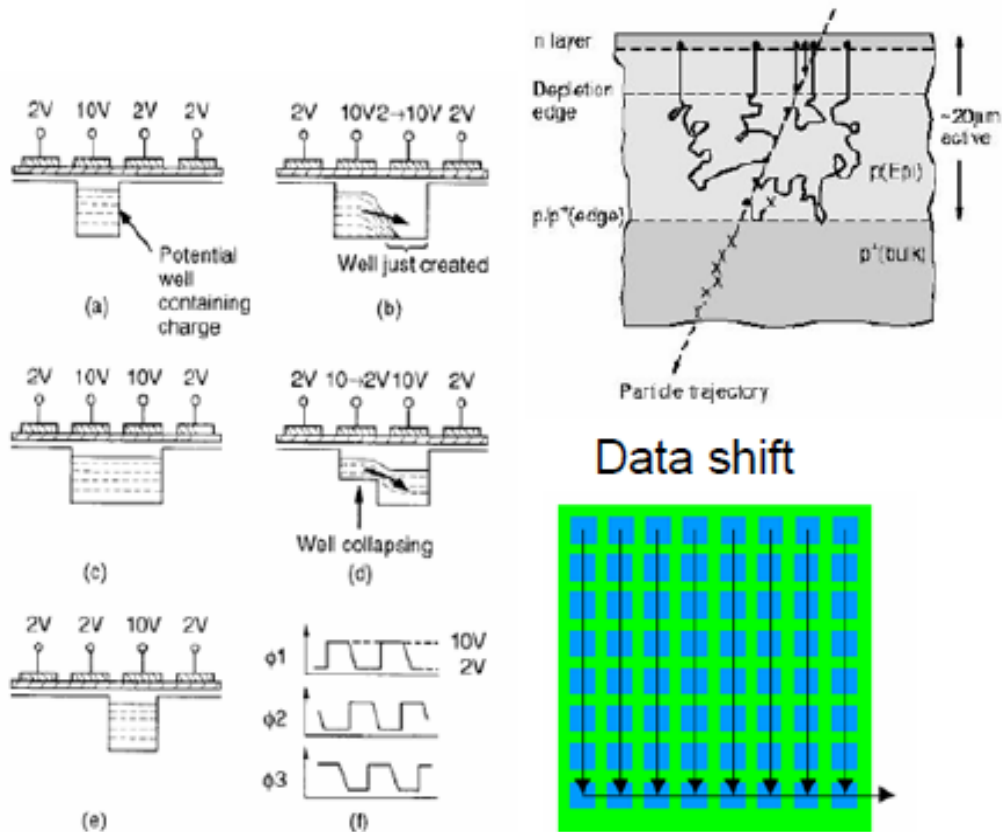


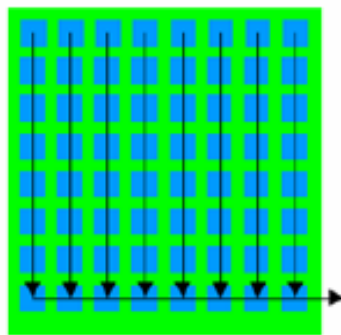
Fig. 1.64 Bump bonding at PSI for the CMS pixel detector. The *left* shows a bare contact on the pixel silicon sensor. In the *middle* part, an electron microscope picture of the structured indium bumps before the reflow process is shown. On the *right*, the bump ball after reflow is shown. The distance between bumps is 100 μm, the deposited indium is 50 μm wide while the reflowed bump is only 20 μm wide [34]

Charge Coupled Device (CCD)

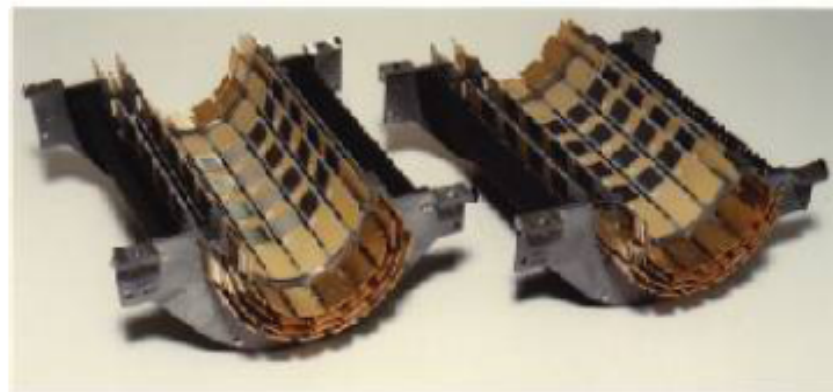
CCD pixel detectors : Still the active depth is usually quite small (typically $15\mu\text{m}$) so the ionization signal is small. The charge is kept isolated in the pixel and then shifted as shown:



Data shift



The SLD silicon pixel vertex detector: the first pixel detector in a collider experiment had $20\mu\text{m} \times 20\mu\text{m}$ pixels and achieved about $4\mu\text{m}$ resolution.



By changing the potential on the gates in one out of 3 rows at a time, one can achieve a “bucket brigade” effect of shifting the charge to the next “well” without it spreading.

MAPS Monolithic Active CMOS

(Complimentary Metal-Oxide Semiconductor)

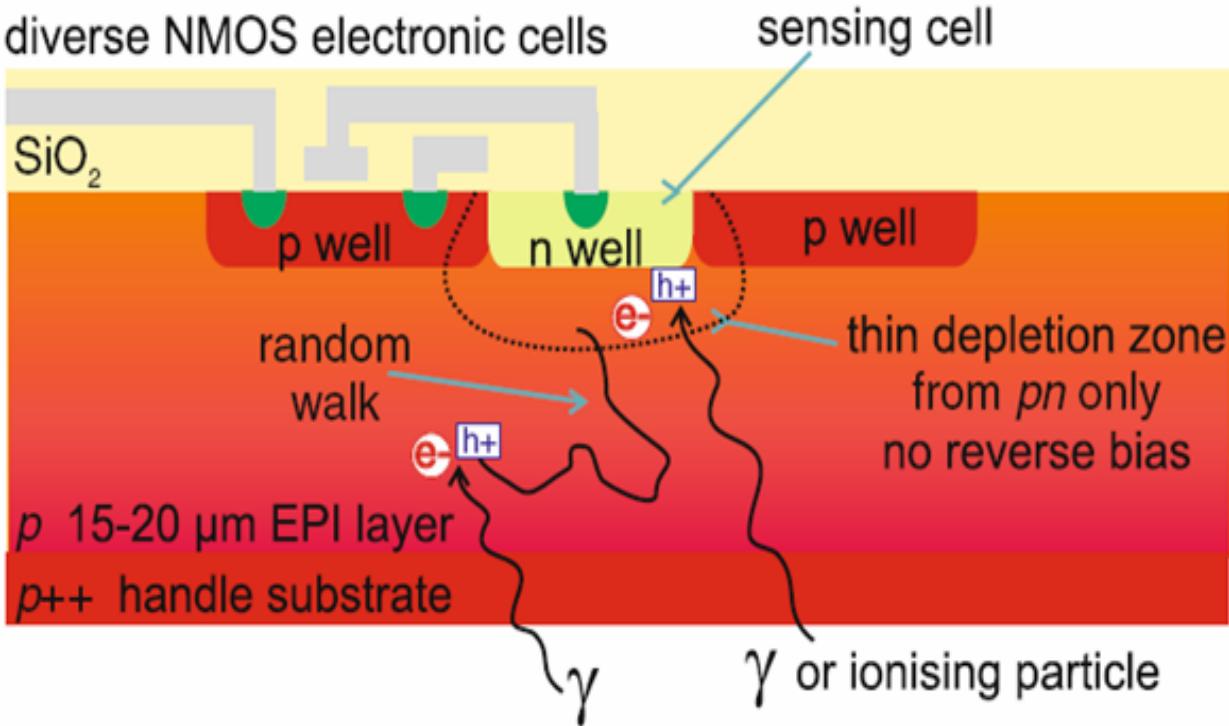


Fig. 1.65 Cross section of a CMOS sensor, one pixel. The scheme nicely depicts an example of NMOS transistors and the N-well to collect electrons from ionization or photo-effect. Electrons created inside the shallow depletion zones are fully collected while electrons from the EPI layer randomly walk towards the N-well and with an excellent lifetime behaviour only some of them will be trapped. Nevertheless, CMOS devices have an excellent signal-to-noise ratio due to their very small capacitances and low currents, therefore the low noise compensates for the low signal

Silicon on Insulator (SOI)

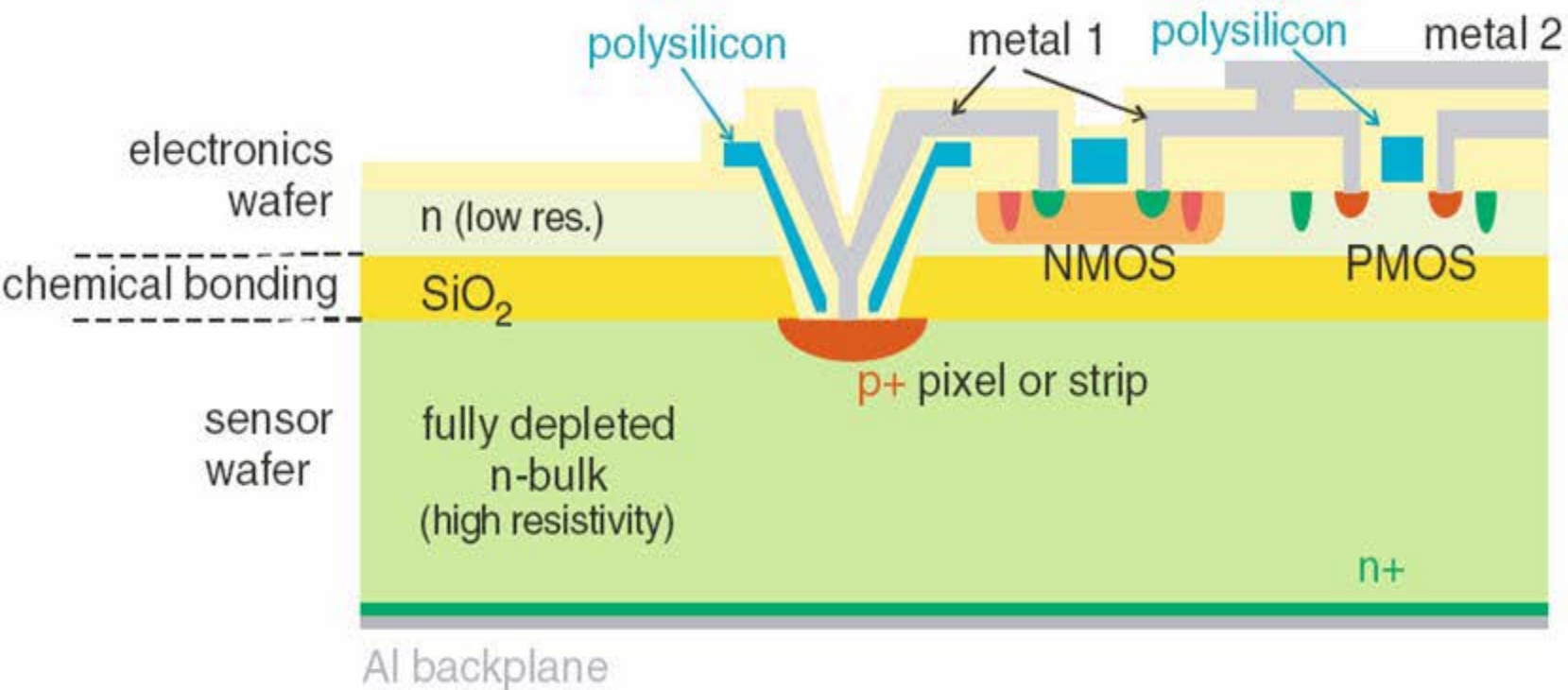
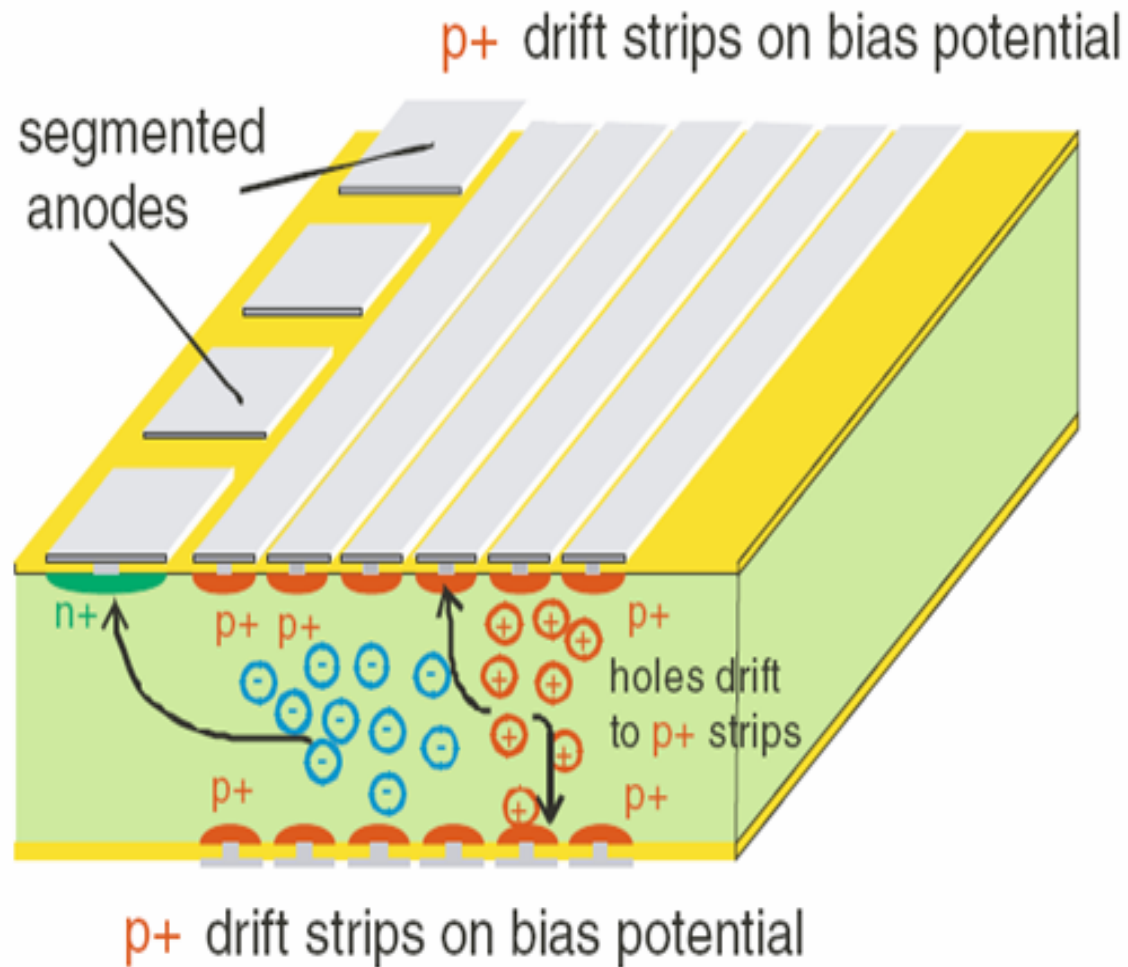


Fig. 1.66 Scheme of a silicon on insulator sensor. The scheme shows the basics of a SOI sensor. Passing charged particles create electron–holes pairs moving to the electrodes in a fully depleted high resistivity *n*-type sensor while the electronics are realized in a low resistivity *n*-type base material, separated by a layer of SiO₂. The connection of both parts is realized by etching while the electronics processing follows standard IC methods. In difference to CMOS devices the sensor wafer can be thick, of high resistivity and depletion is possible. NMOS and PMOS transistors are possible to be processed on the electronics wafer

Silicon Drift Detector

Fig. 1.67 The concept of a silicon drift sensor. Several $p+$ strips on the same potential build a homogeneous field between sensor planes while the edge is structured with $n+$ elements where the free charge carriers drift to; the Y-coordinate is defined by the $n+$ elements while the X-position is defined by the drifting time. Depletion zone builds up horizontally



Used in ALICE

Depleted Field Effect (DEPFET)

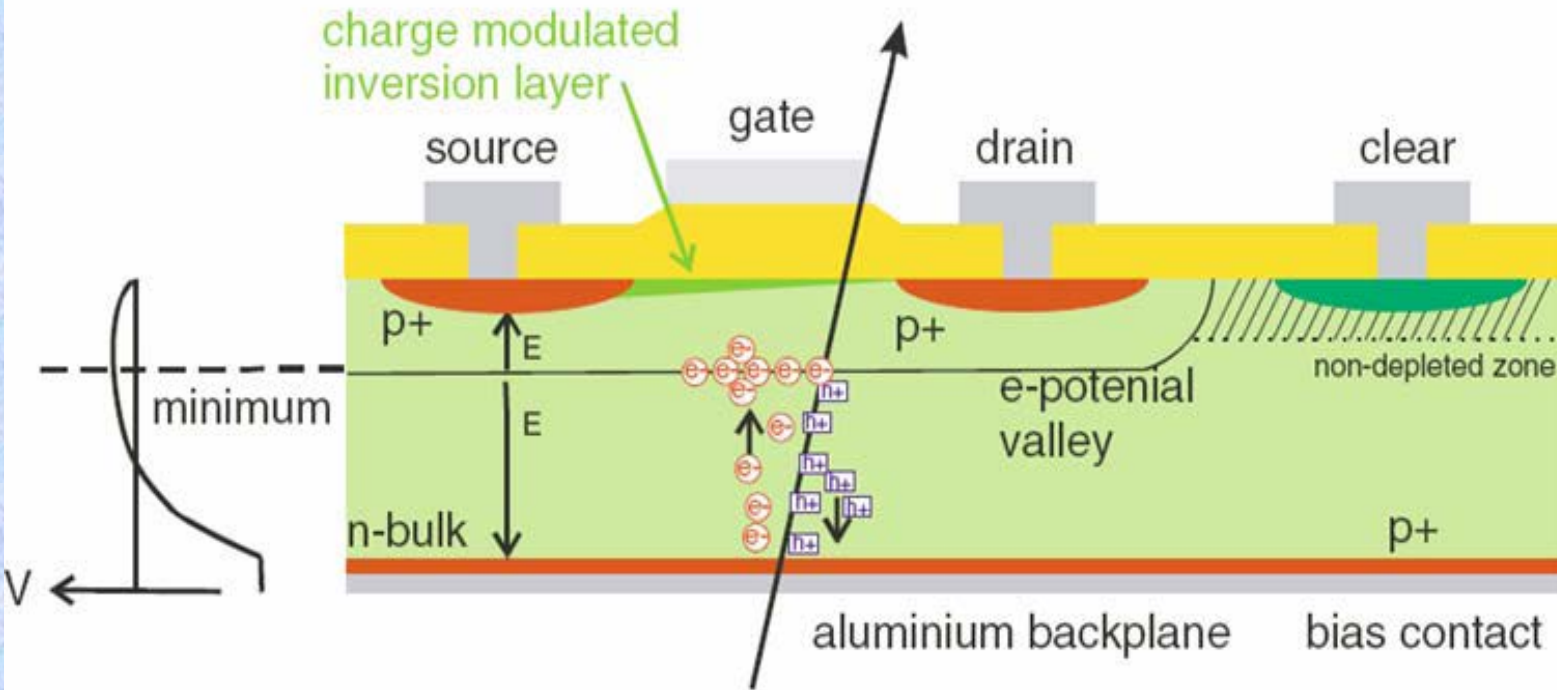
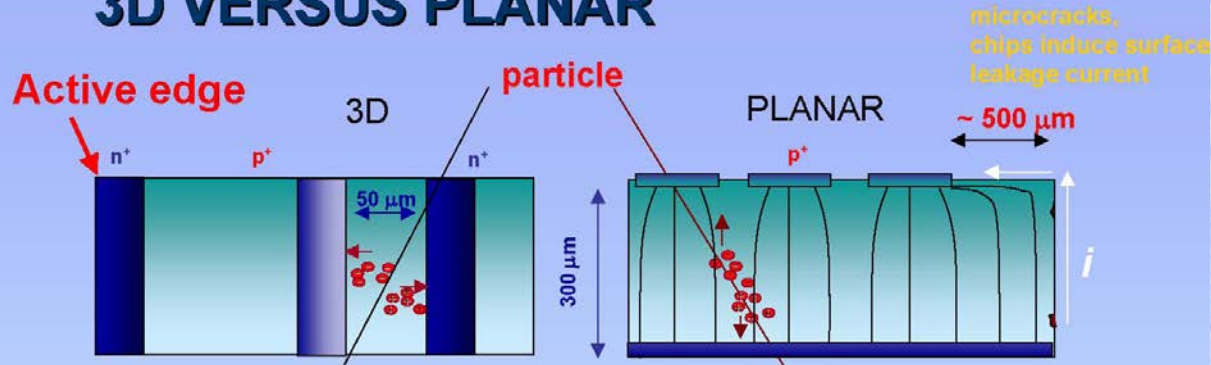


Fig. 1.68 The concept of a DEPFET sensor. The volume is depleted from the side n+ strips down to the back p+ implantation. The potential minimum of the sideways depletion is shifted towards the FET side by optimizing bias configuration. An ionizing traversing particle creates electron-hole pairs in the depleted volume. Holes are lost in the back of the device, while electrons travel to and accumulate at the potential minimum below the external GATE at the so-called internal GATE, thus increasing charge density and thus modulating *source-drain* current of the FET. The electrons stay there until actively *cleared* [111]

3D Silicon Sensors

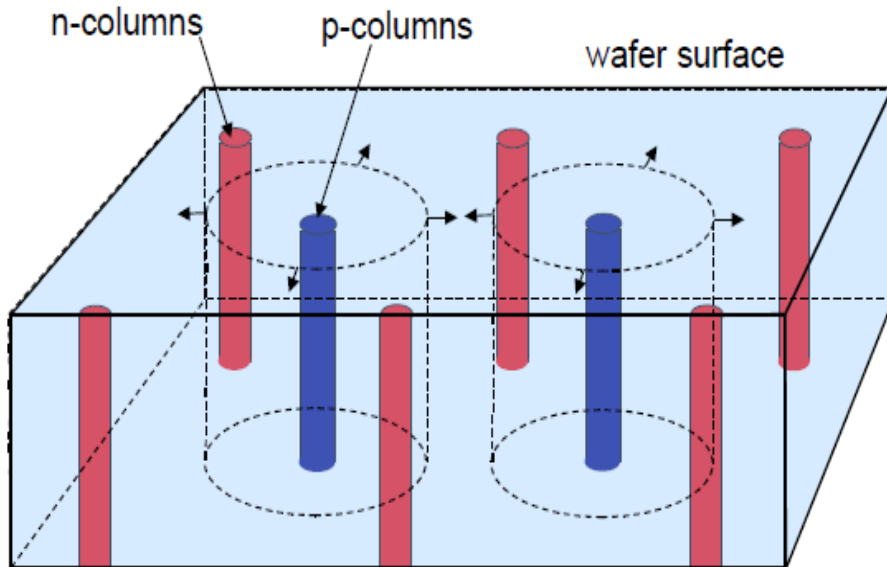
Challenges for tracking at the future LHC upgrade (sLHC) → current planar-Si sensors technology is not radiation hard to survive to the end of sLHC in the innermost layer ($R \sim 4$ cm)

3D VERSUS PLANAR



Very small depletion & drift distances:

**hole diameter: 10 μm
distance ~20-50 μm**



Maximum drift and depletion distance governed by electrode spacing:

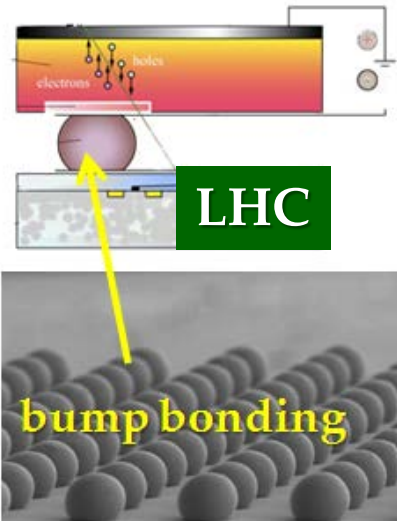
- Lower depletion voltages
- Faster/more efficient charge collection
- Small leakage currents
- Higher radiation hardness
- Narrow dead regions at the edges

→ At the price of more complex processing

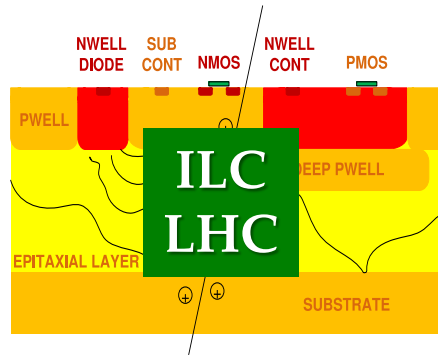
Solid State Tracking: Detector-Electronics Integration Trends

- **Radiation hardness** improvements demand newer technologies
- **Improved functionality** can only be achieved with **higher integration**
- **Power dissipation** and material budget must be **reduced**

TODAY: Pixels
50 – 100s μm

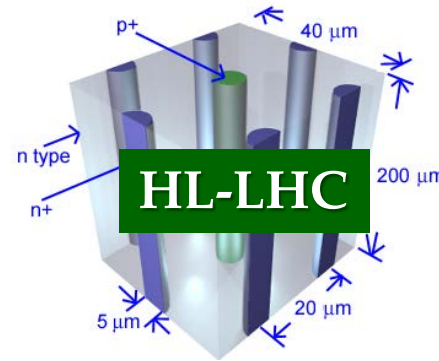


TODAY: Monolithic
25 – 50 μm



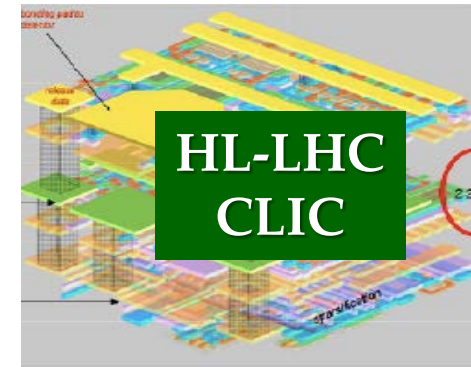
Integrated sensor & electronics: Less X0, no bonding, low noise

TOMORROW: 3D Detectors (25–50 μm)



Lower V_{dep} (power)
Faster charge collection

Day After Tomorrow:
3D TSV (< 20 μm)



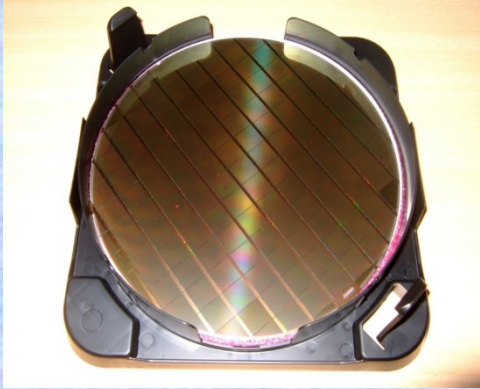
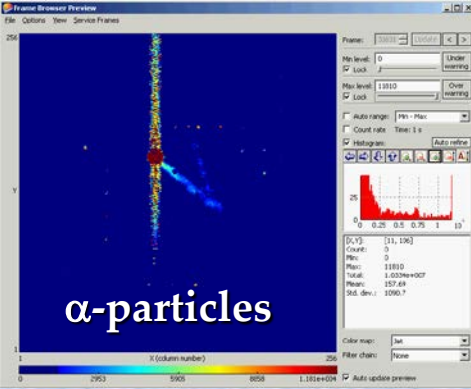
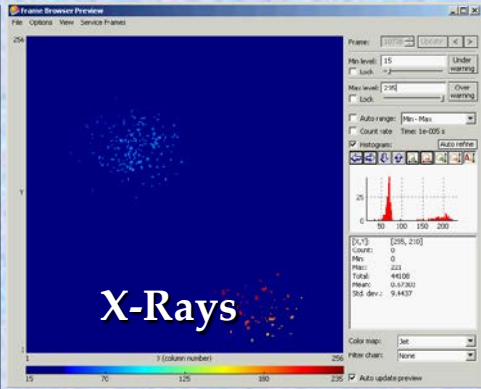
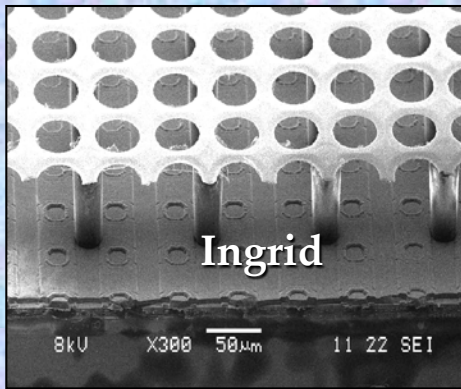
3D vertical Integration (TSV)

Motivation to develop new Pixel Detectors:

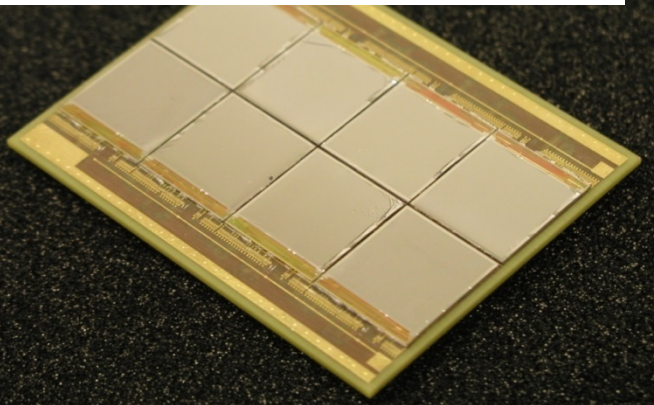
- Decrease fabrication cost
- Develop thinner pixel systems
- Easy fabrication of large area devices
- **Integrate More (= denser) Intelligence**

Trends and Perspectives:

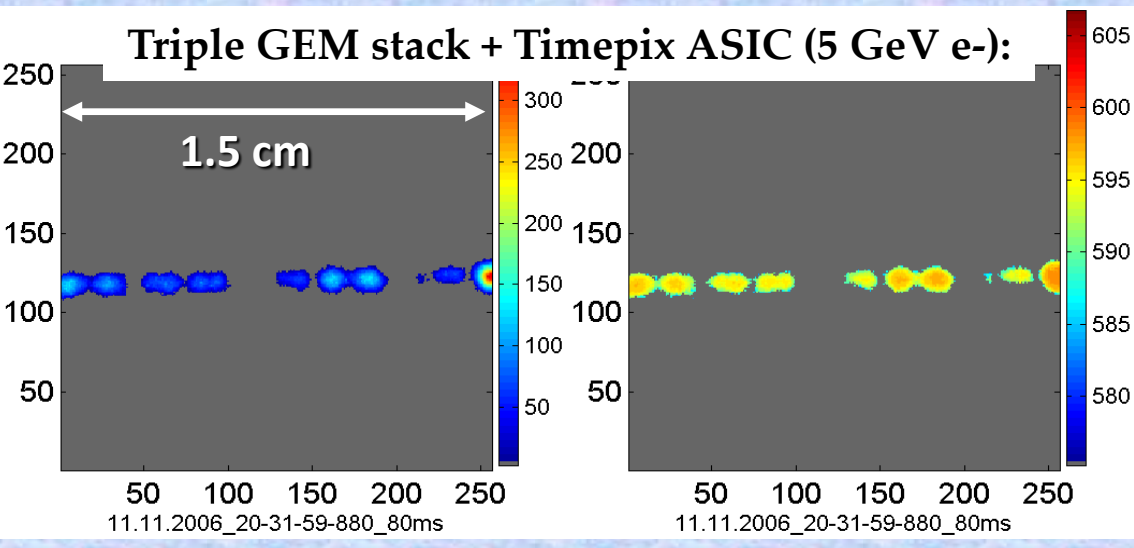
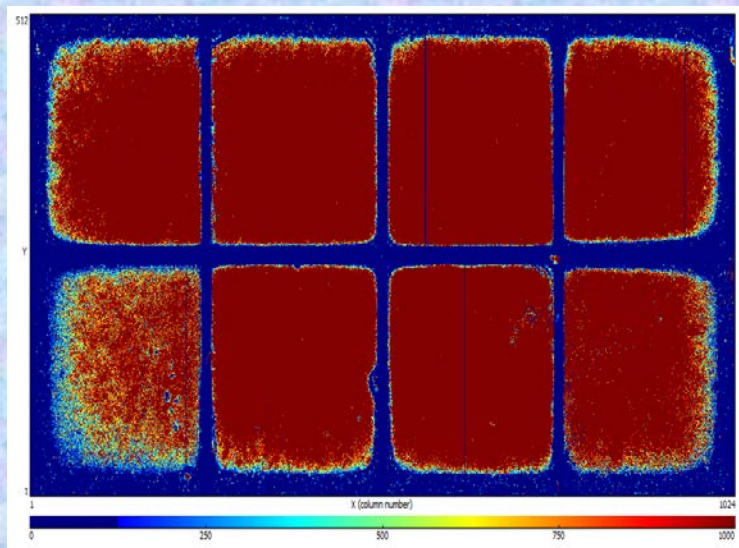
- Improve rad. hardness (p-type bulk)
- Reduce the thickness to 50 μm
- From 6" to 8" and 12" wafers
- **R&D on SLID/TSV interconnect.**



“Octopuce” (8 Timepix ASICs):



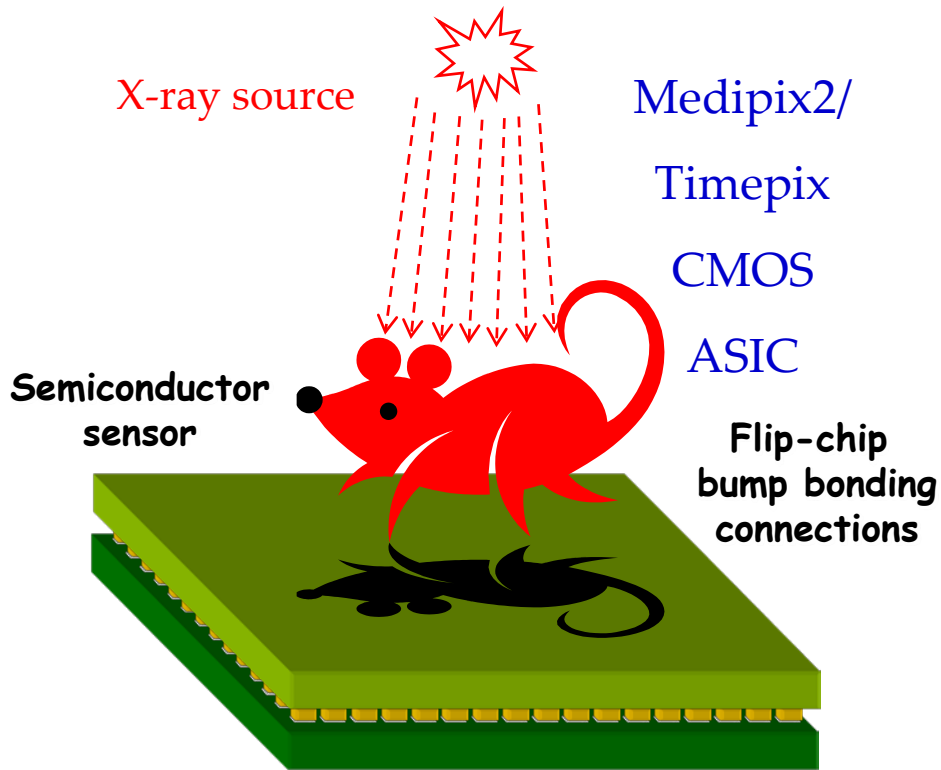
**INSTRUMENTATION FRONTIER:
 PIXEL READOUT OF MPGDs –
 Ultimate Gas-Silicon Detector Integration**



Pixel Readout of Micro-Pattern Gaseous Detectors: Ultimate Integration

Use a CMOS Pixel ASIC (w/o Si sensor), assembled below MPGDs (GEM/Micromegas), as **charge collecting anode and fully integrated readout electronics** for a TPC at LC

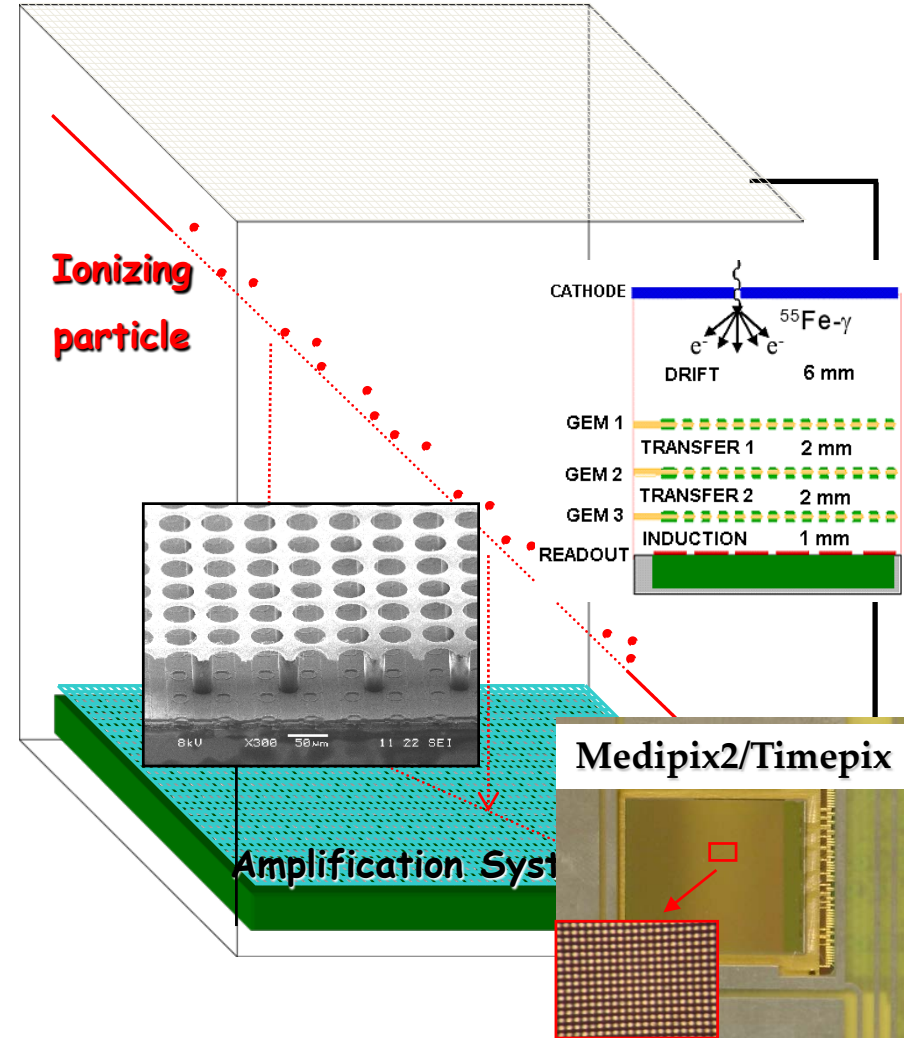
Solid state pixel detector



Medipix2 / Timepix ASIC ($0.25 \mu\text{m}$ –IBM/CMOS)

- 256×256 pixels of $55 \times 55 \mu\text{m}^2$ size
- **Medipix2**: digital with 2 THR (low and high)
- **Timepix**: 2 modes (TOT \approx integrated charge TIME = Time between hit and shutter end)

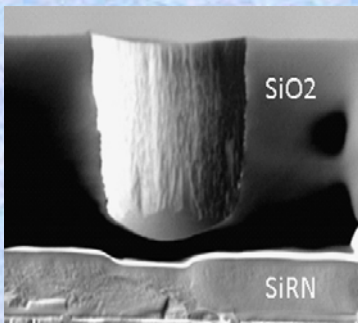
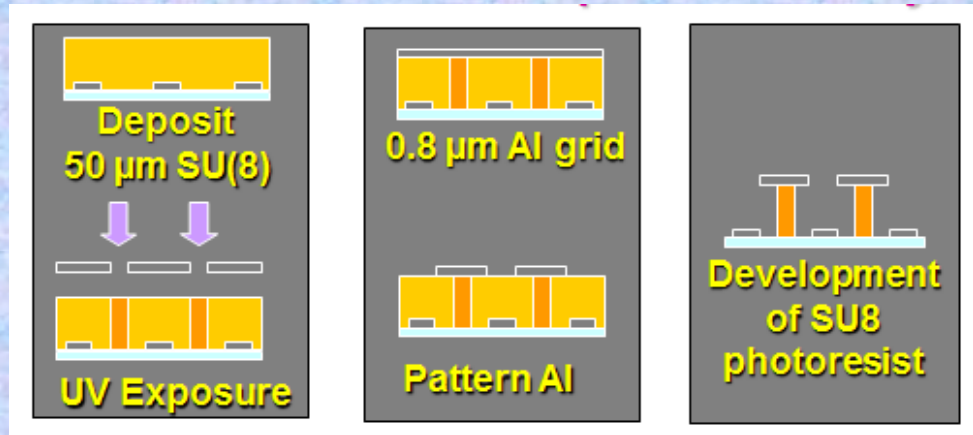
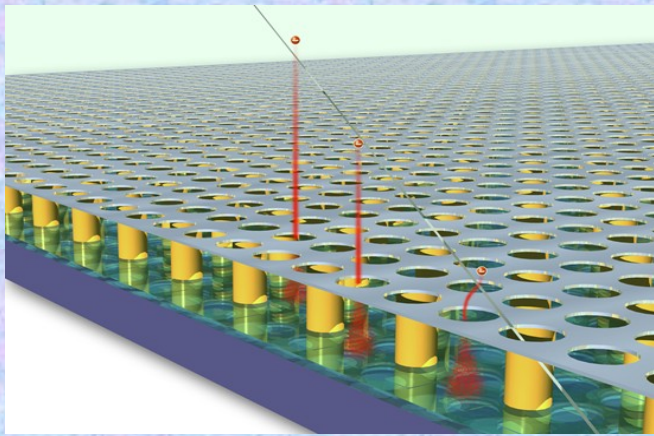
Gaseous detector



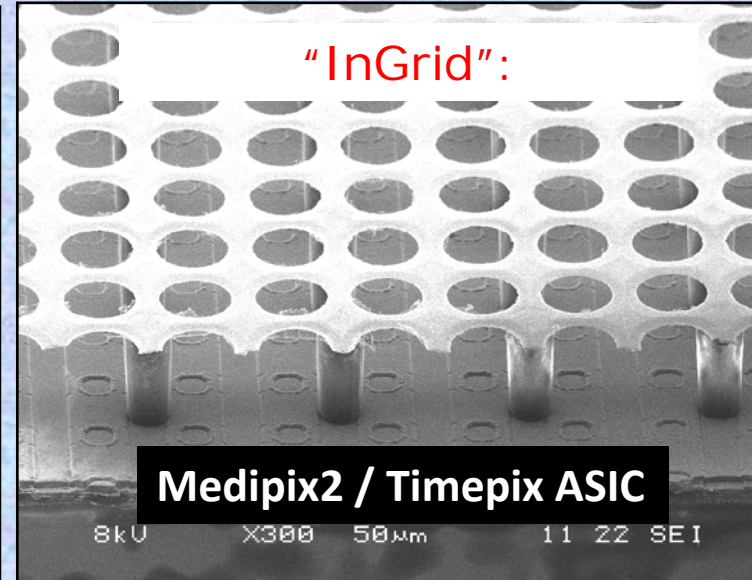
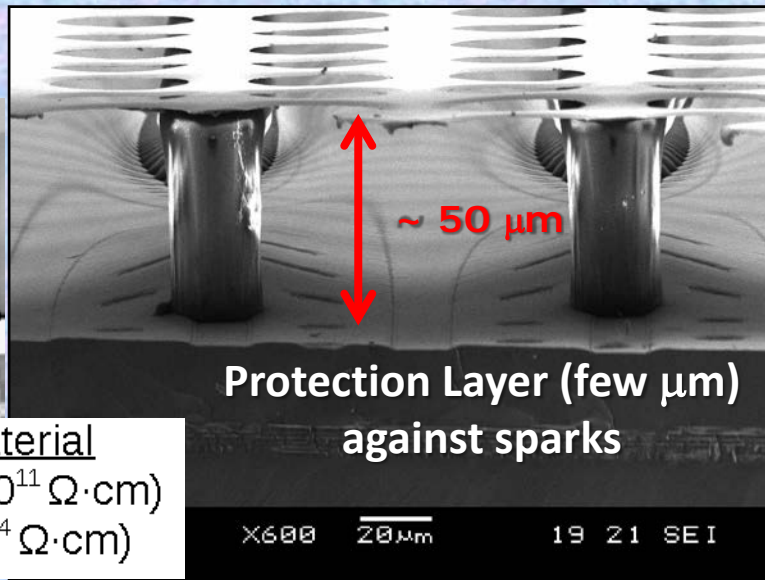
Pixel Readout of MPGDs: "InGrid" Concept

"InGrid" Concept: By means of advanced wafer processing-technology **INTEGRATE** **MICROME GAS** amplification grid directly **on top of CMOS ("Timepix") ASIC**

3D Gaseous Pixel Detector → 2D (pixel dimensions) x 1D (drift time)



high resistive material
15 μm aSi:H (~10¹¹ Ω·cm)
8 μm Si_xN_y (~10¹⁴ Ω·cm)



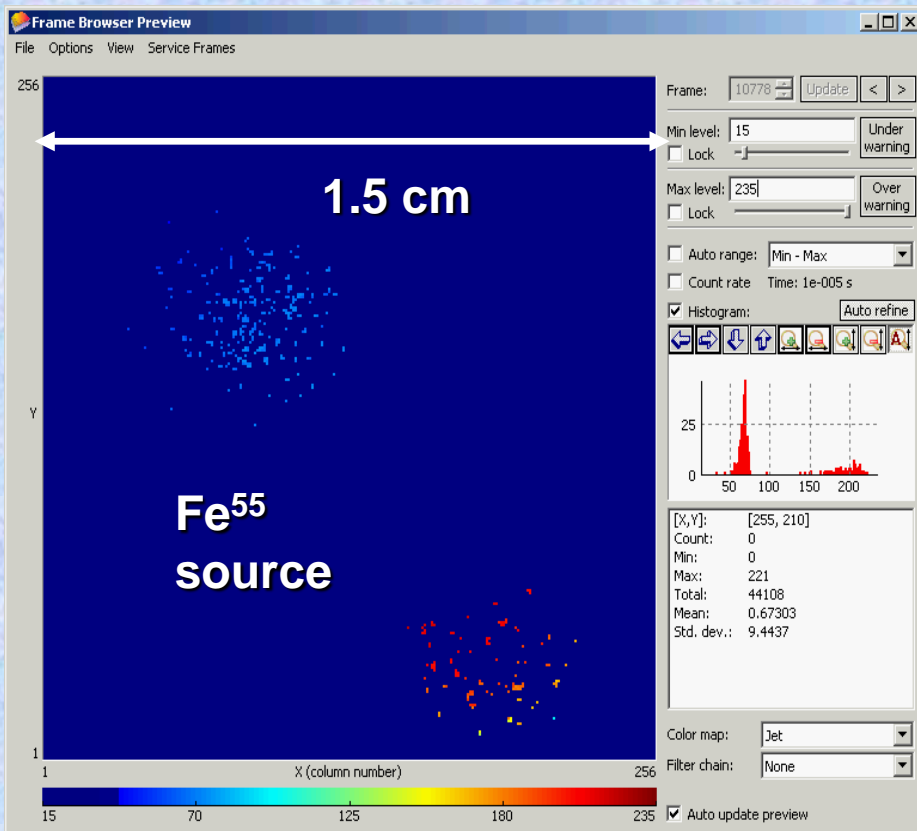
"InGrid" Detector: Single Electron Response and Discharges

Observe electrons (~ 220) from an X-ray (5.9 keV) conversion one by one and count them in micro-TPC (6 cm drift)

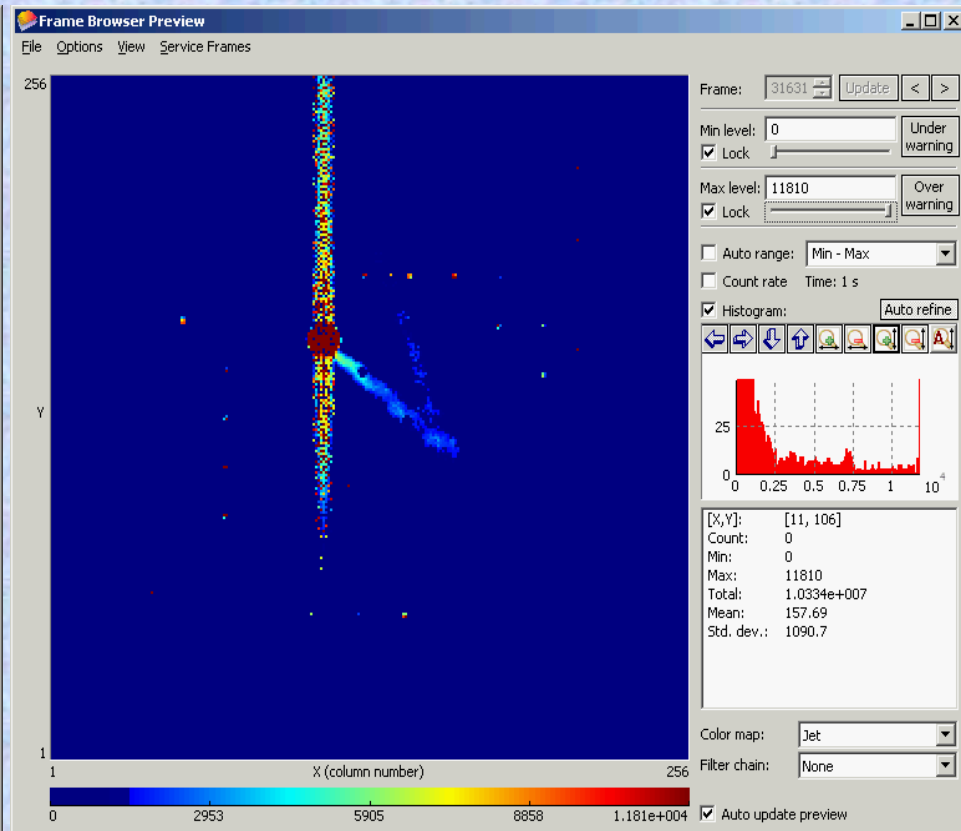
→ Study single electron response

Provoke discharges by introducing small amount of Thorium in the Ar gas - Thorium decays to Radon 222 which emits 2 alphas of 6.3 & 6.8 MeV

→ Round-shape images of discharges



P. Colas, RD51 Collab. Meet.,
Jun.16-17, 2009, WG2 Meeting



M. Fransen, RD51 Collab. Meet.,
Oct.13-15, 2008, WG2 Meeting

Fiber Trackers

- Trackers also work with scintillating fibers

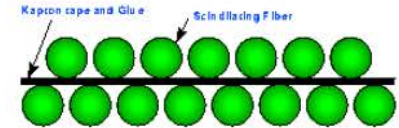
- fiber tracker of D0 (at Tevatron)
- 71'680 fibers of \varnothing 835 μm each in several layers

- Read-Out by VPLCs (Visible Light Photon Counter)

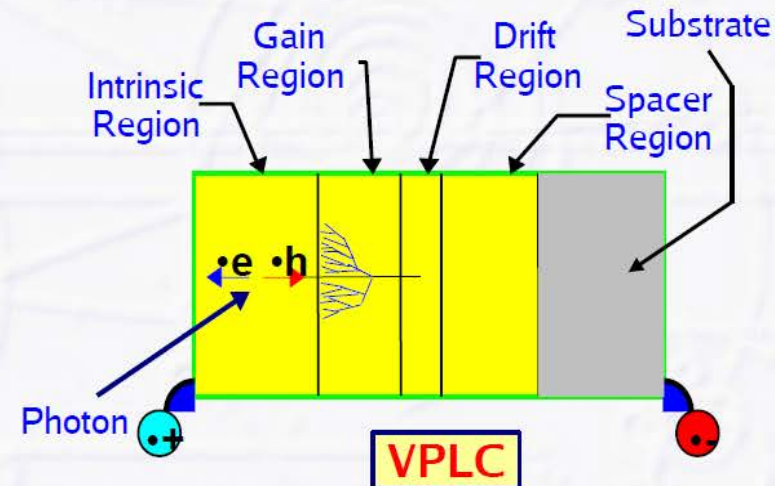
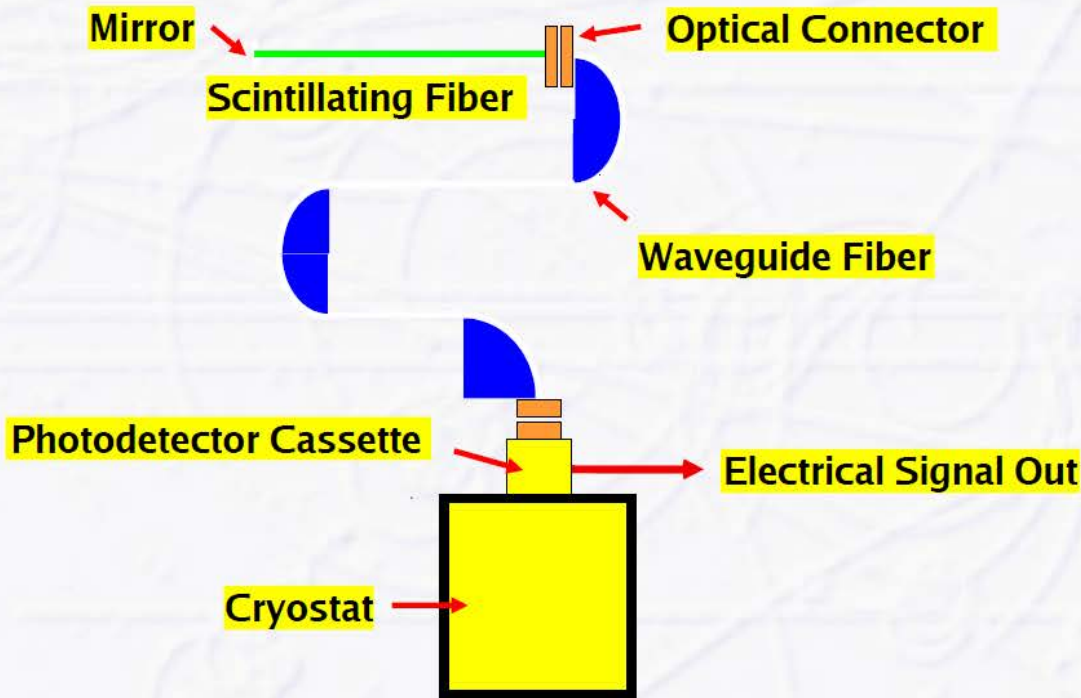
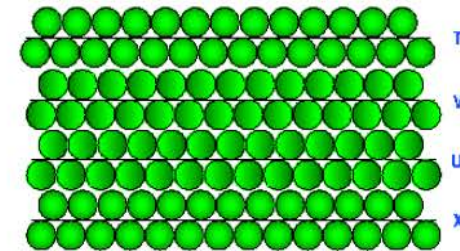
- high quantum efficiency (80%), gain 20'000 – 50'000 when operated at cryogenic temperatures (6 – 10 K)

Fibers&Ribbons

The schematic layout of a ribbon



The schematic layout of a superlayer



Fiber Trackers

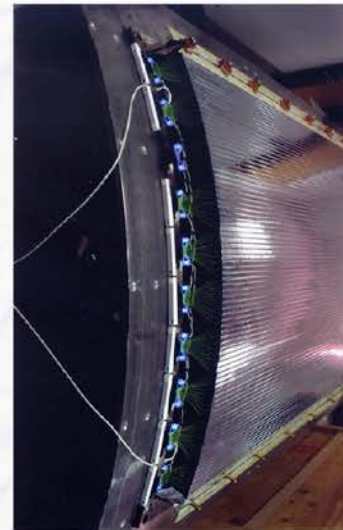
D0 fiber tracker



4 Superlayers in barrel



visual inspection



part of superlayer



optical connectors

Modern Tracking Detectors Summary

● Mainly two (three) types of tracking detectors

→ **wire detectors** (gaseous) since 1960s

◦ **point resolution limited to $\sim 50\text{-}150\ \mu\text{m}$**

→ **silicon detectors** since early 1990s

◦ **very good point resolution**, many electronics channels, “thick” compared to wire chambers

→ **fiber tracker** with scintillating fibers + photon detectors

● Momentum resolution has two (three) main contributions

→ **error from multiple scattering**

◦ **dominates at low momenta**, requires thin/light detectors

→ **error from point measurements (intrinsic resolution)**

◦ **dominates at high momenta**, (large track length helps: $\propto L^2$ + high magnetic field: $\propto B$)

→ **error from calibration/alignment (systematics)**

◦ **additional contribution** to point measurements + **systematic shifts** in momentum measurement